



**UNIVERSIDAD DE INVESTIGACIÓN DE
TECNOLOGÍA EXPERIMENTAL YACHAY**

Escuela de Ciencias Biológicas e Ingeniería

**TÍTULO: Characterization of carbon fibers synthesized from banana
stem and decorated with cerium oxide (CeO₂) nanoparticles**

Trabajo de integración curricular presentado como requisito
para la obtención del título de Ingeniera Biomédica

Autor:

María Gabriela Pineda Molina

Tutor:

Dr. rer. nat. Julio C. Chacón-Torres

Urcuquí, Imbabura, Ecuador

August 22nd, 2022

**SECRETARÍA GENERAL
ESCUELA DE CIENCIAS BIOLÓGICAS E INGENIERÍA
CARRERA DE BIOMEDICINA
ACTA DE DEFENSA No. UITEY-BIO-2022-00021-AD**

En la ciudad de San Miguel de Urcuquí, Provincia de Imbabura, a los 22 días del mes de agosto de 2022, a las 15:00 horas, en el Aula S_CAN de la Universidad de Investigación de Tecnología Experimental Yachay y ante el Tribunal Calificador, integrado por los docentes:

Presidente Tribunal de Defensa	DAVALOS MONTEIRO, RAUL LEANDRO , Ph.D.
Miembro No Tutor	Dra. GONZALEZ VAZQUEZ, GEMA , Ph.D.
Tutor	Dr. CHACON TORRES, JULIO CESAR , Ph.D.

Se presenta el(la) señor(ita) estudiante **PINEDA MOLINA, MARIA GABRIELA**, con cédula de identidad No. **1004450126**, de la **ESCUELA DE CIENCIAS BIOLÓGICAS E INGENIERÍA**, de la Carrera de **BIOMEDICINA**, aprobada por el Consejo de Educación Superior (CES), mediante Resolución **RPC-SO-43-No.496-2014**, con el objeto de rendir la sustentación de su trabajo de titulación denominado: **"Characterization of carbon fibers obtained from banana stem and decorated with cerium oxide (CeO2) nanoparticles"**, previa a la obtención del título de **INGENIERO/A BIOMÉDICO/A**.

El citado trabajo de titulación, fue debidamente aprobado por el(los) docente(s):

Tutor Dr. CHACON TORRES, JULIO CESAR , Ph.D.

Y recibió las observaciones de los otros miembros del Tribunal Calificador, las mismas que han sido incorporadas por el(la) estudiante.

Previamente cumplidos los requisitos legales y reglamentarios, el trabajo de titulación fue sustentado por el(la) estudiante y examinado por los miembros del Tribunal Calificador. Escuchada la sustentación del trabajo de titulación, que integró la exposición de el(la) estudiante sobre el contenido de la misma y las preguntas formuladas por los miembros del Tribunal, se califica la sustentación del trabajo de titulación con las siguientes calificaciones:

Tipo	Docente	Calificación
Miembro Tribunal De Defensa	Dra. GONZALEZ VAZQUEZ, GEMA , Ph.D.	10,0
Tutor	Dr. CHACON TORRES, JULIO CESAR , Ph.D.	10,0
Presidente Tribunal De Defensa	DAVALOS MONTEIRO, RAUL LEANDRO , Ph.D.	10,0

Lo que da un promedio de: **10 (Diez punto Cero)**, sobre 10 (diez), equivalente a: **APROBADO**

Para constancia de lo actuado, firman los miembros del Tribunal Calificador, el/la estudiante y el/la secretario ad-hoc.


PINEDA MOLINA, MARIA GABRIELA
Estudiante


DAVALOS MONTEIRO, RAUL LEANDRO , Ph.D.
Presidente Tribunal de Defensa


Dr. CHACON TORRES, JULIO CESAR , Ph.D.
Tutor


Dra. GONZALEZ VAZQUEZ, GEMA , Ph.D.
Miembro No Tutor


ALARCON FELIX, KARLA ESTEFANIA
Secretario Ad-hoc

AUTORÍA

Yo, **MARÍA GABRIELA PINEDA MOLINA**, con cédula de identidad 1004450126, declaro que las ideas, juicios, valoraciones, interpretaciones, consultas bibliográficas, definiciones y conceptualizaciones expuestas en el presente trabajo; así como, los procedimientos y herramientas utilizadas en la investigación, son de absoluta responsabilidad de él/la autor(a) del trabajo de integración curricular. Así mismo, me acojo a los reglamentos internos de la Universidad de Investigación de Tecnología Experimental Yachay.

Urcuquí, 22 de Agosto de 2022



María Gabriela Pineda Molina

CI:1004450126

AUTORIZACIÓN DE PUBLICACIÓN

Yo, **MARÍA GABRIELA PINEDA MOLINA**, con cédula de identidad 1004450126, cedo a la Universidad de Tecnología Experimental Yachay, los derechos de publicación del presente trabajo de integración curricular, sin que deba haber un reconocimiento económico por este concepto. Declaro además que el texto del presente trabajo de titulación no podrá ser cedido a ninguna empresa editorial para su publicación u otros fines, sin contar previamente con la autorización escrita de la Universidad.

Asimismo, autorizo a la Universidad que realice la digitalización y publicación de este trabajo de integración curricular en el repositorio virtual, de conformidad a lo dispuesto en el Art. 144 de la Ley Orgánica de Educación Superior.

Urququí, 22 de Agosto de 2022



María Gabriela Pineda Molina

CI:1004450126

DEDICATION

*To my parents, Mauricio and María Augusta for letting me dream.
To my siblings and soul mates, Francisco and Camila for adding color to my days.
To my grandparents, especially to Humberto for his endless support and
to Magdalena because a piece of my heart will always be hers.
To my whole family, because you are the reason for what I become today.
To my dearest friends, who gave me love and emotional support on this journey,
but above all a new appreciation for the meaning of friendship.*

ACKNOWLEDGEMENTS

Un agradecimiento especial a mi tutor, el Ph.D. Julio Chacón Torres por su apoyo incondicional, su predisposición, sus consejos y la motivación constante; porque supo compartir sus conocimientos y a la vez contagiarme de esa pasión por la ciencia que se ha quedado grabada para siempre en mí. Mis más sinceros agradecimientos a la Escuela de Ciencias Físicas y Nanotecnología en especial a Gema González, Luis Corredor, Carlos Reinoso, Jonathan Escorza y Darwin Méndez por la predisposición, la orientación, el asesoramiento y la motivación constante en cada etapa de este proceso. Gracias a cada uno de mis profesores de la Escuela de Ciencias Biológicas e Ingeniería por su esfuerzo y dedicación, por llenarme de tanto conocimiento, por creer en mí; pero sobre todo por dejarme ese amor por la ciencia y enseñarme lo que no está escrito en los libros. Gracias a ustedes, Yachay Tech me hizo comprender que enseñar es dejar huella en la vida de una persona.

Gracias a mis padres, Mauricio y María Augusta por dejarme soñar, por ser mi inspiración, mi soporte, porque muchas veces me pusieron sobre sus hombros para que pudiera ver más lejos y hacer de mí la mujer que soy. Gracias a mis compañeros de vida, Francisco y Camila, por darle color a mis días y ser mis cómplices en tantas aventuras. Gracias a mis abuelos, en especial a Humberto por su apoyo incondicional y a Magdalena porque una parte de mí siempre estará con ella. Gracias infinitas a mis padres espirituales Galo y Gladys por ser tan incondicionales y ser parte de este proceso. A toda mi familia, gracias infinitas, tenerlos en mi vida me ha permitido convertirme en quien soy.

Gracias a cada uno de mis amigos que se convirtieron en mi segunda familia, haberlos encontrado ha hecho que cada segundo de este viaje sea maravilloso. Gracias por dibujar tantas sonrisas, por celebrar mis triunfos como si fueran suyos, por el apoyo incondicional, porque supieron abrazarme con el alma cuando más lo necesitaba y por ser ese paraguas en los días de lluvia. Dicen que hay personas mágicas escondidas por los rincones del planeta y ustedes Diana, Jefferson, Mario, Romina, Emilia, Anthony, William, Melanye, Mateo, Evelyn, Rafael y Rossmery encajan perfectamente. Los tengo a todos en mi corazón.

Un agradecimiento especial a quién me enseñó que los genios no son buenos para todo, pero saben sacar lo mejor hasta en circunstancias completamente adversas y que el trabajo duro recompensa más que el talento. Gracias Michael por apoyarme, por enseñarme tanto, pero sobre todo por hacer brillar a mi corazón.

Nadie ha dicho que un ave que emprenda vuelo y abra sus pequeñas alas completamente a lo desconocido, ha de regresar con las manos vacías. Esta etapa me ha llenado de experiencias, miles de sueños y razones para disfrutar cada detalle. A todas las personas que me acompañaron en este proceso, este logro es tan suyo como mío. Simplemente, profundamente y repetidamente gracias por su apoyo incondicional.

Con mucho cariño,

María Gabriela Pineda Molina

RESUMEN

El desarrollo de compuestos de fibras de carbono a partir de precursores de biomasa ha estimulado el interés de los científicos debido a sus propiedades físicas y químicas únicas, pero sobre todo por su biodegradabilidad, disponibilidad, peso ligero y bajo costo. Ecuador como uno de los mayores exportadores de banano del mundo, produce una gran cantidad de residuos agroindustriales. En el presente estudio, las fibras de carbono (CF) obtenidas del tallo del banano se tratan mediante un proceso de descomposición química inducido térmicamente, denominado pirólisis, donde la biomasa se convierte en sus constituyentes simples por acción del calor. En este sentido, con el fin de mejorar las interacciones de las CF y agregar funcionalidades suplementarias para aplicaciones biomédicas, las CF se funcionalizan con nanopartículas de óxido de ceria (CeO_2) a concentraciones de 3.57 mM y 7.14 mM generando y/o uniendo grupos funcionales a la superficie. Con la finalidad de realizar un análisis cuantitativo y cualitativo a nivel superficial se utilizan dos técnicas de caracterización. La microscopía electrónica de barrido (SEM) se aplica para dilucidar la morfología de la superficie, el tamaño de las partículas y su distribución así como la información cuantitativa sobre los diámetros de las fibras. Con este análisis, se registra un promedio de $1.35 \mu\text{m}$ para el diámetro de la fibra y los tamaños de las partículas se encuentran entre 0 y 200 nm. Además, según la concentración, se puede evidenciar diferentes tamaños en las aglomeraciones y la distribución de las partículas a lo largo de la fibra de carbono. Por otro lado, la técnica de caracterización de espectroscopia Raman apoya la interpretación de la información estructural, las interacciones de los grupos funcionales y los enlaces químicos. El análisis de deconvolución de los datos obtenidos presenta cinco contribuciones (bandas D1, D2, D3, D4 y G) mismas que exhiben una estructura desordenada o amorfa. Finalmente, según la relación de intensidad máxima (I_D/I_G) se confirma la presencia de nanopartículas de (CeO_2) a lo largo de las fibras de carbono.

Palabras clave: Fibras de carbono, nanopartículas de óxido de ceria, Microscopía electrónica de barrido (SEM), Espectroscopía Raman.

ABSTRACT

The development of carbon fibers composites from biomass precursors have stimulated the interest of scientists due to their unique physical and chemical properties but above all by their biodegradability, availability, lightweight and low cost. Ecuador, as one of the largest exporters of bananas in the world, produces a large amount of agro-industrial waste. In the present study, carbon fibers (CFs) obtained from banana stem are treated by thermally induced chemical decomposition process, denominated pyrolysis, where biomass is converted in its simple constituents by action of heat. In this regard, to enhance interactions of the CFs and add supplementary functionalities for biomedical applications, CFs are functionalized with cerium oxide nanoparticles (CeO_2) at concentrations of 3.57 mM and 7.14 mM generating and/or attaching functional groups to the surface. In order to perform a quantitative and qualitative analysis at the surface level, two characterization techniques are used. Scanning electron microscopy (SEM) is applied to elucidate surface morphology, particle size and distribution, as well as quantitative information about the diameters of the fibers. With this analysis, an average of $1.35 \mu\text{m}$ is registered for fiber diameter and the particle sizes between 0 to 200 nm. In addition, depending on the concentration, different sizes can be evidenced in the agglomerations and the distribution of the particles along the carbon structure. On the other hand, Raman spectroscopy characterization technique supports interpretation of structural information, interactions of functional groups and chemical bonds. The deconvolution analysis of obtained data presents five contributions (D1, D2, D3, D4 and G bands) that exhibit a disordered or amorphous structure. Finally, according to the maximum intensity ratio (I_D/I_G), the presence of nanoparticles of (CeO_2) along the carbon fibers is confirmed.

Keywords: Carbon fibers, Cerium oxide nanoparticles, Scanning electron microscopy (SEM), Raman spectroscopy.

Contents

List of Figures	x
List of Tables	xi
1 Theoretical Background	1
1.1 The era of Biomaterials	1
1.1.1 Biomaterials: A historical perspective	1
1.1.2 Biomaterials and Biocompatibility: Key Definitions	3
1.1.3 Biomaterials Classification	5
1.1.4 Properties of Biomaterials	6
1.1.5 Principal applications of biomaterials	8
1.1.6 Impact of Biomaterials and their relation with Bionanotechnology	10
1.2 State of the art of Carbon Fibers as Biomaterials	12
1.2.1 Carbon fibers: an approach	13
1.2.2 Application of carbon fibers as biomaterials in biomedicine	15
1.2.3 Synthesis of carbon fibers derived from biobased precursors	17
1.3 Pyrolyzation as thermal decomposition process	18
1.3.1 Types of pyrolysis	20
1.3.2 Pyrolysis applied for Cellulose-based Carbon Fibers	21
1.4 Cerium oxide nanoparticles	22
1.4.1 Physicochemical and Biological properties	22
1.4.2 Synthesis and Characterization alternatives	23
1.4.3 Biomedical applications	24
2 Introduction	27
2.1 Problem Statement	28
2.2 Motivation and Research Objectives	29
2.2.1 General Objective	29
2.2.2 Specific Objectives	29
3 Methodology	31
3.1 Synthesis of carbon fibers functionalized with (CeO ₂) NPs	31
3.1.1 Recollection and Pyrolysis of carbon fibers	31
3.1.2 Synthesis of Ceria (CeO ₂) nanoparticles	33
3.1.3 Decorating carbon fibers with (CeO ₂) NPs	34
3.2 Fundamentals of Characterization Techniques	35
3.2.1 Surface analysis	35

3.2.2	Scanning Electron Microscopy (SEM)	36
3.2.3	Raman Spectroscopy	39
4	Results and Discussion	45
4.1	Scanning Electron Microscopy (SEM)	45
4.1.1	Pristine CFs	46
4.1.2	Carbon Fibers decorated with (CeO ₂) NPs	46
4.2	Raman Spectroscopy	51
4.2.1	Pristine CFs	52
4.2.2	Carbon Fibers decorated with (CeO ₂) NPs	53
5	Conclusions and Outlook	61
	Bibliography	63
	Abbreviations	75

List of Figures

1.1	Principal Classification of biomaterials	7
1.2	Diagram illustrating the top-down and bottom-up approaches for nanoparticle synthesis . .	12
1.3	Schematic representation of principal precursors of CFs and their representative carbon structure	18
1.4	Crystal structure for ceria nanoparticles	23
1.5	Potential biomedical applications of cerium oxide nanoparticles	25
3.1	Banana fibers characteristics before and after pyrolysis	32
3.2	Tubular Furnace, OTF-1200X at Yachay Tech University, Ecuador	32
3.3	Heating ramp for batch of raw banana carbon fibers	33
3.4	Dispersions at 7.1369 and 3.5684 mM nanoparticles concentration	34
3.5	Schematic diagram of the principal components of an SEM microscope	38
3.6	Phenom-ProX model scanning electron microscope (SEM)	39
3.7	Schematic representation of the Rayleigh and Raman scattering processes	41
3.8	Schematic diagram of experimental set-up for Raman Spectroscopy	42
3.9	LabRam HR Evolution microscope	43
4.1	Morphological characteristics of pristine CFs obtained from banana stem	46
4.2	Characteristics of banana CFs decorated with (CeO ₂) NPs at 3.57mM	48
4.3	Characteristics surface morphology of banana CFs decorated with (CeO ₂) NPs at 7.14 mM	50
4.4	Raman spectra of banana CFs decorated with(CeO ₂) NPs at 3.57 and 7.14mM	51
4.5	Raman spectroscopy of Pristine carbon fibers and proposed deconvolution	54
4.6	Raman spectroscopy and proposed deconvolution for decorated carbon fibers at 3.57 mM .	55
4.7	Raman spectroscopy and proposed deconvolution for decorated carbon fibers at 7.14 mM .	56
4.8	Raman spectroscopy of ceria contribution with proposed deconvolution for decorated carbon fibers at 3.57 and 7.14 mM	59

List of Tables

1.1	Key Applications of Biomaterials in the field of medicine and health	8
1.2	Principal characteristics and clinical applications of carbon fiber composite biomaterials. .	16
1.3	Characteristics of Pyrolysis Processes based on their main operating parameters	20
3.1	Pyrolysis treatment and heating ramp parameters for batch of raw banana carbon fibers. . .	33
4.1	Fitted parameters for D4, D3, D2, D1 and G bands.	52
4.2	Summarized Fitted parameters for D4, D3, D2, D1 and G bands of decorated carbon fibers at both concentrations 3.57 and 7.14 mM.	53
4.3	Fitted parameters for cerium oxide contribution at 3.57 and 7.14 mM.	57
4.4	Comparative intensity ratio for Pristine CFs and decorated CFs at 3.57 and 7.14 mM. . . .	58

Chapter 1

Theoretical Background

1.1 The era of Biomaterials

1.1.1 Biomaterials: A historical perspective

The history of biomaterials dates back to antiquity. Many of the early thrusts were attempts by man to repair abnormalities, as surgical techniques were restricted to the body surface in the days before anesthesia and asepsis. For dental applications, gold was utilized by the Aztecs, Romans and Chinese since the beginning of civilization¹. Dental implants made of sea shells were discovered by the Mayans, with findings showing real bone integration¹. With the evolution of human civilization, the field of biomaterials evolved involving different materials at multiple length scales from nano- to micro- to macro level with a simple focus to improve quality and extend human life². Over 1000 years back, silver in different forms was used as an antimicrobial agent to prevent infections. During early stages of civilization, different types of surgical procedures were also found. However, the most significant developments took place in the field of biomaterials over the years 1901–2000 were artificial joints, which improved the quality of life for millions of people over the past 60 years, resorbable sutures to simplify surgical procedures, and many cardiovascular devices saved millions of lives, just to name a few¹.

Biomaterials as we know them now did not exist just over 70 years ago, even less the term “biomaterial”. There were no manufacturers of sophisticated medical devices, except those dedicated to external prosthetics such as limbs, dental and fracture fixation devices, glass eyes and fairly rustic fillings, there were no regulatory approval processes, biocompatibility studies, or academic courses on biomaterials²¹. However, crude biomaterials have been utilized in the past, with typically poor to mixed outcomes, for that reason it is convenient to organize the history of biomaterials in its four most representative eras, which include prehistory, the era of the surgeon-hero, the era of designed biomaterials or those engineering devices, and finally the contemporary era that leads us into the new millennium. The last era is positioning the limits of science today by tissue engineering and organ regeneration, making the years 2001–2100 in the field of biomaterials increasingly interesting¹.

Throughout history, non-biological elements have been introduced into the human body. One example could be the remains of a human, dated to be 9000 years old, which present a spear point embedded in his hip. This unintended implant illustrates the body’s capacity to deal with implanted foreign materials. Another example is the tattoo, as a technique of the introduction of foreign material into the skin, dated at over 5000 years ago¹. Also, according to one of the first surgical textbooks dated around 600 BC, the earliest documented record of skin-graft methods include a technique for repairing damaged earlobes

with cheek skin and reconstructing the nose from a flap of forehead skin³. In terms of dental implants Mayan people fashioned nacre teeth from sea shells in roughly 600 AD¹. Similarly, a wrought iron dental implant discovered in a corpse in France was dated to the year 200 AD⁴. With the aforementioned, two important points to consider beyond success and longevity is the adaptive nature of the body and the need to restore some of the lost functions of certain physiological and / or anatomical parts with an implant.

Another of the most successful approaches are artificial hearts and organ perfusion. In the fourth century BC, Aristotle named the heart as the most important organ in the body, highlighting the importance of its study. Some years later, in 1628 the doctor William Harvey adopted a relatively modern view of the function of the heart as a pump, which became a logical idea of thinking as a pump that could replace the heart artificially¹. This is how a large number of experiments on perfusion of organs with pumps were carried out from 1828 to 1868⁵. One of the key events in the history of artificial organs was the publication of the book called "The Culture of Organs" in 1983, where Charles Lindbergh and Alexis Carrel (Nobel prize) addressed questions about the design, sterility, blood damage, nutritional needs of the perfused organs and the mechanics of the pump, also known as the Lindbergh pump. Leaving a precedent that would lead Dr. Paul Winchell to patent the first artificial heart in the mid-1950s and Dr. Willem Joff and his entire team of scientists tested it on animals seven years later¹.

During World War I, particularly at the end, the high performance of ceramic, metal and especially polymeric materials that were developed in this period, transitioned from restricted to have high availability⁶. For this reason, the possibilities for using these inert and durable materials grew exponentially in health areas due to the need to replace damaged or diseased parts of the body. The materials that were originally manufactured for airplanes, clocks, automobiles and radios, were taken by surgeons and applied to solve medical problems. Among these early biomaterials included polyurethanes, silicones, teflon⁷, methacrylates, nylon, stainless steel, and titanium¹.

All of this historical context help us to understand the trajectory and contribution of biomaterials, especially after World War II when doctors and dentists left a precedent for collaboration between health professionals with scientists and engineers. In this period, many materials were tested, some were successful while others fortuitously succeeded. In most cases, these were high-risk trials conducted where other options were not available. At this point, the term "surgeon-hero" makes sense, since surgeons had the responsibility of preserving the lives of thousands of people but had to make sure to provide them a true quality of life, based on it they found necessary to give a great technological and professional leap¹.

In this way, advances in the area of biomaterials led to crucial scientific and engineering contributions, marking a real change in decision-making before implementing new procedures, as well as different government regulations regarding quality control. Thus, thanks to the growing collaboration between the different areas of science with public and private entities important applications of biomaterials have been developed for medical purposes such as intraocular lenses, hip and knee prostheses, vascular grafts, stents, pacemakers, heart valves, breast and dental implants, artificial organs such as kidney and heart and several medical devices for drug delivery and controlled release⁷.

In the 1960s, the field of biomaterials was establishing its principles regarding cell surface receptors, growth factors, cell attachment proteins, control at the nuclear level for the expression of proteins and phenotypes, gene delivery and stem cells⁶. This is how the community of scientists and researchers receive irrefutable credit for exploiting and embracing new ideas from biology and materials science, giving rise to multiple manufacturing techniques and surface analysis that are part of the toolbox that is used and adopted in the field of biomaterials. Thus, in the Modern Era, biomaterials have evolved by leaps and bounds due

to scientific advances but also to rapid developments in research and technology. Boundaries in the field of medical devices and many other areas continue to be expanded with the study and incorporation of first-generation materials concepts with later-generation approaches¹.

The base of ideas and materials developed for the biomaterials field was built by creative and committed individuals, so it is undoubtedly important to look at this base to understand many of the common trends, attitudes and several factors related to materials that have led us to those that we actually have. So, the main approaches to biomaterials science include therapeutics and diagnostics involving basic science, engineering, and medicine. However, translation of biomaterials to medical devices depends on clinical realities, in-vitro tests performed on both animals and humans, robust engineering-based designs, and the involvement of the industry involved in manufacturing and commercialization¹.

1.1.2 Biomaterials and Biocompatibility: Key Definitions

The words "biomaterial" and "biocompatibility" have been used in the previous paragraphs without giving a formal definition, below are some definitions adopted during the last years. One of the definitions most supported by experts in the field is:

"A biomaterial is a nonviable material used in a medical device, intended to interact with biological systems".⁸

Analyzing the previous definition, when "medical" term is used it is mainly limited to applications that can be therapeutic or diagnostic in the health area. However, by eliminating this word, the definition becomes broader and can cover a wide variety of applications of biomaterials, as has been evidenced in recent years. Additionally, by using the term "nonviable" the definition is limited to non-living cells, however, in recent years new technologies have been used to develop hybrid artificial organs and the benefits of tissue engineering that make use of living cells⁹.

Another of the concepts adopted by David Williams to define a biomaterial according to the National Institute of Biomedical Imaging and Bioengineering (NIBIB) is given by the following expression:

"Any matter, surface, or construct that interacts with biological systems".¹⁰

However, it does not specify medical applications and is imprecise for the context being used. The following is another of the definitions suggested by Williams in 1999, which lost validity as it was considered too cumbersome and due to its similarity to the definition adopted by the Food and Drug Administration (FDA) that emphasized into very specific applications:

"A material intended to interface with biological systems to evaluate, treat, augment or replace any tissue, organ, or function of the body".¹¹

Another valid option published by Williams in 2009, in one of his essays on the nature of biomaterials, was given as follows:

"A substance that has been engineered to take a form which, alone or part of a complex system, is used to direct, by control of interactions with components of living systems, the course of any therapeutic or diagnostic procedure, in human or veterinary medicine".⁹

It refers to both human and veterinary applications, where the last one was relevant due to the number of clinical trials involving animals. However, the importance of including the veterinary aspect to define a biomaterial continues in endless debate. Given the foregoing arguments, David Williams recommended that the more succinct derivative of the last definition should be used for consensus voting¹. As a result, the suggested definition of “Biomaterial” was as follows:

“A substance that has been engineered to take a form which can direct, by control of interactions with living systems, the course of any therapeutic or diagnostic procedure”.⁹

After some minor grammatical alterations and slightly better wording, the definition for a biomaterial is as follows:

“A substance that has been engineered to take a form which can direct, by control of interactions with living systems, the course of any therapeutic or diagnostic procedure”.⁹

Over the years the definitions have been acquiring more specificity depending on the area of application. The most widely accepted definition of biomaterial is the one adopted by the American National Institutes of Health (NIH), which defines it as follows:

“any substance or combination of substances, other than drugs, synthetic or natural in origin, which can be used for any period of time, which augments or replaces partially or totally any tissue, organ or function of the body, in order to maintain or improve the quality of life of the individual”.¹²

However, the majority of biomaterials (that fulfill the particular biocompatibility criteria) cause a non-specific biological reaction known as the foreign-body reaction⁹. This leads to a commonly used definition of biocompatibility.

“Biocompatibility is the ability of a material to perform with an appropriate host response⁸ in a specific application”.¹³

This definition has been adapted from the European Society of Biomaterials (ESB), it is used and will be used internationally by regulatory agencies and experts working in the field of biomaterials. In this sense, a biomaterial is considered biocompatible if it is friendly to the biological system or in other words, it must not cause any type of damage either at the cellular or system level. Therefore, any material that is biocompatible must elicit an appropriate response from the host and perform its intended function without presenting any type of adverse reactions¹⁴.

With everything mentioned above, then a biomaterial can be defined as any systemically, pharmacologically inactive substance or combination of substances used for implantation within or integration with a biological system to augment or replace functions of live tissues or organs⁷. In order to do this, a biomaterial must be in contact with live tissues or bodily fluids, resulting in a living-nonliving interface. Also, many authors define a biomaterial as a material, synthetic or natural, that can be used in medical applications to perform a body function or replace a body part or tissue². For that, a biomaterial is intended to interact at the interface of biological systems or also it could be used as a delivery system for drug or biological factors.

1.1.3 Biomaterials Classification

Once the broad meaning of biomaterials has been defined, it is necessary to recognize that there are a great variety. Biomaterials are classified depending on their crystalline structure, bonds, macrostructures², atomic and molecular interactions, biomaterials-tissue responses among other aspects that give it certain physical and chemical properties¹ that allow their categorization. Each subgroup of biomaterials is organized based on certain properties that show evidence of some kind of similarity and in this way they can be studied as a set for different applications.

Depending on the characteristics these present due to their crystalline structure, bonds and macrostructures, biomaterials can be classified into: metals, polymers, ceramics and composites.

Metals

Metals are materials that have a crystalline structure and are held together by metallic bonds. These possess several qualities that are unique such as the ability to conduct heat and electricity, they have low ionization energy and electronegativity, that is, they are prone to give up electrons to form cations. This last quality is due to the availability of free electrons when forming metallic bonds. This is how all these characteristics make them malleable, ductile and with a lustrous or shiny appearance². But above all the aforementioned characteristics, metals are used for their mechanical strength which is necessary to guarantee mechanical stability in the early stages of fracture healing¹¹. In general, metals are necessary for the design and manufacture of many medical devices because they have the required mechanical properties that no other biomaterial can replicate¹.

Polymers

Polymers are materials that consist of long carbon chains formed by a large number of smaller units, called monomers, which are principally linked by covalent bonds with other secondary bonding². Due to the versatility with which they are joined, polymers can be linear, branched or networks, which makes them in the broadest category of materials used in medicine for their ability to adapt for specific molecular architecture, molecular mass and chemical composition¹. Furthermore, due to the presence of covalent bonds, most polymers have low conductivity and can present multiple structures depending on their crystalline structure², the distribution and composition of the monomers¹.

Ceramics

Ceramics are generally opaque, solid, inorganic and non-metallic materials formed by metallic, non-metallic or metalloid atoms that are mainly linked by ionic and / or covalent bonds². They can have crystalline, semi-crystalline or non-crystalline atomic structures and, with the exception of glass, ceramics do not have a glass transition behavior. Since ionic and covalent bonds do not have the ability to leave free electrons, ceramics cannot conduct heat or electricity¹. However, there are some types that show conductivity as the temperature increases due to the movements of the defects¹⁵. Ceramics are utilized to replace, repair, or regenerate skeletal system, joints, teeth or comprising bone because it contains a variety of hard inorganic components¹. Most clinical applications of bioceramics relate to the repair of the skeletal system, comprising bone, joints and teeth, and to augment both hard and soft tissue¹⁶.

Composites

Composites are materials that have two or more different phases or materials (mainly metals, ceramics and polymers) in their minimal structure¹¹, which maintain their inherent characteristics on a microscopic or macroscopic size scale².

In addition, if a focus is made on the unit cell or the basic building unit of the biomaterial, they can be classified into three groups: crystalline, semi-crystalline and amorphous. Basically, if the unit cell of the material is repeated in all direction axes and they maintain a wide range of order, they are called crystalline. In contrast, there are many materials where the unit cell or minimum unit does not repeat in all directions and has a minimum order range; these are called amorphous or vitreous. In general, these glass-like materials have a glass transition temperature (T_g), which is a range for which certain material that is in the liquid phase transforms to a more rubbery-solid phase¹. Finally, those materials that share both glassy and crystalline characteristics in their configuration are known as semi-crystalline².

On the other hand, if the convergence for classification is made based on the source from which certain materials come, they are classified in natural materials for those which are available in nature such as rocks, wood, corals or bones; and are denominated synthetics, to those that are designed by humans for certain functionality generally improving certain characteristics². Besides, taking into account the macrostructure or, in other words, the structure at the macroscopic level (*greater than 1000 nm*), biomaterials can be classified according to their porosity as porous or dense biomaterials², or give them broader classifications depending on the surface coatings and internal or external microcracks¹⁷.

Depending on the responses between biomaterials and tissue, or vice versa these can be classified into four different subgroups as follows: bioinert, toxic, bioactive and bioresorbable. Any nontoxic substance that, once implanted in the human body, has minimal interaction with the surrounding tissue is referred to as bioinert. Toxic materials are substances that may cause death to surrounding tissue if it is placed or enters into the body. A material that is nontoxic but is capable of inducing a specific response that triggers the formation of a bond between the tissue and the material due to the biological interaction between the parts is called bioactive. Bioresorbable is the term used to describe a nontoxic material that upon placement within the body dissolves (resorbed) and slowly replaces in vivo tissue². In Figure 1.1 is illustrated schematically the main classification of biomaterials, it is important to note that any type of biomaterial can fit into several of these categories.

The relative significance of the different characteristics that are necessary for the intended medical application widely influences the selection or design of a specific biomaterial. All mentioned before, has direct consequences on the roadmap of biomaterials that includes the development, testing, clinical applications and translational research phases. Therefore, the selection criteria of a biomaterial is based mainly on most of the characteristics mentioned below, such as non-toxicity, biocompatibility, availability, faculty to be processed in the desired form, mechanical properties, cost effectiveness, if it has the ability to be sterilized under certain procedures, stability, degradability, among others.

1.1.4 Properties of Biomaterials

Experts in the field of biomaterials should have a good appreciation for materials science that includes the use of metals, ceramics, polymers, composites, and biological materials. This can be influenced by

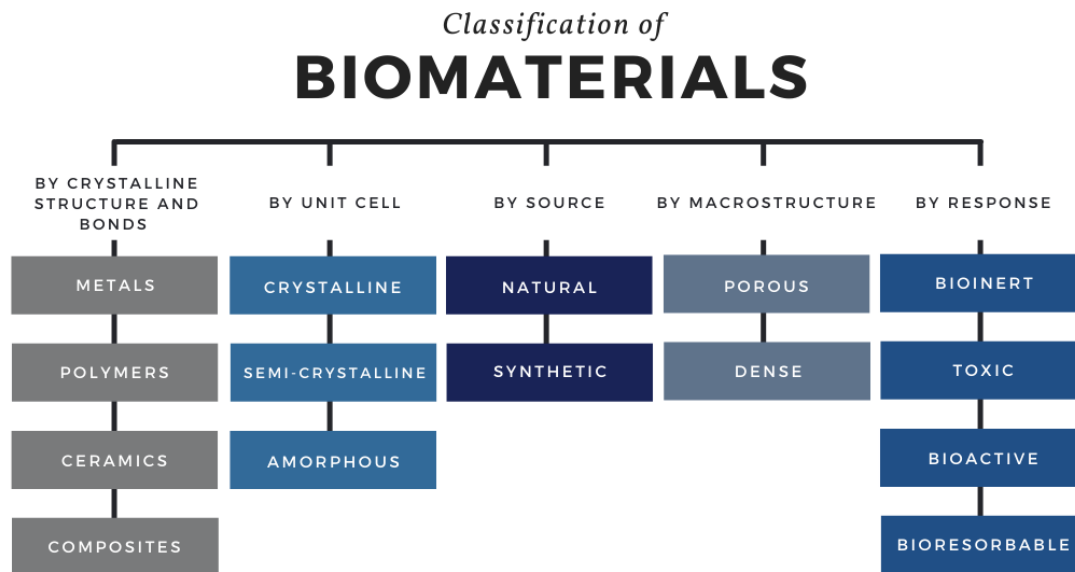


Figure 1.1: Principal Classification of biomaterials

the domain of the theoretical part and the practice especially by the understanding of the properties of biomaterials. Depending on the application to be given to a biomaterial, suitable combinations of specific properties will be sought in order to adequately satisfy the design needs for the medical device under manufacturing and development. Among various properties that are assigned to biomaterials, the most important are chemical, physical, mechanical and biological that are directly related to their properties both at the surface level and in bulk.

Chemical properties

Chemical properties describe the "potential" of materials to undergo some change in their chemical composition, the bonds and the structures that compose them at the atomic level, as well as the type of reaction that they can present under specific conditions of the environment in which they find. Thus, the acidity or basicity, electronegativity, reactivity¹⁸, ability to degrade and resistance to corrosion¹⁹ of a biomaterial are chemical properties that are determined by information about its atomic structure.

Physical properties

Physical properties refer to those characteristics that can be observed or measured without altering the composition of the materials, they are generally used to describe the materials depending on the size and extension¹⁵. Thus, physical properties refer to density, color, conductivity¹⁵, malleability, microstructures¹⁸, phases, different types of porosity²⁰, among other qualities that can be evidenced in a biomaterial.

Mechanical properties

Mechanical properties are concerned with quantifying and describing those physical properties that a material exhibits after the application of forces. Among the most studied mechanical properties are toughness, tensile strength², hardness, modulus of elasticity, elongation, fatigue limit²⁰, among others that biomaterials can present.

Biological properties

Biological properties are those characteristics that define the behavior of biomaterials under certain conditions of a biological environment². Depending on the biological environment, it is in-vitro if an environment is recreated in a closed environment, usually a petri dish⁷. On the other hand, they are called in-vivo properties if the characteristics are measured from the reactions that the material can trigger within an animal or human body⁷. With the study of biological properties, relevant characteristics such as biocompatibility, bioinertness and biofunctionality of biomaterials can be determined¹⁵.

Surface properties

Surface properties of the biomaterials can be determined in the outermost layer of a material where not all the interactions and bonds are completed and there are many dangling bonds that can present qualities very different from the inherent properties of the bulk material⁷.

1.1.5 Principal applications of biomaterials

Biomaterials are applied in multiple fields such as medicine, pharmaceutical industry, food and textile industry, technology development, environmental remediation and many other applications that have significantly transformed the quality of life of human beings. On the field of Biomedicine, biomaterials are one of the areas of greatest interest due to their diverse application in the manufacture of implants, implements to improve drug delivery, prostheses, medical devices, artificial organs, as well as in the regenerative medicine field with the use of specific scaffolds.

The selection of biomaterials depends on the use to be given, for example, if they need to be applied to the dental and orthopedic area, they must meet certain conditions of stability, hardness, mechanical strength, prolonged degradation periods, biocompatibility, even at an aesthetic level. Below, Table 1.1 presents some applications of modified synthetic and natural biomaterials in the medical and health area.

Table 1.1: Key Biomaterials applied in Medicine and Health

APPLICATION	BIOMATERIAL USED
SKELETAL SYSTEM	
Joint replacements for hip, knee and shoulder	Alumina, Zirconia, Ti pure and coated with ceramic alloys, Cobalt-Chromium, Polyethylene ¹ , Teflon or PTFE, Glass UHMW-PE ⁷ , Steel, Ti and Co-Cr alloys, Aluminium oxide

Devices used for trauma fixation (screws, pins, plates, and rods)	Cobalt-Chromium, Titanium, Ni-Ti, Stainless steel ¹ , Polyetheretherketone (PEEKs), poly(lactic acid) (PLA) ²¹ , Polyaryletherketones (PAEKs)
Intervertebral disc regeneration and repair	Titanium, Nitinol ²² , Polyether ether ketone, Stainless steel, Alginate, Agarose, Gelatin, Collagen ²³
Bone disease or defect repairment	Calcium phosphates and sulfates, Bone products from human samples ¹ , Bioactive glass, Hydroxyapatite (HA) ²⁴
Bone cement employed for fixation	Glass polyalkenoate, Polymethyl methacrylate (PMMA), Calcium phosphate cements ¹
Tendon, cartilage, or ligament repair and replacement	Decellularized porcine tissue, Collagen ²³ , Hyaluronic Acid lubricants, Poly(lactide) and metallic fixation devices
Tooth fixation or dental implant	Titanium (Ti) and its alloys (mainly Ti-6Al-4V) ⁷ , Zirconium, Au alloys, Stainless steel, Chromium alloys with Co and Ti ⁷ .
CIRCULATORY OR CARDIOVASCULAR SYSTEM	
Vascular and stent grafts, patches	Nitinol ²⁵ , Cobalt-chromium, Stainless steel, Dacron, expanded poly(tetrafluoroethylene) ²⁶ , treated tissue
Heart valves	Cobalt-chromium, fixed bovine and porcine tissue, Dacron, Carbon based, stainless steel, Nitinol ²²
Pacemakers	Titanium and polyurethane (PU) ¹
Implantable defibrillators	Titanium and polyurethane (PU) ¹
Stents for coronary, peripheral vasculature and nonvascular	Stainless steel, Nitinol ²⁵ , Cobalt-chromium, Pt, tantalum, Mg alloys, poly(styrene-b-isobutylene-b-styrene), poly(n-butyl methacrylate), polyethylene-co-vinyl acetate ¹ , phosphoryl choline containing block copolymers, poly(lactic-co-glycolic acid), PLA ²¹
Catheters: cardiovascular, urologic, and others	Polytetrafluoroethylene (PTFE) ²⁶ , poly(vinyl chloride), silicone, polyurethane ¹
Cardiac assist devices	Titanium alloy, stainless steel, polycarbonate, PTFE, poly(ethylene terephthalate)
Blood oxygenator	Polycarbonate, polymethylpentene, polypropylene, polysiloxane, poly(vinyl chloride)
Blood bags	Poly(vinyl chloride) and antimicrobial coatings
ORGANS	
Hemodialysis	Silicone, polyvinyl chloride, Polysulfone ¹ , modified cellulose, polyacrylonitrile, polycarbonate ²⁶
Skin substitute for wounds and burns	Collagen ²³ , alginate, cadaver skin, carboxymethylcellulose, polyurethane, nylon, silicone
OPHTHALMOLOGIC	

Contact lens	PMMA, silicone (polydimethylsiloxane [PDMS]) ²⁷ , polyhydroxyethylmethacrylate (PHEMA) ²⁶ , polyvinyl alcohol, polyvinyl pyrrolidone ¹
Intraocular lens	PDMS ²⁷ , polyacrylate-PMMA, PHEMA, PMMA ²⁶
Glaucoma drains	Cross-linked collagen ²³ , stainless steel, silicone, polypropylene
DRUG DELIVERY SYSTEMS (DDS)	
Oral	Silk, fibrin, Polylactic acid (PLA) ²¹
Ocular	Hyaluronic acid, Silicone ²⁶
Pulmonary	Poly(lactide-co-glycolide) (PLGA), poluvinylpyrrolidone (PVP) ²⁶ , Nanopolymeric particles consisting of (HPMC)
Implantable	Silk fibrin, Hydroxyapatite (HA) ²⁴
Systemic	Cholesterol-modified poly(ethylene glycol)-polylactide, Lyophilized lettuce cells (ACE2/ANG-(1-7)) ²⁸
Vaginal	Palm oil and hyaluronic acid, Silicone matrix polymer
Topical	Polylactic acid ²¹ , collagen, polyvinyl alcohol, carbopol
OTHER	
Cochlear prostheses	Titanium, aluminum oxide ¹ , platinum, platinum-iridium, PDMS ²⁷
Breast implants	Polydimethylsiloxane (PDMS) ²⁷
Hernia and body wall repair meshes	Polypropylene, polyester, expanded PTFE, decellularized porcine/bovine tissue ¹
Sutures	Silk, nylon, polyester copolymers ²⁶ , poly(glycolic acid), PLA ²¹ , polydioxanone, polypropylene, PTFE, processed bovine tissue
Tympanostomy	Silicone, PTFE ¹
Intrauterine device	Stainless steel, PDMS, copper polyethylene ²⁹

1.1.6 Impact of Biomaterials and their relation with Bionanotechnology

Throughout the previous few decades, the increasing relevance of biomaterials in our society may be seen from a variety of approaches, including the advance of biomaterials as an academic field and a significant industry. The extraordinary ability to convert biological activity into synthetic materials including the development of technologies, mainly for the research and manufacture of biomaterials, made them one of the science and research areas with the greatest interest in recent decades. Biomaterials is one of the major fields of study in the United States with approximately 16,000 enrolled students until 2005 in more than 75 biomedical engineering departments³⁰. As a result, in recent years, the number of medical devices, gene transfer, tissue engineering, biotechnology and drug delivery alternatives developed in order to improve the quality of human life has grown exponentially. In the last few years, it has been clear that a common theme about the influence of structural properties of biomaterials at the nanoscale has run across a lot of publications published in these sections³¹

Biomaterials is undergoing a revolutionary shift, with biological sciences taking equivalent precedence over materials science and engineering. Simultaneously, advances in Nanotechnology have considerably increased the sophistication with which biomaterials are designed allowing the fabrication of biomaterials with more complex functionalities³⁰. This is the case of Bionanotechnology, which emerged as an extraordinary fusion between Biotechnology and Nanotechnology, debuting as a young subdiscipline of nanotechnology where biological interactions are the basis for inspiring and creating solutions. To elucidate, nanotechnology or perhaps more precisely the nanotechnologies, refer to the knowledge and manipulation of engineering approaches at the nanoscale. The prefix nano- denotes a measure of 10^{-9} units, the nature of which is decided by the following word. Nonetheless, the extraordinary attributes of these materials are summarized in the properties they can offer unlike bulk material, which can be applied to positively influence the quality of life through advances in medicine and biotechnology³¹. As we know, Biotechnology is an interdisciplinary area where living organisms and biological systems use technology including the principles of chemistry and biology to design novel products³².

Despite the variety of bionanotechnology fields, they have one fundamental thing in common: the capacity to construct molecular machineries with atomic-scale accuracy or specifications³³. Bionanotechnology practice has much wider scope, it can be applied for biological self-assembly, bio-nanorobotics, medicine, pharmaceutical, agriculture, food, cosmetical, cosmeceutical and environmental alternatives. To emphasize, self-assembly combines the versatility of peptides, proteins, ribosome and DNA complexes to design geometrical nanostructures with customized morphologies as well as the creation of more stable complexes with preferred functionalities³². Bio-nanorobotics are able to actuate, sense, process information and provide automatic intelligence handling, for their adaptability, based on what occurs in nature, is principally used in space applications to map and sense planetary terrains, enhance health management and also for protection systems³⁴. Bionanotechnology is also applied in electronics, biosensors and among several other applications³², as an example utilizing DNA oligomers, fibrils of protein, or peptide nanotubes can be create metal nanowires which can be interconnected with other physical components at the nanoscale³⁵.

To sum up, advances in biomaterials and bionanotechnology, above all in the health area, need the exceptional combination of more functional medical biomaterials including the understanding of biological complex and dynamic behaviours to assure the reproduction of functionalities and properties that are currently unavailable. The creation of smart and multifunctional biomaterials for usage in human bodies will most likely be focused on research in the new generation of bioinspired materials that fulfill fundamental inputs from chemical and physical stimuli. Surely this type of biomaterials will be applied in anatomical regions that allow real-time monitoring which can help to report and activate responses in the midst of biological crises³². For that, it is undoubtedly to ensure that future generations of biomaterials will be critical components in many applications that modern society demands.

1.2 State of the art of Carbon Fibers as Biomaterials

During the last few decades, biomaterials made up of nanomaterials have emerged as an alternative to many issues with potential applications in multidisciplinary science. Nanomaterials are materials with at least one external dimension that is smaller than 100 nanometers and their properties are substantially influenced by their size. For the manufacturing and synthesis of nanomaterials, the methodology is chosen depending on the properties, morphology and applications of each material. There are different approaches to synthesize nanomaterials, including the bottom-up and the top-down approaches (see Figure 1.2). A bulk material is trimmed down to the necessary NPs using various methods in the top-down approach, whereas NPs are generated at the atomic level and then integrated into the desired material in the bottom-up approach³⁶.

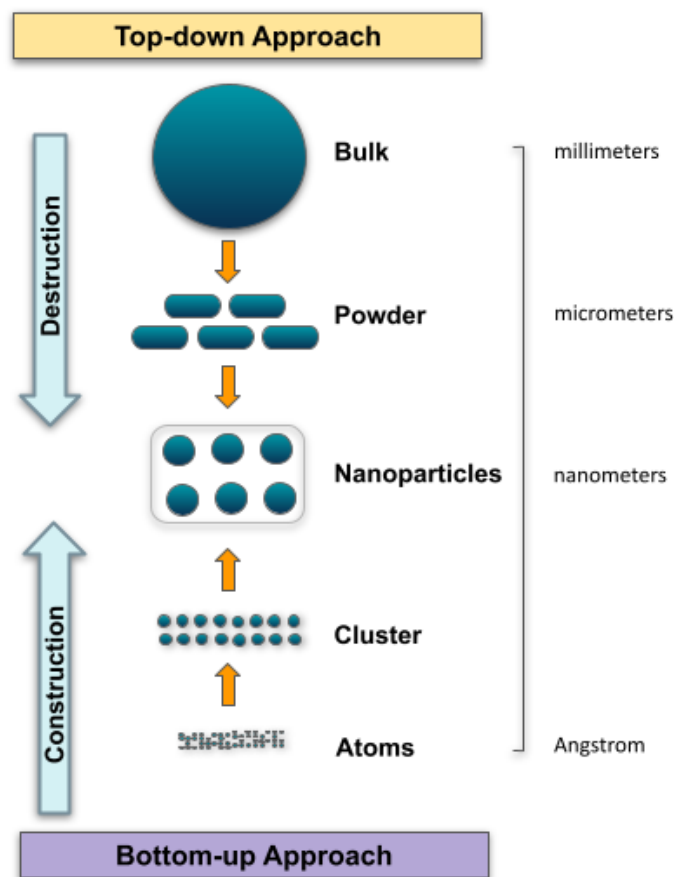


Figure 1.2: Diagram illustrating the top-down and bottom-up approaches for nanoparticle synthesis

In addition, nanomaterials are categorized as follows based on spatial dimensionality: as zero-dimensional (0D) nanomaterials for those that have all their dimensions in nanoscale (sized below

100 nm) where spherical, hollow sphere, nanorod, cube, polygon, metal, core-shell materials and also quantum dots are included³⁷. One-dimensional (1D) materials comprehend two dimensions at nanoscale and only one not, these materials include ceramic, metallic, polymeric, nanotubes, nanorod filament, nanofibers and nanowires³⁶. In addition, two-dimensional nanomaterials (2D) consist of one dimension in nanoscale while the other two are not. 2D incorporate single and multi layered materials, with crystalline or amorphous structure, and also thin films, patterned surfaces, nanocoating and nanoplates³⁷. On the other hand, three-dimensional (3D) materials are structures with many dimensions apart from 100 nm, these materials comprehend a combination of multiple nanocrystals in several directions e.g. polycrystals, pillars, fibers, foams, nanotubes, nanobuds, fullerenes, honeycombs and multiple designs of layer skeletons³⁶. For the above mentioned reasons, the surface area of nanoscale materials is intimately related to chemical reactivity and electrical properties. As well as their behavior is dominated by quantum theory which involves the optical, magnetic and electrical behavior.

1.2.1 Carbon fibers: an approach

According to their chemical composition, nanomaterials are divided into several groups, such as single constituent NPs and composites, under which are further types. Carbon-based nanomaterials are one of the main subdivisions; these materials have unique properties and play a crucial role in a variety of fields. Carbon is a solid-state allotrope that exists in a variety of shapes and sizes, including graphite, amorphous carbon, and diamond³⁸.

Following the previous definition, carbon fibers (CFs) are a 3D strand material of interconnected hexagonal carbon atoms, in most of cases present a diameter size between 1-10 μm . CFs can adopt forms like filaments, rovings, yams or tows that contain at least 92 percent by weight of carbon which is presented at non-graphitic state³⁹. Also, these materials can be crystalline, amorphous, or partially crystalline depending on the production conditions. The crystalline region resembles to graphite because the carbon atoms present a sp^2 hybridization and are bonded by covalent interactions forming a honey-comb lattice which constitute the graphene layer. The sp^2 hybridization of orbitals allows the overlapping and delocalization of π electrons in each graphene layer, similar to metallic bonding. In fact, the remarkable electrical and thermal conductivity of CFs is due to these hybridized π -bonds and, by using weak van der Waals interactions these graphene layers are layered parallel to one another. Nonetheless, flawless crystalline carbon in carbon fibers is difficult to obtain, and most carbon fibers have a turbostratic layer stack as their basic unit⁴⁰.

Carbon fibers have been categorized into the following classes based on parameters like the fiber structure and degree of crystallite orientation, as well as mechanical performance: Low elastic modulus type (LM), Standard elastic modulus type (HT), Intermediate-modulus (IM), High-modulus (HM) and Ultrahigh-modulus (UHM)⁴¹. Following the tensile elastic modulus, UHM and HM are the type of CFs with a high modulus (>350 GPa) while the IM and HT types are considered as high strength fibers but characterized by their low modulus due to the lower thermal treatment temperature ($\sim 1500 - 2000$ °C). Finally, but not least, LM is the CF subclass with lowest modulus (<100 GPa) due to their random crystallite orientation, also denominated as isotropic carbon fibers⁴⁰.

As expected, CFs are also classified according to their precursors such as poly(acrylonitrile) (PAN), pitch⁴², cellulose and lignin as well as those graphene and carbon nanotubes (CNTs) based CFs. Thus cellulosic, pitch and PAN precursors are the most popular for carbon fiber manufacturing while others precursors such as phenolic resins, poly(vinylidene chloride), and graphene have been investigated but do not easily reach the standards for large scale of manufacturing. Easy carbonization, a high carbon yield, and a simple fiber processing are all requirements for carbon fiber precursors. In most cases, CFs are manufactured by polymerization of the precursors, then drawing and solidifying a precursor polymer to form the fiber which is followed by thermal stabilization process, carbonization and finally graphitization (at very high temperatures) performed in vacuum conditions⁴⁰. The high-thermal process cause a violent vibration at molecular level and expel a great amount of non-carbon atoms i.e. carbonization¹.

According to historical background, Thomas A. Edison was the first one to use carbon fibers. Edison carbonized cotton threads into pure carbon fiber filament⁴³ for his incandescent light bulb tests in 1897. Years later, Roger Bacon designed the first high-performance carbon fibers⁴⁴ in the late 1950s. For manufacture process of carbon fibers, PAN was the first precursor recognized by Shindo in 1961 and still today it constitutes the most important precursor for CFs⁴⁰.

Nowadays, CFs were not commonly established in industrial applications by themselves, these were generally used to reinforce or give special function to materials composed mainly of plastic, ceramic, metal, and so on⁴². Carbon fibers are now being used extensively in the aerospace sector due to their unique qualities of being lighter and stronger than metal equivalents. However, depending on the properties which are directly related to the manufacturing process and the starting precursor, not all CFs are strong enough for the aerospace industry⁴⁰ but can be successfully applied for other purposes. A remarkable characteristic of CFs is their specific strength⁴⁵ and modulus which is roughly four times greater than steel⁴⁶. The applications of carbon fibers have diversified over time, they continue leading alternatives in the field of fibers due to their properties as their tensile strength, low densities, mechanical resistance, considerable thermal¹ and electrical conductivity but above all by their high thermal and chemical properties in order to maintain stability⁴⁰.

Carbon fibers (CFs) have received increasing attention because of their specific strength and stiffness, above all in the field of lightweight composites. Nonetheless, their high cost and dependency on fossil-based raw resources evidence the need for more cost-effective and renewable alternatives⁴⁷. As mentioned above, more than 96% of the commercial CFs for composite applications are made from PAN, an expensive fossil-based polymer. Only minor amounts are produced from petroleum and Rayon⁴⁸, a type of regenerated cellulose. PAN precursors are manufactured using spinning techniques in solution and then through a series of thermal processes such as oxidative stabilization (between 200 and 350 °C) and carbonization (greater than 1000 °C) are converted into CFs. In order to improve Young's modulus the CFs are graphitized at temperatures above 2000 °C, giving it a notable advantage with Young's modulus value greater than 350 GPa⁴⁷.

However, as a result of thermal treatments the toxic byproducts of the process accompanied by the amount of organic solvent with hazardous characteristics determines that CFs obtained from

PAN is not an eco-friendly procedure⁴⁶. Therefore, the expensive costs of manufacturing CFs, along with environmental concerns over PAN, is accelerating research into alternative bio-based precursors and green processing methods. With the motivation to develop cost-efficient and high availability alternatives based on renewable resources, lignin and cellulose are in growing interest as carbon fiber precursors⁴⁹. The relevance of recent studies are focused on the most abundant and renewable biomass constituents, cellulose and lignin to appropriately convert into precursor or carbon fibers. However, the major limitation that present this type of constituents are based on the maximum yield reached at large scale production, for example upon thermal decomposition of cellulose rarely is reached a 44.4% of carbon content⁵⁰. Likewise, lignin has a mass carbon yield of 55% which presents a thermoplastic nature compared with PAN and residence times above 100 hours⁵¹ which involve challenges in the melt spinning and higher production costs⁴⁹.

In addition to the aforementioned, CFs based on lignin and cellulose exhibit limited mechanical properties but, interestingly they may be used in other applications that do not require a tensile strength greater than 3 GPa⁵². As a result, interest in developing cellulose or lignin as precursors has resurfaced. Recently, some studies have shown that using 1,5-diazabicyclo[4.3.0]non-5-ene-1-ium acetate ([DBNH]OAc) for solvent-based spinning technique allows the continuous spin of cellulose and lignin filaments with considerable molecular orientation and improved mechanical properties⁵³. This resulted in a whole new approach to the use of lignin and cellulose as potential precursors because of their carbon-forming chemical structure and low cost. A great example is the new bio based hybrid precursor manufactured by blending cellulose with lignin and then dry-jet wet spun using [DBNH]OAc as the solvent for its qualities as an ionic solution. Thus, limitations of the separated constituents in terms of carbon fiber development can be overcome by appropriate combination of cellulose and lignin in a single hybrid composite⁴⁹.

1.2.2 Application of carbon fibers as biomaterials in biomedicine

Since the late 1970s, carbon fibers have been extensively utilized and also studied for their use as biomaterials. One of the most important benefits of carbon fibers, as biomaterials, are their mechanical properties (light weight, high strength, flexibility) but also they are easy to combine due to their variety of morphologies and radiolucency origin carbon fiber composites. In terms of biocompatibility, CFs present high affinity and considerable *in vivo* stability⁴². In order to take advantage of these characteristics, multiple studies of medical applications have been carried out, mainly focused on the reinforcement of pre-existing conventional biomaterials as well as the incorporation of carbon fibers for certain medical devices and orthopedic implants⁴², such as spinal fixation cages.

The vast majority of applications that have been registered are based on composites designed on the basis of biomaterials used regularly. Much research has been reported emphasizing the use of carbon fibers with other carbon materials, some polymers, and certain metals. The main objective of making these combinations is to reinforce the material, reduce its weight, high strength, fixation power, add flexibility, and so on. In Table 1.2 are mentioned some carbon fiber composites according to their secondary constituents. It is important to emphasize that

the most commonly used carbon composites in the medical area, specifically in orthopedics, are those that include polyether ether ketone (PEEK) in their composition⁴². As matter of fact, CFs can be braided with fibers of multiple polymers to develop artificial ligaments and tendons. As mentioned above, a common example are the CFs reinforced with PEEK or polysulfone (PSU) polymers to improve the stem of hip prostheses¹.

In addition, regenerative medicine for distinct tissues has experienced exponential growth during the last years. Depending on the technique or method, this field is directly related to cytokine therapy, cell and gene therapy, and many studies of these are applied separately or in combination⁵⁴. However, to achieve great regeneration performance in any of these techniques, effective scaffold material with specific properties that holds cells or cytokines at the local site and facilitates the regeneration of new tissue is required⁵⁵. In this way, CFs are good candidates for regenerative medicine, specifically in scaffolds⁴² because they exhibit two opposing properties in interaction with biological systems: bioinertness and bioactivity⁵⁶. CFs are denominated as a bioinertness biomaterials because they present a high strength like metals but they do not corrode in applications directed in-vivo, so this is favorable both for scaffolding and for any type of biomaterial.

On the other hand, in response to their location in the live organism, CFs can exhibit a variety of bioactivities. For example, for damaged bone tissue these areas are easily regenerated in presence of CFs and in-vitro studies have shown that surrounding osteoblasts are activated and present an improvement in their cell adhesion⁵⁶. However, it is now being investigated whether the bioactivity of CFs is caused by some surface properties, or structure, among many other factors that allow researching possible interactions of CFs with other tissues. Without a doubt, if these properties of carbon fibers can be successfully exploited, they will be extremely helpful as scaffolds in regenerative medicine.

Table 1.2: Principal characteristics and clinical applications of carbon fiber composite biomaterials.

Types of carbon fiber composite biomaterials	Base materials	Characteristics	Applications
Carbon Fiber + Carbon composite	Carbon	Light weight, high strength, chemical stability, durability, and good in-vivo and in-vitro, biocompatibility	Artificial joint ⁵⁷ , Middle ear implant, Plate ⁵⁸ and screws for fracture fixation, Maxillofacial implants ⁵⁹
Other carbon fiber composites	Co-Cr-Ni alloy	Good biocompatibility and mechanical properties	Aneurism clip ⁶⁰
	Hydroxyapatite (HA)	Good bone ingrowth	Artificial trachea ⁶¹
	Epoxy resin	Superior adhesive force, high dimensional stability, high resistance to water and chemicals	Fracture treatment plates, housing of pacemakers ⁶²

	Polyether ether ketone (PEEK)	Specific modulus similar to bone which avoids interface disruption and bone loss	Fracture fixation plates, femoral stem of hip joint prostheses ⁶³ , sliding parts of artificial joint and spinal fixation cages ¹
Carbon fiber + Polymer composite	Ultra high molecular weight polyethylene (UHMWPE or UHMW)	Not compatible with metallic surfaces, low adherence with polyethylene surface	Sliding parts of artificial joint, artificial hip and knee joints ⁶⁴
	Polyamide 12 (Nylon 12)	Good compatibility with the surrounding bones and high fixation between stem and bone	Femoral stem prostheses ⁶⁵
	Polysulfone	Light weight, high strength, good biocompatibility, and superior mechanical properties	Fracture treatment screws, Femoral stem prostheses ⁶⁶
	Polycarbonate polyurethane (PC-PU)	High flex fatigue	Artificial joint, catheters, general purpose tubing, hospital bedding, surgical drapes, wound dressings, short-term implants ⁶⁷
	Polymethyl methacrylate (PMMA)	Impact resistance and prolonged load-carrying ability	Replacement of neoplastic bone, tougher bone cement ⁶⁸
	Biodegradable polymer	Green synthesis and high biocompatibility	Scaffold for tendon repair ⁶⁹ , screws, pins, and rods and filler after a tooth extraction

1.2.3 Synthesis of carbon fibers derived from biobased precursors

According to Ogale et.al PAN the synthetic precursor is used to make the vast majority of high-performance commercial carbon fibers. However, employing bio-based precursors can help alleviate some of the environmental issues and related costs involved with this method. In this regard, cellulose and lignin are considered as potential biomass precursors because of their low cost and the ability to form carbon chemical structures. One the most abundant source of biomass is raw wood which is constituted of about 40-50% of cellulose, 23-32 percentage of hemicellulose and only 15 to 30% belongs to lignin constituent⁷⁰.

A simplified schematic of lignin, cellulose, poly(acrylonitrile) PAN and mesophase pitch precursors with their respective final carbon structure is presented in Figure 1.3. Indeed, lignin, cellulose, and PAN produce CFs with nongraphitic or turbostratic structures⁷⁰ that elucidates a noncrystalline configuration i.e. at the molecular and atomic level are not organized in a definite lattice pattern structure. In contrast, mesophase pitch after thermal process at temperatures above

2400 °C generates a high graphitic with a characteristic crystalline structure⁷¹

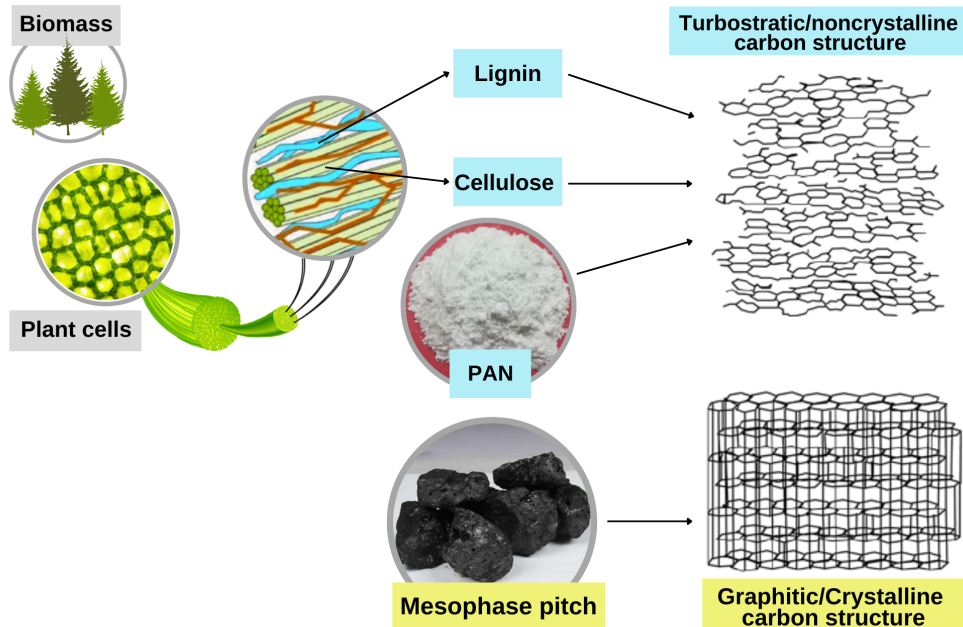


Figure 1.3: Schematic representation of principal CFs precursors (Lignin, cellulose, PAN and mesophase pitch) with their final carbon structure.

However, unlike carbon fibers that include synthetic precursors in their manufacture, most cases biomass has a high content of ash and minerals. This triggers a series of drawbacks with the tensile strength and purity of the resulting CFs because generate defects within the structure of the fibers. Based on these criterion, it can be assured that the separation of lignin and cellulose from biomass is very important. Also, due to the cross-linked form of lignin, it is necessary to break it down and separate it from cellulosic fibers. This process requires a drastic chemical decomposition treatment that is achieved by chemical pulp⁷⁰.

1.3 Pyrolization as thermal decomposition process

Pyrolization, also known as pyrolysis process, is a thermally induced chemical decomposition process where biomass is converted in its simple constituents by action of heat. This process is carried out in the absence of oxidizing agents e.g. oxygen, nitric oxide, nitrogen dioxide, and generally takes place in the temperature range from 300 to 650 °C at atmospheric pressure⁷². However, the product yield depends on several parameters including the heating rate, the final temperature reached and the residence time⁷³.

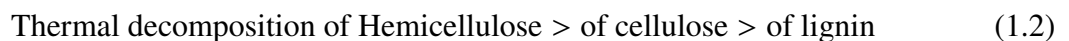
Typically, in pyrolysis applied for biomass feedstock the decomposition of the matrix produces polyaromatic chars, biochar (solid), bio-oils (liquid), and syngas (gaseous) as a result of the breakdown of organic materials⁷². In other words, large and complex hydrocarbon molecules of components stemming from cellulose, hemicellulose and lignin are broken down into smaller and simpler gaseous, liquid, and solid products during the pyrolysis process. To summarize, a general reaction can be used to illustrate the pyrolysis process, as follows:



As mentioned above, pyrolysis involves the breakdown of complex to single molecules into the products. In concordance to the previous reaction, there are three principal types of products: Liquids that are presented as tars, water and heavier hydrocarbons such as benzene, ethyl benzene, toluene, and phenols⁷⁴. Solid products that are commonly char or carbon in the form of fillers and fibres and the last but not the least, gaseous products, that are generally CO_2 , H_2O , CO , C_2H_2 , C_2H_4 and C_6H_6 ⁷⁵. Also, biomass is constituted by three principal structural components as hemicellulose $(C_5H_8O_4)_m$, cellulose $(C_6H_{10}O_5)_n$ and lignin $(C_{81}H_{92}O_{28})$, but also presents minor amounts of extractives.

These constituents depend directly on the pyrolysis variations in terms of mechanisms, pathways, different rates, size of particles, temperature, residence time, but above all the products of interest. Specifically, because lignin decomposes across a larger temperature range than cellulose and hemicelluloses, which breakdown fast over smaller temperature ranges, it seems to be more thermally stable during pyrolysis⁷⁵. For example, from cellulose can be obtained several sub-products like methane, hydrogen, carbon dioxide, carbon monoxide, steam, phenol, acetic acid and benzene as a result of the pyrolysis process⁷².

Thus, in accordance with the above, the properties of these principal constituents under a thermal decomposition process can be summarized as follows⁷⁶:



Lignin decomposes over a wider temperature range compared to cellulose and hemicellulose, which rapidly degrade over narrower temperature ranges, hence the apparent thermal stability of lignin during pyrolysis. So, the rate and extent of degradation is dependent on several parameters of the process like the reactor type, particle size, temperature, heating rates and pressure⁷⁵.

To our knowledge, dehydration, depolymerisation, isomerisation, aromatisation, decarboxylation, and charring are just a few of the reactions that take place during pyrolysis. These reactions can be categorised in primary and secondary but also there are reactions that comes from different conditions. In primary reactions, char formation, depolymerisation and fragmentation are included⁷⁷. More in detail, charring is the result of condensation or combination of benzene rings during pyrolysis⁷⁸ while during depolymerisation bond connections between the monomers are cracked obtaining derivatives such as volatiles and gases⁷⁹. Moreover, in secondary reactions, are contemplated those reactions triggered due to the low stability of the primary compounds

Table 1.3: Characteristics of Pyrolysis Processes based on their main operating parameters

Pyrolysis Process	Final Temperature (°C)	Heating Rate	Residence Time	Products
Torrefaction	280	Very small	10 - 60 min	Torrefied Biomass
Carbonization / Slow	>400	Very low	Days	Charcoal ⁷⁵
Conventional	>575	Low	5 - 30 min	Gas, bio-oil and char
Fast	~500	Very high	<2 s	Bio-oil ⁸²
Flash	<650	High	<1 s	Bio-oil, chemicals, gas ⁸³
Ultrarapid	~1000	Very high	<0.5 s	Chemicals, gas
Vacuum	400	Medium	2-30 s	Bio-oil
Hydropyrolysis	<500	High	<10 s	Bio-oil
Methanopyrolysis	>700	High	<10 s	Chemicals

formed during primary reactions, such as the recombination or cracking processes. In this regard, from cracking lighter products will be produced while heavier compounds will result from the recombination⁸⁰.

On the other hand, reactions from different conditions refer to those which impact the reaction network. For instance, higher production of char can be determined by lower heating rate, while more volatile compounds can be the result of fast heating. Following this definition, also temperature has a major impact on product dispersion. To sum up, and based on all of the study that has been conducted thus far, it can be determined that secondary reactions are the governing processes that can result in the formation of products with specific properties⁸¹.

1.3.1 Types of pyrolysis

For the above mentioned reasons, in all pyrolysis processes, parameters such as the biomass composition, pyrolysis temperature, heating rate, particle size and the effect of catalyst are crucial to determine the final properties of a material or obtained products. In relation to the effect of temperature, it affects both the composition and yield of the pyrolysis product because temperature has a direct influence on the gases production and release rates. The effect of rate of heating and residence time apart from generating compositional and yielding changes, has a substantial implication of secondary reactions which induces a secondary product formation. In regard to biomass particles, finer or smaller particles offer less resistance to release gases preventing secondary cracking. Larger particles, oppositely, promote secondary cracking by the higher resistance to escape first products. And, the catalyst effect exert a considerable influence in liquid yielding⁷⁵. In this sense, according to the range of the main operating parameters for the thermal decomposition process of pyrolysis, it is classified into torrefaction, conventional, carbonization or slow, fast, flash, ultrarapid, vacuum, hydropyrolysis and methanopyrolysis⁷⁵. In Table 1.3 are compared some specifications about each of the different pyrolysis processes in relation to the principal parameters and their products⁷².

1.3.2 Pyrolysis applied for Cellulose-based Carbon Fibers

Studying the chemical processes of each main component of biomass is an effective and necessary first step in figuring out how pyrolysis works. According to Suhani et.al the analysis of chemical composition of banana trunk fibers report about 59% of high cellulose, 15% of hemicellulose and a characteristic low content of lignin of 13% related to nonwood fiber type. The low content of lignin in nonwood fibers is due to it function as adhesive to bind the cellulose in fiber increasing strength which make it unbreakable⁸⁴.

In this regard, cellulose is a polymer chain formed by linked linearly D-glucose units connected via $\beta(1 \rightarrow 4)$ glycosidic bonds⁸⁵. Thus, the degree of polymerisation of cellulose varies depending on the source. It might reach above 5000 units depending on the source⁸¹. When compared to other carbon fiber precursors such as PAN and pitch, the cellulose structures reveal a low carbon content and challenging carbonization. For that, many efforts have been made to understand how cellulose is pyrolyzed and carbonized⁴⁰. Moreover is necessary to understand that requires of three principal steps for a correct pyrolysis as follows: stabilization, carbonization and graphitization steps.

For the first step, according to Tang and Bacon, stabilization is analyzed into four stages: First, water is desorbed from cellulose at temperatures from 25 to 150°C. Second, at temperatures between 150 - 240 °C dehydration from the -OH and -H fragments occurs. Thus, at intra-molecular level the formation of new C-C bonds and ketone groups take place⁸⁶. The thermal breakage of the glycosidic bond and production of tar, H_2O , CO, and CO_2 happened in stage III with the free radical reaction at temperatures from 240 to 400 °C. Finally, at temperatures exceeding 400 °C, each cellulose unit eventually broke down into four carbon atoms and condensed into a graphite-like structure⁸⁷. For the above mentioned reasons, in the past years pyrolysis for cellulose-based carbon fibers suggested that a slow heating rate is the best option to reduce carbon lost due to the elimination of oxygenated compounds, aldehydes and so on in the depolymerization reaction⁸⁸ which also prevents the formation of levoglucosan⁸⁶. Also, slow pyrolysis was proposed to improve microstructure, density and porosity of fibers as well as pyrolysis in reactive atmosphere, use of organosilicon compounds and flame retardants⁴⁰.

According to Frank et.al, for the second step pyrolysis stops and the key chemical reactions are finished at temperatures about 400°C with a carbon content of about 60 - 70%. Thereby, the carbonization process is carried out at temperatures ranging from 900 to 1500 degrees Celsius in an inert gas environment. When non-carbon atoms are released, a carbon-rich residue (95%) is formed⁸⁶. Generally, the processes that occur during carbonization are difficult and complex to see using analytical techniques. In theory, during pyrolysis, the depolymerized, amorphous char is reorganized and condensed to create polycyclic rings, aromatic structures, and then graphite-like layers. As a result, a micro crystalline material composed of sp³- and sp²-hybridized carbon is formed. Fiber shrinkage, density gain, and an increase in tenacity are all linked to the creation of the aromatic structure after carbonization⁸⁹.

Finally, temperatures between 1500 and 3000 °C are necessary for graphitization, which

results in a carbon content of more than 99 percent and the formation of graphitic layers. This process is a highly power-consuming and strongly depends of the desired application of CFs. In order to improve mechanical properties of the final carbon fiber, graphitization under stress, or hot stretching, is carried out by improving the alignment of the carbon ribbons along the fiber axis⁸⁶.

1.4 Cerium oxide NPs: properties, synthesis, characterization and applications

The term nano denotes a billionth of a unit quantity. Particles of size ranging from 1 to 100 nm are denominated nanoparticles, and they exhibit higher surface ratio as well as unique electronic, magnetic, optical and mechanical properties due to their shape and size⁹⁰. Cerium is non-toxic, cheap and the most abundant of the rare earth alkali metals. It belongs to the group of Lanthanides with an atomic number equal to 58, is located in the period 6 within block f. Cerium oxide is an n-type semiconductor with a wide-bandgap of 3.19 eV and a high excitation energy⁹¹. However, the most important property is attributed to the ability of ceria to store and release oxygen via simple Ce^{4+}/Ce^{3+} redox cycles, which is highly dependent on the concentration and kinds of oxygen vacancies in the lattice, as well as surface structures and states. Above mentioned easily reduction is due to at bulk state CeO_2 exists in both +3 and +4 oxidation states. For that, at low oxygen partial pressures, cerium oxide may be readily reduced from CeO_2 to $CeO_{2-\delta}$ by surface reduction⁹².

1.4.1 Physicochemical and Biological properties

Cerium has a density of 6.77 g/cm^{-3} and a molar mass of approximately $140.12 \text{ g/mol}^{-1}$. At room temperature it is malleable and oxidizes easily. Also, cerium shows excellent thermal properties with a boiling point of $3424 \text{ }^\circ\text{C}$ and a melting point equivalent to $798 \text{ }^\circ\text{C}$ ⁹¹. It can be found in minerals such as hydroxyl bastnasite, zircon, synchysite, monazite, rhabdophane, bastnasite and sällanite. As previously stated, it has a remarkable ability to cycle between the two ionic forms of Ce^{4+} and Ce^{3+} . This is owing to the existence of a ground-state electron in the 4f orbital in concordance with its electronic configuration $[\text{Xe}] 4f^1 5d^1 6s^2$, which allows it to display redox properties. Further, the cerium in its oxide form is made up of a face-centered cubic (fcc) typical fluorite lattice with eight oxygen atoms bound to the cerium atom⁹¹ as shown in Figure 1.4. At nanoscale it maintains the same structure with oxygen deficiencies. In other words, as a result of great efforts undertaken toward a better understanding, the building blocks of nanoparticles is directly related to the crystallite nature of the particle. For that, in the cerium oxide nanoparticle polycrystallinity is more common, but evidently crystal structure depends on the synthesis method⁹¹.

Hence, the relationship between the ceria atom and oxygen vacancies is directly associated to the reduction of the cation of Ce^{+4} resulting in a triplet due to the location of the atom of Ce^{+3} . The main reason behind oxygen vacancies is due to the method of synthesis and the size of ceria crystals⁹⁴.

In addition, to mention electrochemical properties cerium oxide is one of the most suitable

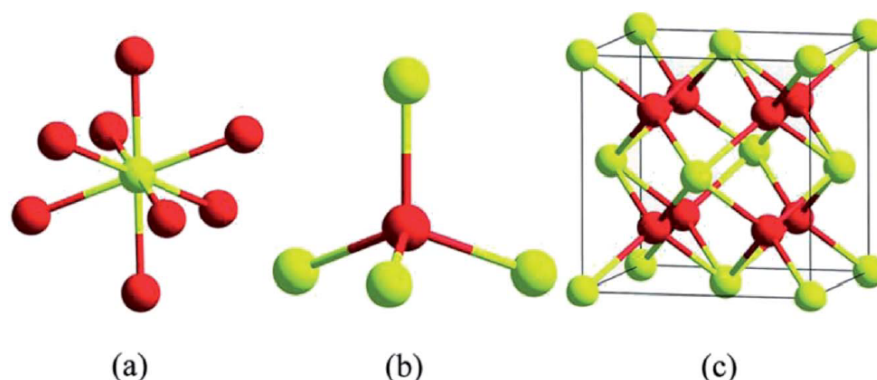


Figure 1.4: Crystal structure for ceria (Ce_4O_8) nanoparticles. Yellow color is attributed to eight-folds of cerium atoms and red represents four-fold atoms of oxygen for both (a) and (b). The basic fcc fluorite lattice structure of (Ce_4O_8) is presented in (c). Adapted from Reed et.al⁹³

intern transition metal candidates to be used as electrode, sensors and supercapacitor constituents because show outstanding electrochemical properties such as higher thermal stability, exceptional oxygen storage, conductivity and electrical diffusivity⁹⁵.

Ceria nanoparticles have demonstrated three crucial biological properties such as Superoxide Dismutase (SOD) and Phosphatase mimetic activity. Cerium oxide nanoparticles, by their high ratio of +3 and +4 affect significantly the SOD-mimetic activity because present similarities at Ce^{+3} fraction activities. Also, Seal et al. revealed that nanoparticles ranged between 3 and 5 nm manifest stable catalytic rate which translates into excellent SOD activity even much higher than the SOD enzyme activity⁹⁶. In addition, several studies determined that the existence of Ce (+3) sites in cerium oxide NPs are suitable to break phosphate bonds of O-phospho-L-tyrosine and *para*-nitrophenylphosphate. Furthermore, the application of these nanoparticles with plasmids of DNA produce bonds without hydrolysis products. As a result, it may be argued that several proteins and ATP molecules can be phosphorylated without causing any type of DNA damage⁹⁷.

1.4.2 Synthesis and Characterization alternatives

As mentioned before, there are two approaches applied to the synthesis process such as bottom-up and top-down. Also, most parameters related to the capping and reducing agents play an important role in the synthesis methods because it determines the physical, chemical and biological properties of nanoparticles⁹⁸. As a result, every day are created new strategies for the synthesis of nanoparticles with specific characteristics based on the two last mentioned approaches. In this regard, between the methods for NPs synthesis are included biological, physical and chemical procedures. Many of these implicate the use of chemicals and precursors of biological origin. However, over the years and with regard to the large amount of research studies; the best method for NPs synthesis is the biological alternative due to that it reduces the difficulties related to biocompatibility and originate non-toxic and environmentally friendly nanoparticles without neglecting that it is simpler and cost-effective⁹¹. Among the chemical

methods are sol-gel process, pyrolysis, hydrothermal synthesis, sonochemical synthesis, coprecipitation and mechano-chemical processes. On the other hand, for biosynthesis the use of plant, fungus, nutrients and natural polymer mediated alternatives are booming due to the countless benefits⁹¹.

The appropriate characterization requires powerful equipment and high-precision techniques to ensure the highest quality in the design and manufacturing processes of nanoparticles. To date, thanks to the advances that result from research and technological development, there are a large number of characterization techniques that can be used for the analysis of the properties of nanomaterials. These can be categorized into qualitative and quantitative or based upon nanomaterial properties. For qualitative analysis, are included Fourier transform infrared spectroscopy (FT-IR), UV-Vis spectrophotometry, Scanning electron microscopy (SEM), X-ray diffraction (XRD), Raman scattering and Atomic force microscopy (AFM)⁹⁹, while quantitative consists of Transmission electron microscopy (TEM), Annular dark-field imaging (HAADF), Liquid Chromatography - Mass Spectrometry (LC-MS/MS), Intracranial pressure (ICP), Thermogravimetric Analysis (TGA), Dynamic Light Scattering (DLS) and Zeta potential⁹⁸. Arguably, this classification may be controversial since many of the equipment that has been designed are combining quantitative and qualitative techniques in a single device. And, it has been possible to evidence the design of external devices that adapt to several of these in order to obtain a better study of the properties of the new materials.

1.4.3 Biomedical applications

Cerium oxide nanoparticles, after silver oxide NPs, are one of the most promising metal oxide nanoparticles that have attracted attention in recent decades. They may be used in a wide number of fields, including agriculture, industry, environment, and biomedicine. According to the scope of this study will focus only in biomedical research.

In Figure 1.5 the possible applications of cerium oxide NPs in the field of Biomedicine are summarized. Among the most relevant applications in recent years can be found: Theragnostic agent for cancer, Bio-scaffold, Anti-oxidative agent, Biosensors, Antimicrobial agent, Drug and gene delivery, Therapeutic agent and Anti-inflammatory.

To mention a few examples, as theragnostic agent for cancer treatment, cerium oxide NPs exhibit cytoprotective properties that induce the formation of reactive oxygen species (ROS) making them a potential anticancer agent due to changes in the regulation of antioxidant enzyme expression and the resulting acidic environment at the level of cancer cells⁹¹. This leads to the production of reactive nitrogen species (RNS) that act together with ROS to cause nitrosative stress in damaged¹⁰⁰.

As already mention, cerium oxide nanoparticles exhibit outstanding properties such as non-toxicity, large surface area, large capacity of storage, biocompatibility, good conductivity for oxygen ions, as well as high mechanical strength. These properties allow the development of biosensors, a good example is the biosensor manufactured from a film of indium-tin-oxide (ITO) coated glass where cholesterol oxidase was immobilized for the detection of cholesterol which become in a cost-effective alternative for coronary diseases¹⁰¹.

As antibacterial or antimicrobial agent, in concordance with the ability of cerium oxide NPs

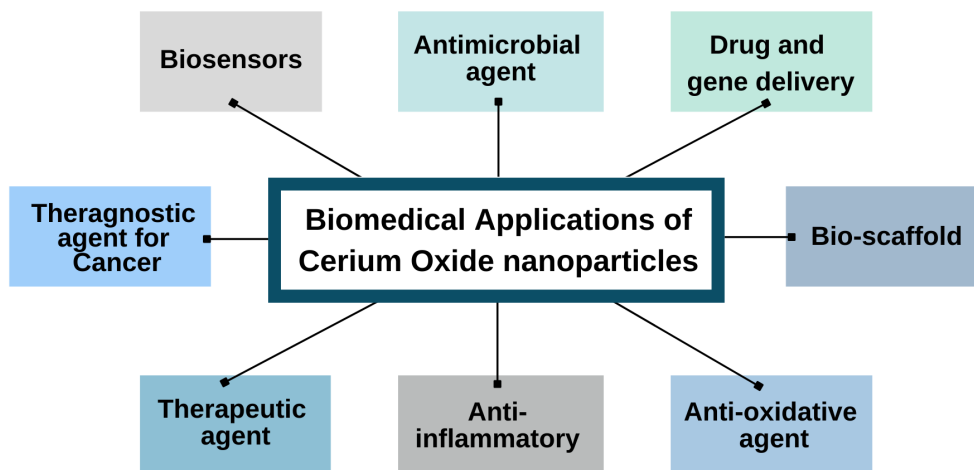


Figure 1.5: Potential biomedical applications of cerium oxide nanoparticles.

to produce ROS, when NPs interact with bacterial cells they release some ions that react with thiol functional groups characteristic of the protein structure of bacterial cell membrane. As a result, this generated acidic environment decreases the permeability of the membrane and produces cell death¹⁰². In addition, ceria nanoparticles exhibit anti-oxidant potential properties and act as a neuroprotective agent. When NPs are exposed to rat brain tissue, shows a substantially increasing of thiol content and trigger caspase-3 protein expression, decreasing oxidative DNA damage and lipid peroxidation¹⁰³.

Undoubtedly, cerium oxide NPs show pharmacological potential due to their oxygen buffering qualities, a suitable example is the porous bioactive glass scaffolds used for regeneration and enhance of osteoblastic differentiation without requirement of additional osteogenic supplements¹⁰⁴. Just as some examples have been mentioned, multiple applications can still be listed in which cerium oxide nanoparticles demonstrate a high potential to be used in biomedical applications.

Chapter 2

Introduction

The development of natural fiber composite (NFC) is based on two primary strategies: preventing the loss of forest resources and delivering high economic returns¹⁰⁵. Thus, natural fiber composites have stimulated the interest of scientists due to their biodegradability, multifunctionality, lightweight¹⁰⁶, specific strength properties, low cost, enhanced energy recovery⁵, and, most significantly, their ease availability⁶. For reinforcing composites, natural fibers come in a variety of forms, including continuous, random oriented, and woven fabric. Furthermore, experts have been searching for the ideal material for certain purposes for years. There is growing interest in the development of carbon fibers composites from biomass precursors in different applications such as supercapacitors¹⁰⁷, aerospace applications, polymer and adhesion research, automotive industry, biosciences, electronics, metallurgy, energy, medical and pharmaceutical industry¹⁰⁸.

Due to their large-scale availability, simplicity of processing, and low cost, a plethora of natural fibers has been studied as fillers in composites. These include biomass from oil palm empty fruit bunches (EFB), rubber wood sawdust, borassus fruit, bamboo¹⁰⁹, coconut husk, pineapple leaves, jute¹¹⁰, and many others¹¹¹ have been investigated as viable precursors for the production of activated carbon fibers. Among the large number of plants available which can be grown by nature, not all are suitable either for reinforcement use or as a natural fiber for the manufacture of composites. In order to choose an adequate type of fiber, certain conditions must be taken into account. The fibers must be easily extracted from various parts of the concerned plant such as the seeds, stems, leaves, fruits and other grass fibres¹¹². Additionally, they must adhere easily with the matrix that is being developed. Finally, but not least, according to several studies the strength and some physical and chemical characteristics of all fibers from natural origin depend on the content of cellulose and lignin¹¹¹. For a natural fiber to be more suitable it must have a cellulose content of at least between 6 - 80% and a lignin content between 5 - 20% by weight¹¹³.

In this sense, composite materials made from diverse natural fibers are rapidly growing. Banana fibers derived from the banana stem and fruit which are consumed by all humans worldwide, is one such natural source¹⁰⁶. Because of its high strength and stiffness¹¹⁴, banana carbon fiber would be used as a reinforcement in both thermoplastic and thermoset matrices or as an eco-friendly alternative for biomedical purposes¹¹⁵. In terms of composition of banana fiber, which has a high cellulose concentration of 63 - 64% and a lignin content of 5%, it represents an

interesting aspect that makes these fibers a potential reinforcing replacement for existing ones¹⁰⁶. Every day, the world moves closer to adopting improved technology, which has an indirect impact on the usage of outdated materials. In this regard, researchers are concentrating on the creation of new novel materials from a variety of renewable sources. For that, metals, polymers, and ceramics are all used in the production of biocomposites, which is a challenging process to be applied as drug/gene delivery, orthopedics, tissue engineering, and aesthetic orthodontics among other biomedical applications. The acceptance of these materials as biomaterials by the human body is the first and most important requirement. In order to be used in the human body, a biomaterial must possess a number of key common properties, which can be used alone or in combination to replace or act as a framework for the regeneration of damaged or degraded tissues or organs, therefore enhancing the quality of life for patients¹¹⁶.

In recent decades, nanoparticles and nanocomposites have opened bright horizons to develop new alternatives for potential-biomedical-applications in order to improve clinical performances and reduce toxic or adverse side effects. More specifically, a new era of nano-level control of carbon fibers after 30-years of development⁴². For this purpose, coupling agents and/or surface modification techniques can increase fiber/matrix interfacial adhesion in polymer composites. This research project addresses the characterization and utilization of carbon fibers from banana stem decorated with cerium oxide (CeO₂) nanoparticles as a potential future research directed at eco-friendly and biodegradable composites for biomedical applications. Ecuador, being a country with a high banana production level, it may be feasible to manage waste treatment while gaining research and technical benefit to the biomedical field.

2.1 Problem Statement

Because recent technological advancements have enabled nano-level management of carbon fibers, biomaterials applications have likewise moved to the nano-size era. Carbon fibers (CFs) are fibers with microscale diameters that substantially improve the functionalities of traditional biomaterials and enable the production of novel composite materials. According to Holmes in their research conducted in 2014, the demand for carbon fibers (CFs) is increasing each year at a 10% rate and is expected to reach 89000 tons by 2020¹¹⁷. In this context, as science and technology develop, it is important to consider natural and renewable resources for the production of fibers from natural precursors. It should be noted that poly(acrylonitrile) (PAN) is used as a precursor in approximately 98% of CFs. Essentially, this material is made up of extremely thin and fragile acrylic fibers, the majority of which are made up of carbon atoms¹¹⁸. Thus, natural fiber composites have stimulated the interest of scientists due to their biodegradability, multifunctionality, lightweight, specific strength properties¹¹⁷, low cost, enhanced energy recovery, and, most significantly, their ease availability¹¹⁸.

According to the Food and Agriculture Organization of the United Nations (FAO), in 2020 the preliminary results of the Banana Market Review based on the geography and dynamics of economic activities, Ecuador reached an unprecedented high of approximately 6.9 million tons in bananas making it the largest exporter of bananas in the world¹¹⁹. Therefore, being a country with a high level of banana production, it immediately translates into a large amount of

agro-industrial waste. It may be feasible to manage waste treatment while obtaining research and technological benefits for the biomedical field. In order to achieve this, it is indispensable to assure that carbon fibers present chemical and physical properties that translate in biologically essential characteristics and supplementary functionalities. All this is possible thanks to the benefits of functionalization, a process of adding new functions, capabilities, features, or properties to a material by changing the surface chemistry of it. For that reason, carbon fibers from banana stems decorated with Ceria (CeO_2) nanoparticles can be considered as a potential future research directed at eco-friendly and biodegradable composites for biomedical applications.

In order to elucidate the properties of this novel composite, it is essential to carry out a significant surface description that requires the capacity of characterization techniques such as Raman spectroscopy and Scanning Electron Microscopy (SEM). Raman Spectroscopy may be used to determine the chemical composition of materials by detecting vibrational¹²⁰, rotational, and other states in a molecular system¹²¹. On the other hand, SEM is a high resolution surface analysis method that elucidates and images the microstructure¹²², morphology, topography and composition of the outermost layer of the biomaterial¹²³. The more parameters are measured, the description about the surface of carbon fibers from banana stems decorated with (CeO_2) nanoparticles will be more complete, allowing for more effective applications.

2.2 Motivation and Research Objectives

2.2.1 General Objective

To synthesize and characterize carbon fibers obtained from banana stem and decorated with cerium oxide (CeO_2) nanoparticles for biomedical applications.

2.2.2 Specific Objectives

- To obtain information about the morphological composition and surface topography of the banana carbon fibers decorated with cerium oxide (CeO_2) nanoparticles using Scanning electron microscopy (SEM) characterization technique.
- To detect vibrational, rotational, and other states in the molecular system to probe and identify the chemical composition of the carbon fibers decorated with ceria (CeO_2) nanoparticles using Raman Spectroscopy characterization technique.
- To reveal the chemical environment where carbon fibers decorated with cerium oxide nanoparticles exist by the speciation of the respective elements observed to determine the surface specificity of it.
- To quantify chemical composition, relative and absolute concentrations of certain elements and chemical functional groups near the interface between banana carbon fibers and cerium oxide nanoparticles.

Chapter 3

Methodology

This chapter presents a descriptive summary of the methodology carried out in this study. It provides information about the recollection of banana fibers, upon the different parameters for thermal decomposition process (i.e. pyrolysis). As well as, the top-down approach for the synthesis of cerium oxide nanoparticles at concentrations of 3.57 and 7.14 mM. The process carried out for the decoration of the banana fibers with the nanoparticles obtained is described more in detail. Finally, specifications about Scanning Electron Microscopy (SEM) and Raman Spectroscopy characterization techniques that were applied for the characterization of the nanocomposite are described. In this regard, the analysis of characterization techniques start with the fundamental principles and experimental system set-up for proper data collection, qualification and quantification.

3.1 Synthesis of carbon fibers functionalized with (CeO₂) NPs

3.1.1 Recollection and Pyrolysis of carbon fibers

For this study, previous recollected banana carbon fibers were chosen as substrates for pyrolysis. According to Gaona, S. et.al, two types of banana tree samples were used, both belonging to the Family: Musaceae, to the Genus: Musa and to the Species: Musa Paradisiaca¹²⁴. In relation to geographic location, the first sample is obtained from the province of Imbabura (Urcuquí) and the second one from Santo Domingo de los Tsáchilas (Santo Domingo). The first sample is obtained from the pseudo-stem of the banana tree; it presents characteristics of a too young species that does not present fruits with a diameter of trunk equivalent to 20 mm. The second sample belongs to a species that has produced fruits, which were previously cultivated with a trunk diameter equal to 35 mm. To obtain the fibers, after removing the protective layers from the banana trunk, a scalpel was used to make a shallow cut to help break the trunk. Thus, two magnificent batches of raw fibers were obtained from the trunk of the banana bunch¹²⁴.

Raw carbon fibers go through a thermal decomposition process denominated as pyrolysis. In this regard, a system of spike mounting is used which keeps the fibers anchored and thus avoids fiber shrinkage during the thermal treatments inside the tubular furnace. In Figure 3.1 is shown

the contrasting appearance of raw carbon fibers before (a) and after (b) the thermal decomposition process.

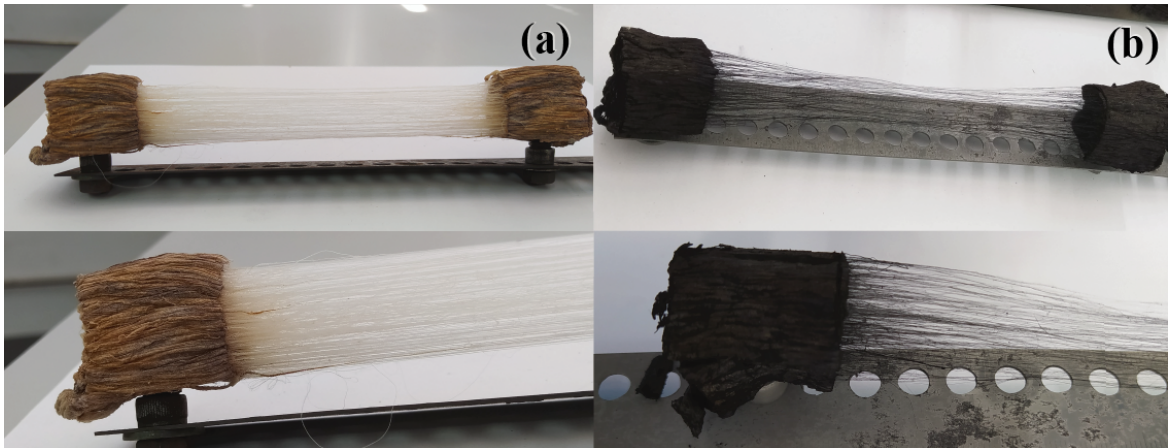


Figure 3.1: Banana fibers characteristics: (a) before and (b) after pyrolysis.

Pyrolysis process is carried out in an Argon (Ar) atmosphere with a precision mass flow of 0.3 L/min in a tubular furnace OTF-1200X shown in Figure 3.2.



Figure 3.2: Tubular Furnace, OTF-1200X at Yachay Tech University, Ecuador

To study the effect of pyrolysis temperature over the time, as evidenced in Table 3.1, all batches worked at a maximum temperature of 900 °C with 60 minutes residence time. A total of three batches of fibers were pyrolyzed according to the conditions specified in Table 3.1 which also can be seen in Figure 3.3.

Table 3.1: Pyrolysis treatment and heating ramp parameters for batch of raw banana carbon fibers.

	Heating ramp									
Time (mins)	0	10	20	30	40	50	60	80	140	
Temperature (°C)	0	100	200	300	500	700	800	900	900	

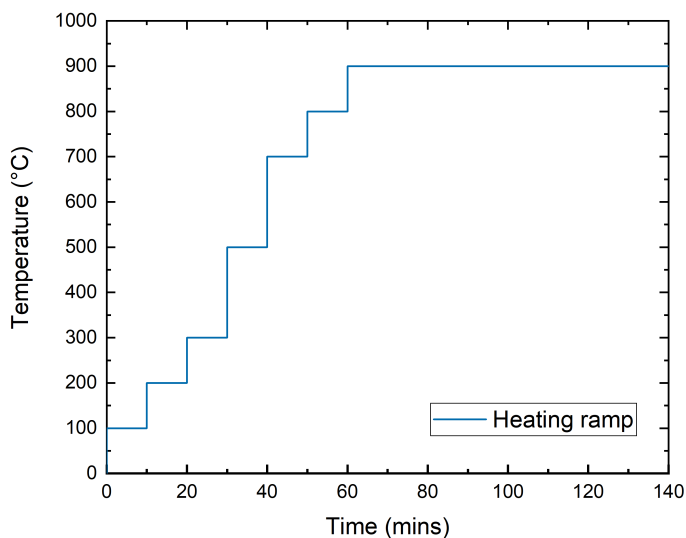


Figure 3.3: Heating ramp for batch of raw banana carbon fibers

3.1.2 Synthesis of Ceria (CeO₂) nanoparticles

Synthesis of cerium oxide nanoparticles follow a top-down also known as destructive approach because large molecules are decomposed into smaller form. For this research, previous synthesized cerium oxide NPs powder were chosen as substrate for solutions used for future immersion process. Method of synthesis of cerium oxide NPs powder was carried out by Maldonado, P. et.al¹²⁵, using cerium sulfate at a concentration of 0.05 M and ammonium hydroxide at 0.5 M. The synthesis procedure started with the addition of 10 mL of cerium sulfate (Ce(SO₄)₂) in a beaker with constant stirring, this step is followed by the addition of 50 mL of ammonium hydroxide (NH₄OH) dropwise to the solution, as a result is evidenced the gradual production of a precipitate. Then, the solution was drained into a hydrothermal autoclave reactor and placed into a furnace for 5 h at 180 °C. After several minutes, until that reactor reaches an appropriate room temperature, the solution is placed in falcon tubes to be centrifuged for a period of 5 minutes at 2000 rpm. Subsequently, the supernatant is discarded in an appropriate container and the pellet was washed with 40 mL of pure water. Then, each tube is shaken until obtain a homogeneous solution and centrifuged at the same conditions as before. As already mentioned above, the liquid phase was also discarded and the procedure is repeated four times before drying the pellet at 80 °C for 4 hours.

Powdered ceria oxide nanoparticles were used to prepare two type of colloidal solutions

in which previously pyrolyzed banana fibers were placed. To prepare the dispersions, a 0.1% (w/v) solution of SDS (Sodium Lauryl Sulphate Extra Pure) was first prepared in 25 mL of distilled pure water. An aliquot of the dilution (2 mL) was taken to prepare the variants in nanoparticle concentration. In this way, two types of colloidal nanoparticle solutions were obtained after ultrasound assisted extraction as follows: the first one at a concentration of 3.5684 mM when add 1 mg in 2 mL of the 0.1% (w/v) SDS solution and the second variation at a concentration of 7.1369 mM when adding 2 mg in 2 mL of the 0.1% (w/v) SDS solution. At greater concentration of cerium oxide nanoparticles the solution appears with less transparency. Thus, clearly in Figure 3.4 the solutions with dispersed nanoparticles where is evidenced a variation in nanoparticles concentration as well as a particle size distribution that decreases from left to right can be observed.

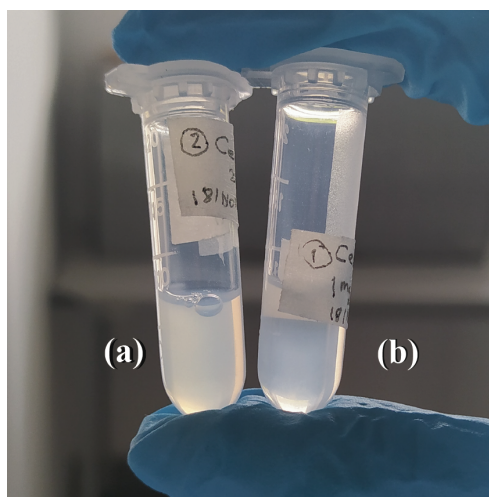


Figure 3.4: Dispersions of nanoparticles of varying nanoparticles concentration, with the particle size distribution decreasing from left to right. (a) At concentration of 7.14 and (b) 3.57mM.

3.1.3 Decorating carbon fibers with (CeO₂) NPs

As explained earlier, after the thermal decomposition process all carbon fibers obtained from banana stem were decorated with (CeO₂) NPs at 7.1369 and 3.5684 mM nanoparticles concentrations. In-situ functionalization of CFs was performed by the principles of immersion method, in other words carbon fibers were introduced in ceria nanoparticles solutions for 3 days to be late dried at room temperature until the fibers appears more separated from each others with a hair-like shape. With the previous step, it is expected to obtain significantly adhesion of the (CeO₂) NPs along the surface of the CFs, thanks to the interaction between the functional groups and the nature of the nanoparticles.

3.2 Fundamentals of Characterization Techniques

For characterization purpose, SEM-EDS images or micrographs were obtained from a Phenom-ProX with software Pro-Suite detector fast SDD from AMPTEK and the Raman spectra for the different samples of pristine and decorated CFs was obtained from a Horiba scientific LabRAM HR evolution Raman spectrometer.

3.2.1 Surface analysis

The elements present (the types of atoms) and how these constituents link to one another establish the characteristics of matter in one way or another. The shape of the outer layer therefore determines how a solid or liquid is seen by the outside world. Most types of matter in the solid or liquid state have a surface layer that is distinct from the underlying material. Chemical (composition and/or speciation) or structural (variations in bond angles or bond lengths) differences, or both, might be the cause of this difference and these properties are mainly determined by the physical and chemical properties of its surface layer¹⁰⁸.

This is the appropriate point to discuss general points about surfaces, particularly solid surfaces. First, it should be noted that the surface region of a material exhibits unique reactivity. This characteristic allows the development of catalysis and microelectronics studies that mainly take advantage of the reactivity and the structure of the surface and in the field of biology, this characteristic is also used and improved to understand the behavior of some materials with other substances. Second, the surface has a minimal amount compared to the total mass of the material. Third, the surface of a material is completely different from the bulk. Within the traditional characterization techniques that are used to elucidate the characteristics of the material, none are found that are suitable for the surface, since they do not have the necessary sensitivity to analyze the minimum amount of the material that allows adding information about its composition and chemical structure. Fourth, the surface molecules of a material often can exhibit reasonable mobility. Finally, it is important to take into account that the surfaces of the materials are prone to being easily contaminated with components that are present in the vapor phase (among them it is quite common to find silicones, hydrocarbons, iodine and sulfur compounds). If materials are placed under ultra-high vacuum conditions, that is, at pressures lower than 10^{-7} Pa, any type of contamination can be delayed. However, the vast majority of medical devices are used at normal atmospheric pressure conditions, which leads us to learn to live with a certain amount of contaminants².

More specifically, the surface can differ in composition and/or structure from that of the underlying bulk material in most forms of matter and its fact depends on two agents, external forces of the outer layer or those related to internal forces. As a result of these agents modifications, adhesion, adsorption, biocompatibility, corrosion, desorption, interfacial electrical properties, reactivity, texture, wear and tear, wettability among other physical and chemical properties can be changed. A characterization gives the ability to modify (tailor) some specific properties of the surface and/or the formulation of new biomaterials as needed becomes available. Besides, the surface of a solid or liquid, as the term is most generally used, can be defined as the outermost layer or the upper limit of an object that is the region that determines the behavior of a solid or

liquid with its surroundings. Applying this concept, a surface can span as little as one atomic layer (0.1–0.3 nm) to several hundreds of atomic layers (100 nm or more) depending on the material, its environment, and the property of interest¹⁰⁸. Considering a single strand of human hair to put these measurements into context, it has a diameter of 50 - 100 μm (0.05 - 0.1 mm). The outer surface is made up of atoms with a diameter of around 0.2 nm¹⁰⁸. Hence, the manner in which a specific solid or liquid interacts with its environment can be better understood if the surface composition and speciation can be characterized.

However, due to the scale that these surfaces handle, the magnification needed ($\sim 30,000,000\times$) can only be reached using a very limited number of techniques to reveal the physical structure of the object in question¹⁰⁸. In terms of chemical properties, spectroscopy or spectrometry techniques are needed. Despite the existence of a large number of spectroscopies and spectrometries, there are really few that provide information on the active chemistry of the outermost surface, that is, within the outer 10 nm of a solid.

Among the available techniques, which require relative ease and minimal sample preparation, and fit perfectly with the objectives of this study are Scanning Electron Microscopy (SEM) and Raman Spectroscopy. Raman Spectroscopy by detecting vibrational, rotational, and other states in a molecular system may be used to determine the chemical composition of materials. Furthermore, Scanning Electron Microscopy (SEM) is a high resolution surface analysis method that elucidates and images the microstructure, topography, morphology and composition of the outermost layer of the biomaterial². To sum up, having in mind the great efforts undertaken toward a better understanding the more parameters are measured, the description about the surface of biomaterial will be more complete, allowing research into more effective biomedical applications.

3.2.2 Scanning Electron Microscopy (SEM)

Over the years, due to the limitations in the resolving power of human eyes, multiple instruments have been developed, but the most relevant is the microscope for its magnificent efficiency to study and characterize a wide variety of materials. This instrument depends on the quality and number of lenses you have in your setup, but especially on the wavelength of the light from the source to produce the image¹²². Based on the above, the microscope can be classified into optical or light microscope (OM) and electron microscope (EM) depending on the resource that produces the image¹²³. Basically both have the same operating principle, the main difference lies in the resource, OM uses visible light while EM uses a focused accelerated electrons beam³¹.

In terms of resolution, optical microscope is limited due to diffraction properties while electron microscopy exhibits much higher resolution because the electrons are more energetic than photons in visible range as a result of their shorter wavelength. Thereby, two main types of electron microscopes are available, transmission electron microscopy (TEM) and scanning electron microscopy (SEM). The first, TEM, was conceived by Knoll and Ruska in 1931 and seven years later Von Ardenne introduced the first SEM, which only in 1965 came to market as a powerful tool to understand scientific phenomena¹²³.

Scanning Electron Microscopy (SEM) is a multipurpose, versatile and advanced instrument which is able to examine and analyse surface phenomena of the materials under vacuum conditions. The pressure inside the SEM chamber is usually low in the range of 0.1 to $10^{-4} Pa$ ¹²². Basically, the sample is hit by a high energy electron beam exciting and ejecting X-ray electrons to be analysed at the outcoming. These captured electrons provide information about composition, morphology, topography, orientation of grains, crystallographic information, magnetic and electrical features, among other characteristics from the sample's material¹²³. In other words, this characterization technique indicates parameters such as the shape and size, how the surface looks, providing high resolution images of its texture, roughness or smoothness. But also, gives information about chemical composition and the arrangement of atoms at the outermost layer of material. The chemical information consists in the analysis of their relative ratios as well as the degree and arrangement of atoms in the single crystal particle¹²². In that regard, scanning electron microscope (SEM) is the most advanced instrument for obtaining a high-quality visual picture of a particle with a spatial resolution of 1 nm and magnifications extended 300.000 times over the normal range¹²⁶.

2.2.2.1. Fundamental principles of SEM

Scanning electron microscopy is based on the releasing of primary and secondary electrons. Primary electrons are emitted from the source by providing heat or energy in the range of 1 to 40 keV, while secondary electrons are released from the source as a result of the atomic energy provided by the energy interaction at atomic levels. The high resolution image is obtained by the collection of secondary electrons from the specimen, but is necessary to highlight that all these interactions are only achieved under vacuum conditions. This last requirement avoids interactions with gas molecules or impurities with the electrons of interest¹²³.

In addition, the atomic number, specific concentration of atoms in the specimen, and the input electron energy directly influence electron scattering and interaction volume. This interaction between volume and scattering process will increase if the electron energy or the accelerating applied voltage is also increased¹²². In contrast, if the atom concentration and atomic number are high, the interaction volume and scattering will be low. Another factor to take into account is the angle of incidence of the electron beam which induces the interaction volume and scattering process¹²³.

2.2.2.2. Experimental set-up for SEM

SEM is an optical and electronic system that consists of four principal components: (1) electron gun (electron source and accelerating anode), (2) electromagnetic lenses, (3) vacuum chamber housing the specimen and (3) the column. The last one is basically the set of several detectors to collect the signals emitted from the material sample¹²³. Briefly, inside the vacuum chamber, the gun emits the electron beam in a vertical direction traveling through electromagnetic fields and lenses. Then, the electron beam is directed on the specimen by the objective lens. The focused beam is then rastered over a specific area of the specimen surface with the assistance of deflector coils, which in turn are controlled by the scan generator¹²⁷. Thus, the focused beam scans across a specified region of the specimen surface. After that, the electron beam hits the

material producing a huge number of emitting signals (electron-sample interaction), i.e. x-rays and electrons which are detected and further converted to signals by the detector¹²². These signals provide detailed information about the material to characterize. To illustrate, Figure 3.5 shows the typical structural components of an SEM.

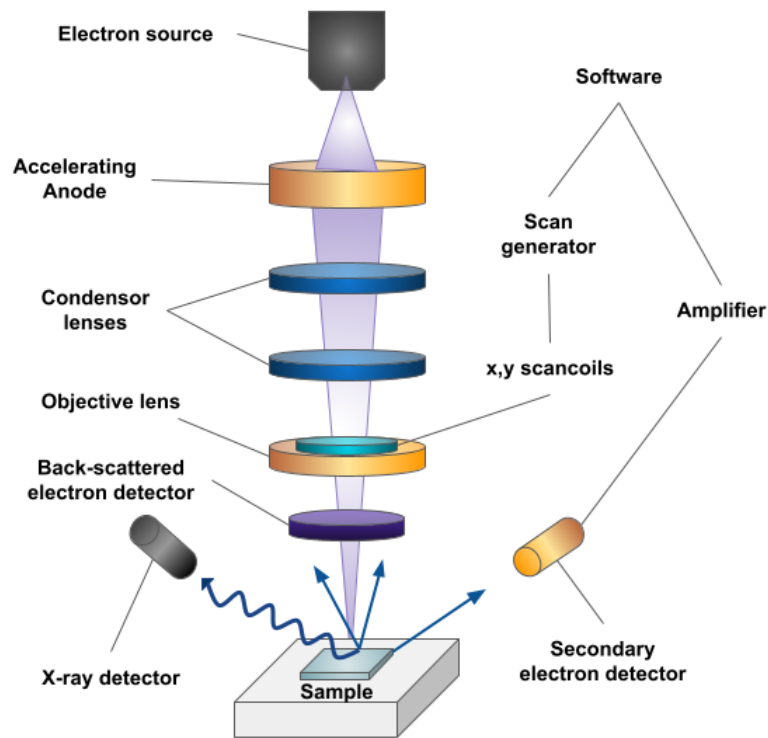


Figure 3.5: Schematic diagram of the principal components of an SEM microscope

2.2.2.3. SEM Data collection, Qualification and Quantification

The morphology and other surface characteristics of the samples were carried out with a Phenom-ProX with software Pro-Suite detector fast SDD scanning electron microscope. Figure 3.6 shows the Phenom-ProX scanning electron microscope at School of Earth Sciences, Energy and Environment at Yachay Tech University (Ecuador). For the sample preparation, all SEM stubs were labeled previously and using a double-sided carbon masking tape, the respective decorated carbon fibers samples were placed.

During SEM analysis, all samples were exposed to a 15.0 kV acceleration voltage and the elastically scattered electrons were detected by a back-scattered electron detector (BSD). Samples imaged with the SEM were taken at 2000x and 20000x with a Field of View (FOV) of 134 and 13.4 μm , respectively. As a result, the micrographs for the pristine fibers and those with nanoceria bound to the surface of the banana carbon fibers illustrate representative characteristics; which

could be explained in terms of physical and chemical interactions between the functional groups at the surface of carbon fibers.



Figure 3.6: Phenom-ProX model scanning electron microscope with software Pro-Suite detector fast SDD at Yachay Tech University, Ecuador

Additionally, in order to measure the fiber diameter, average size of the particles and to determine the distribution along the fiber, the image processing software ImageJ was used. The distribution of fiber diameters was determined from a random sampling of approximately 110 different zones from micrograph while for average particles size about a 80 different structures. The data obtained from aggregates and freely particles, were analyzed separately to avoid the deviation of real data due to the presence of bigger structures.

3.2.3 Raman Spectroscopy

Raman scattering was discovered in 1928 by Krishna and Raman. This technique provides a quantitative and qualitative chemical analysis through the vibrational modes of molecules. Typically, in Raman, a monochromatic light (laser invisible, near-infrared, or near ultraviolet range) is employed, which stimulates the molecules to reach the high-energy states of excitation denominated as “virtual states”. In other words, Raman is based on inelastic scattering between incoming photons and phonons in materials¹²⁸. This characterization technique is a non-destructive, efficient, powerful and favorable to sample preparation that provides information about chemical structure, polymorphy, crystallinity, and molecular interactions which are essential to understand the interaction of light with the chemical bonds of materials in order to elucidate related residual stress, impurities, microstructural changes, among several others¹²⁹. Indeed, to characterize certain specimens it is necessary to analyze Raman spectra according to position and position shift

bands but also full width at half maximum (FWHM) and their respective intensities. Basically, when light interacts with the materials a more deep explanation is given by the synergy of photons and the vibration phonons where the difference in frequency between the incident light and the scattered one gives particular information on the vibrations of the lattice¹³⁰. Therefore, Raman spectroscopy is widely used to contribute for structural fingerprint analysis and identification of specific molecules.

2.2.3.1. Physical principle

As mentioned before, the principle of Raman effect is based on the inelastic scattering mechanism between incident light and the irradiated specimen due to the interaction of chemical structure within the material with the properties of the incident light¹³¹. It all comes down to the distortion process that the electron cloud experiences until it reaches its stability, in other words, the photons will scatter until they find a relatively more stable energy state¹²⁰. As shown in Figure 3.7, when photons fall back to the ground level, also named as initial energy state, there is no energy transfer between the incident light and the dispersed light and consequently photon frequency and wavelength remain unchanged¹³². This process where an elastic collision occurs, is denominated as Rayleigh scattering represented as (a) in Figure 3.7.

As would be expected, when photons move towards a new energy state different from the initial one, an energy transfer takes place, the same that can occur due to the loss or gain of photons¹²⁰. These variations are evidenced in the spectrum by the rise and fall of the laser energy photons providing information about the vibrational system¹²¹. However, Raman scattering can be classified into Stokes Raman scattering and anti-Stokes Raman scattering shown as (b) and (c) respectively in Figure 3.7. In Stokes Raman scattering, the photons are excited going towards a higher energy level (starting from the initial initial energy level) causing that scattering light to have a lower frequency than the incident light. In contrast, in anti-Stokes Raman scattering, photons fall at a lower energy level, so, the frequency of dispersed light is higher than incident light¹²¹.

The intensity of Raman spectrum is proportional to the concentration of each constituent and each peak represents specific shift due to vibrational frequencies which are further used to describe chemical structures. In mathematical terms, Raman shift is defined as the frequency difference ($\Delta\nu$) between the excitation radiation and the Raman scattered¹³³. Raman shifts are typically expressed in wavenumbers (cm^{-1}). It is defined as:

$$Raman\ Shift\ [cm^{-1}] = \frac{10^7}{\lambda_0[nm]} - \frac{10^7}{\lambda_f[nm]} \quad (3.1)$$

where both are wavelengths, λ_0 is for the laser and λ_f is for Raman peak. Besides, in order to convert wavenumbers to wavelength, the following equation is used:

$$\lambda_0[nm] = \frac{1}{\frac{1}{\lambda_f[nm]} - \frac{Raman\ Shift\ [cm^{-1}]}{10^7}} \quad (3.2)$$

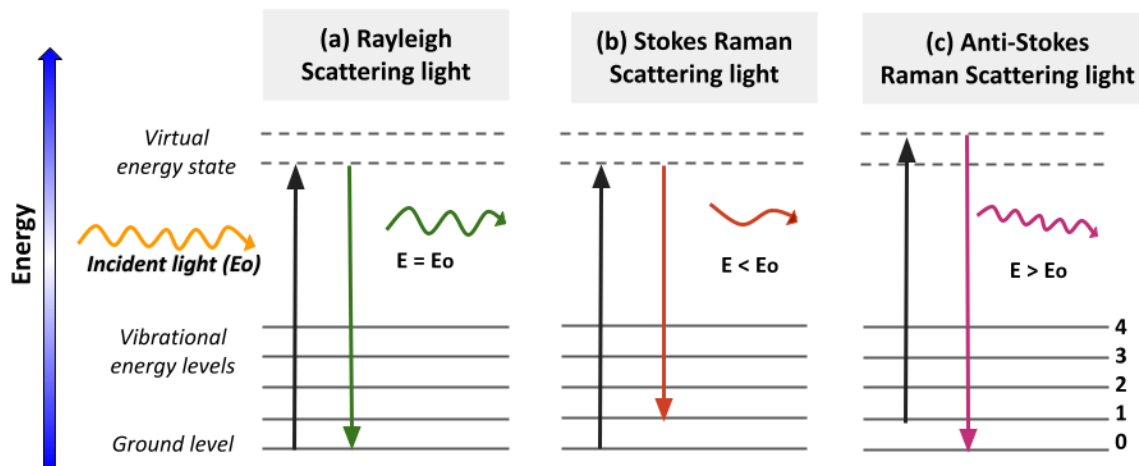


Figure 3.7: Schematic representation of the Rayleigh and Raman scattering processes: (a) Rayleigh scattering, (b) Stokes Raman scattering and (c) Anti-Stokes Raman scattering.

Using wavelength values, an absolute wavelength scale can be plotted. In contrast, using wavenumbers, a relative scale is represented¹³⁴.

2.2.3.2. Experimental set-up for Raman Spectroscopy

A Raman spectrometer is composed of four principal components like the (1) light source, (2) monochromator, (3) sample holder and (4) detector. However, in relation to the characteristics that might impact Raman spectra analysis like high signal-to-noise ratio, instrument stability, and adequate resolution many technologically improved Raman spectroscopy models have been made in the last decades. For example, the development of detectors with highly sensitive coupling with optical fibres and microscopes enhanced significantly the analytical capability. As an excitation source a great variety of lasers can be used like argon and krypton ions, He:Ne, Nd:YAG and diode lasers. Furthermore, many spectrometers use near-IR (NIR) excitation lasers, which have a lesser fluorescence impact than visible wavelength lasers¹²⁰. To elucidate, some applications depending on lasers: Visible lasers (488 nm - 541 nm or 633 nm) are employed for semiconductor, catalyst, biological, mineral, and polymer samples. UV lasers (from 244 nm to 325 nm) are used for biological and catalysts specimens while NIR lasers (785 nm or 830 nm) are used for polymer and biological samples.

As shown in Figure 3.8 the mechanism of Raman spectroscopy is governed by the (1) light source, (2) monochromator, (3) sample holder and (4) detector. The light from laser origin is collected with the diverse optical components and finally the scattering light is reached by the detector to be analyzed as the software spectra obtained. Generally, bandpass and rayleigh filters

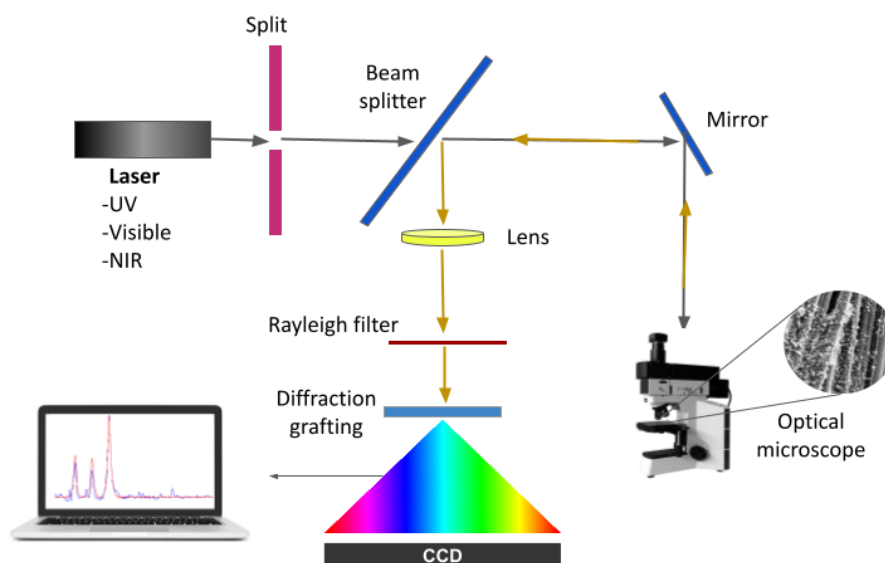


Figure 3.8: Schematic diagram of experimental set-up for Raman Spectroscopy adapted from Baker, M. et.al.¹³⁴

are applied to avoid the pass of undesired wavelengths that are not representative in final chemical analysis.

In addition, to control the frequency stay a bandpass filter is used within a certain range and rejects the other. Besides, the beam splitter, in the component that splits a beam of light in two parts. In this way, the first path goes to the sample and the second one, which comes from the optical microscope, passes to the CCD detector. A diffraction grating is similar to a super prism which divides light into distinct wavelengths while maintaining a high level of resolution¹³⁴.

2.2.3.3. Parameters for Raman Data collection

Raman measurements were carried out with a LabRam HR Evolution microscope, shown in Figure 3.9. Before all experiments, the instrument was calibrated by measuring the Raman peak position of a reference silicon wafer. An excitation from a continuous-wave helium-neon laser at wavelength of 532 nm was used. For the instrument set-up, an objective with a hole and a magnification of 100 as well as a ND Filter of 3.2% were used. Each spectrum is the result of accumulation of 10 spectra, each acquired over 3 seconds from -20 cm^{-1} to 3000 cm^{-1} to eliminate the noise of the final Raman spectra.

All collected Raman spectra were pre-processed by a baseline correction, normalizing and fitted using PeakFit v4.12 software. After subtracting the background using a lineal function as baseline, the peak fitting procedure was completed with the addition, subtraction of redundant peaks, editing parameters and/or functions. Finally, Raman peaks were fitted iteratively until the overall residuals were minimized and a not significant improvement is possible as indicated in the

R^2 . Five Fano peaks (D1, D2 D3 D4 and G) were used, nevertheless as a result of fitting procedure due to the final peak amplitude and large asymmetry these can be classified as Lorentzian peaks.

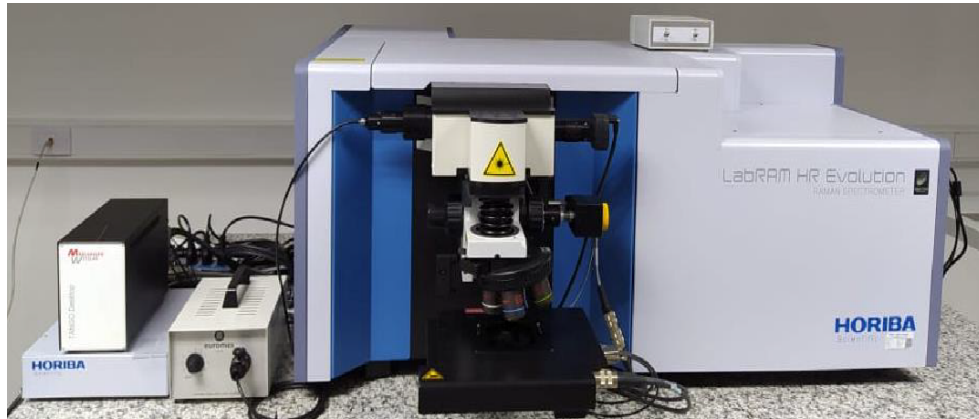


Figure 3.9: LabRam HR Evolution microscope at Yachay Tech University, Ecuador

Chapter 4

Results and Discussion

The results analysis of pristine and decorated banana carbon fibers samples start with the identification of morphology and the main structures present in the pristine fibers, specifically the major presence of (CeO₂) nanoparticles and aggregates after the immersion treatment. To evaluate the distribution and the effectiveness of decoration all of those samples were characterized first by Scanning Electron Microscopy (SEM), to analyze the morphology, distribution and quantitative information about diameter fiber and particle size. Then, for an appropriate characterization, Raman spectroscopy supports interpretation of interactions of functional groups, chemical bonds and structural information at the surface of biomaterial with the light source based on their unique vibrational characteristics (fingerprints) represented in the form of a spectrum.

4.1 Scanning Electron Microscopy (SEM)

Pristine and decorated banana carbon fibers samples analyzed through Scanning Electron Microscopy (SEM) technique, allows to elucidate and observe the surface microstructure and morphology of the samples, giving preliminary information about shape and size of the outermost layer constituents. A SEM micrograph is created by recording the interaction of the electron beam with the specimen, thus the criteria for visibility is tied directly to the contrast represented by a numerical value and the electrical conductivity. Compositional or Atomic Number (Z) Contrast is the principal type of contrast distinguished in micrographs, where the higher atomic number of the element represents higher intensity in the image scanning¹²⁷.

Hence, to identify each specimen in samples, cerium oxide nanoparticles will exhibit more brightness due to their higher atomic number (Z=58) compared with carbon fibers which are composed mainly of carbon atoms (Z=6). According to a series of studies performed by Tschöpe et al., an enhancement of four orders of magnitude related to electronic conductivity when the particle size transitioned from the micro to nanoscale is demonstrated¹³⁵. For that, cerium oxide nanoparticles will show more brightness compared with carbon due to their higher electrical conductivity which depends on the properties of the constitutive atoms and the ways of those are assembled to pass current. In other words, the electrical conductivity of cerium oxide depends both on the structure with many electrons bonded by weak interactions that allow and facilitate

their movement at nanoscale.

4.1.1 Pristine CFs

In Figure 4.1, SEM micrographs elucidates morphology details of pristine CFs samples. Each fiber is composed by several fibrils that maintain a hair-like structure and are parallel grouped forming a kind of bundles. Figure 4.1 (a) shows a micrograph of banana carbon fibers composed by long fibrils that are grouped together which evidence small variations in diameter and minimal curvature along their length. At the surface level, apparently pristine CFs appears straight and homogeneous with a cylindrical structure. Besides, the magnification of the red-highlighted area shown in Figure 4.1 (a) is observed in micrograph (b). Figure 4.1 (b) reveals that each fibril is slender and elongated with an evident variation in diameter scale along their extension. In this regard, in each one of the fibrils is important to note the predominance of some interruptions in their morphology which induces to occasional undulations or crimps of different sizes as well as an adoption of helical waveform.

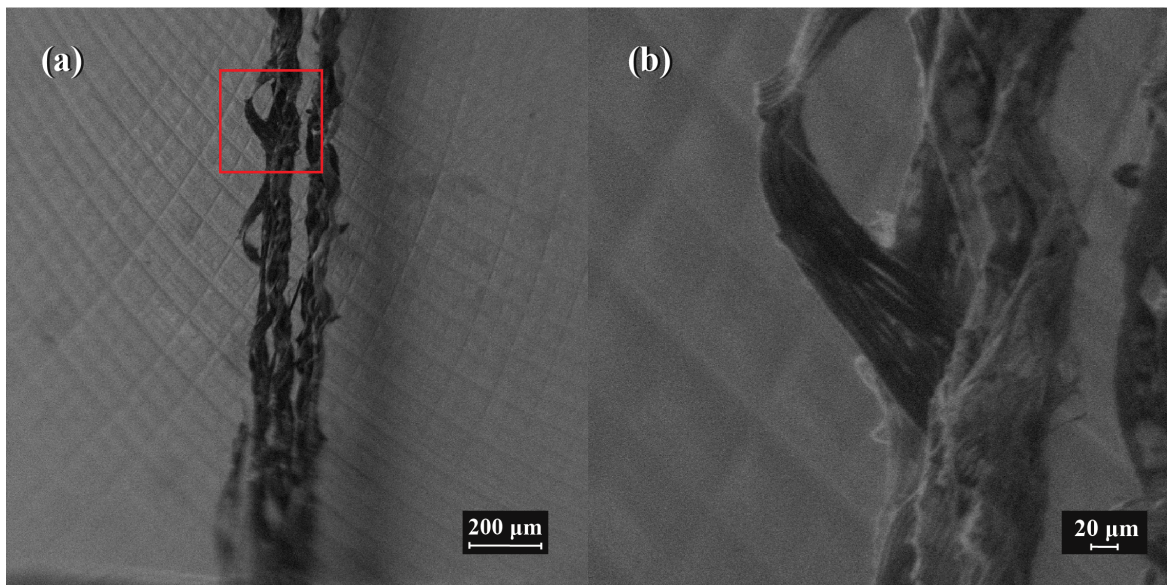


Figure 4.1: Morphological characteristics of pristine CFs. (a) SEM images of pristine carbon fibers. (b) Higher magnification view of the red-highlighted area in (a).

4.1.2 Carbon Fibers decorated with (CeO₂) NPs

At 3.57 mM concentration of (CeO₂) NPs

Figure 4.2 presents the SEM micrographs of nanoceria at a concentration of 3.57 mM bound to CFs samples. The magnification of the red highlighted area shown in Figure 4.2 (a) is observed in

micrograph (b). In depth analysis, in Figure 4.2 (a) banana CFs samples maintain a hair-like shape where each cylindrical fibril presents apparently straight and smooth morphology surfaces with particle deposition. Fibrils are slender, and elongated structures with hierarchical diameter scales that are in parallel, forming a network of aligned fibrils grouped in bundles. In the same way, along the fibrils, some interruptions are observed in their structure due to occasional undulations or crimps of different sizes and others that adopt a helical waveform. As well as, particles of different sizes seems that maintain spherical form and are deposited indistinctly on the surface of carbon fibers.

Besides, Figure 4.2 (b) reveals about twelve smooth-looking cylindrical fibrils, multiple free particles as well as aggregates of them that are randomly dispersed. The particles and aggregates have different shapes, textures and sizes, are distributed and deposited along the fibrils surface. Moreover, the fibers are slightly aligned, some of them have undulations in the form of a fold along their length slightly changing their direction. Mostly, fibers consist largely of fibrils organized in an essentially parallel array along the long axis of the bundle. Probably, the majority of these undulations in the fibers occur due to helical twisting of the constituent fibrils. For that, at both magnifications it is possible to visualize, in terms of contrast and electronic conductivity, the remarkable difference in brightness intensities which confirm the presence of (CeO_2) NPs by reason of higher atomic number and the ability to pass current such as constituents as cerium oxide.

Also, Figure 4.2 (c) shows the histogram of the fiber diameter for decorated CFs at 3.57 mM concentration of nanoceria. Briefly, the fibers were seen to be approximately $0.84 - 2.13 \mu\text{m}$ in diameter. In detail, the fiber diameters follow a typical Gaussian distribution with an average fiber diameter of $1.354 \mu\text{m}$. Observations on the carbon fiber diameters determines that 46.4% of all measured structures have sizes from 1.4 to $1.6 \mu\text{m}$. Further, 35.5% related with sizes between $1.0 - 1.4 \mu\text{m}$, 10.9% associated with diameters between $0.8 - 1.0 \mu\text{m}$, and 7.2% shows sizes from 1.6 to $2.2 \mu\text{m}$.

Finally, Figure 4.2 (d) reports the shape and distribution of particle size frequency of the most visible cerium oxide nanoparticles. According to the analysis of SEM images is possible to determine that 80% of all measured structures have sizes between 100-200 nm. Then, 11.25% is related with sizes from 200 to 300 nm, about 5% shows particles from 0 to 100 nm, also 2.5% related with the formation of the biggest structures from 300-500 nm, and 1.25% are related to aggregates from 800-900 nm observed in the micrograph.

At 7.14 mM concentration of (CeO_2) NPs

Figure 4.3 shows SEM micrographs of cerium oxide nanoparticles at [7.14] mM bound to CFs samples. Higher magnification view of the region indicated with the red box in Figure 4.3 (a) is presented in (b). SEM image, Figure 4.3 (a), shows thin and elongated banana CFs with evident set of fibrils that are indistinctly aligned forming bundles. Each fibril maintain a hair-like shape with minimal helical waveform that is running in a longitudinal and oblique course. Also, is shown a high proportion of rounded fibrils with evident amounts of deformations (wrinkles, kinks and curls) which follows the helical path of the fibrils around the fiber. Gradations in fibril

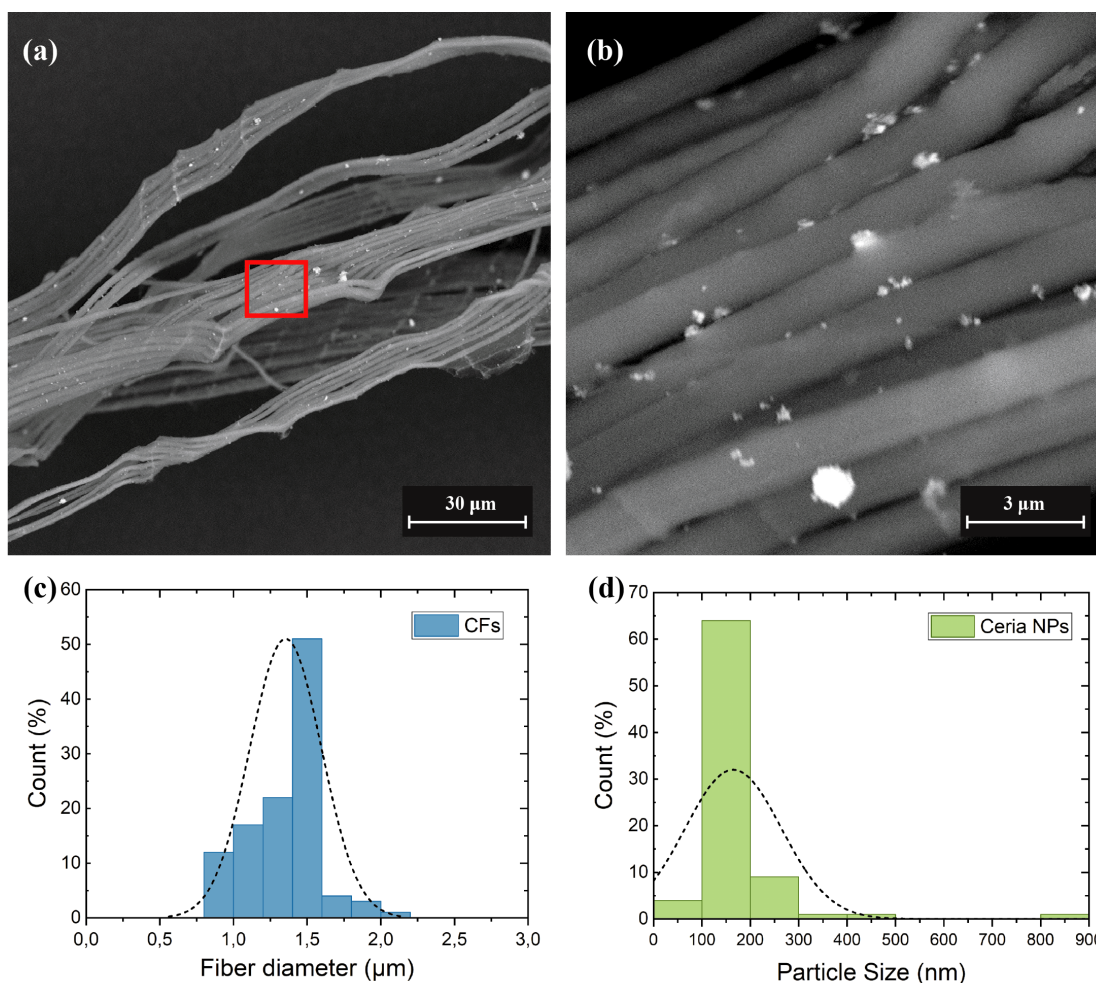


Figure 4.2: Characteristics of banana CFs decorated with (CeO_2) NPs at 3.57 mM. (a) SEM micrographs of nanoceria bound to CFs samples. (b) Higher magnification view of the region indicated with the red box in (a). (c) Histogram of the fiber diameter for decorated CFs extracted from (b). (d) Histogram for the major features of the distribution of cerium oxide NPs size.

thickness can easily be seen while observing whole fibers, but when a magnification is applied are even more evident. About the morphology of the surface of the fibrils, they preserve a cylinder shape with smooth and homogeneous texture. As well as, lustrous-small particles of different shapes and sizes deposited on the surface of CFs can be seen.

Also, in Figure 4.3 (b) smooth-looking cylindrical fibrils with multiple free particles as well as cloud-like aggregates of them are randomly disperse. Those, are spread and deposited along the fibrils surface in a variety of forms, textures, and sizes. As mentioned above, gradations in fibril thickness are more visible at higher magnifications, and effectively fibrils presents a variable diameter along their length. Mostly, fibrils appears with a longitudinal course, that are organized

in an essentially parallel way along the bundle. Also, fibrils show a high proportion of rounded edges with some deformations like wrinkles, kinks and curls. Many of these fiber undulations are most likely caused by helical twisting of the constituent fibrils. In this way, is possible to confirm the existence of cerium oxide nanoparticles, due to Z-contrast and electronic conduction, where (CeO_2) NPs can be identified as free and aggregated structures with a considerably different magnitude of brightness compared with carbon constituents.

In order to report the shape and distribution of fiber diameter and particle size, Figure 4.3 (c) and (d) respectively, shows the percentage of occurrences in the data for each variable. The histogram of the fiber diameter for decorated CFs at [7.14]mM concentration of nanoceria is shown in Figure 4.2 (c). The fibers were seen to be approximately $0.84 - 2.25 \mu\text{m}$ in diameter. Moreover, fiber sizes follow a standard Gaussian distribution, with a $1.363 \mu\text{m}$ average diameter from a statistical sample equivalent to 110 random measurements. According to observations of fiber diameters, 37.2 % of all measured structures have sizes between 0.8 and $1.2 \mu\text{m}$. Thoroughly, 32.7 % related with sizes between $1.2 - 1.6 \mu\text{m}$, while 23.6 % is associated with diameters between $1.6 - 1.8 \mu\text{m}$, and just 6.4 % shows sizes from 1.8 to $2.4 \mu\text{m}$.

Finally, Figure 4.2 (d) presents the shape and particle size frequency distribution of the most visible cerium oxide nanoparticles. Based on SEM image analysis is possible to determine that 63.3 % of all measured structures have diameters between 0 and 200 nm. Then, 23.3 percent is related to aggregates from 200-400 nm, about 8.33 % is related to particles from 400 to 600 nm, while 1.67 % is associated to the formation of the largest structures from 600-800 nm. A small percentage, specifically, 1.67 % is related to aggregates from 1200 to 1400 nm and the largest aggregates are ranged from 1600 to 1800 nm with just a 1.67 % of the total of measurements.

Because of the scanning electron microscope (SEM) allows for direct inspection of complete fibers, it also allows for the detection of changes in fiber shape and distribution of particles over their surface. Regarding the diameter of the carbon fibers, the distribution shows similar intervals for both concentrations that is, we have fibers between 0.8 and $2.25 \mu\text{m}$ with an average of $1.3585 \mu\text{m}$. According to the analysis on the size of particles that have been deposited on the surface of the fibers a large percentage is related to particles between 0 and 400 nm. With a concentration of 3.57 mM, it is evident that the particles are smaller therefore the agglomerations have a smaller size. With all this, it can be said that there is a lower concentration of CeO_2 nanoparticles with a better distribution along the fibers. In contrast, with a concentration of 7.14 mM, it is evident that the particles are of relatively larger size as well as that of the agglomerations. With all this, it can be concluded that there is a higher concentration of nanoparticles distributed indistinctly but agglomerated mostly, in other words there is little distribution on the surface of the fibers forming larger structures. For that, the micrographs appears more lustrous than those at concentration of 3.57 mM and pristine samples.

According to Tanvir and Qiao¹³⁶, as the amount of nanoparticles in a fluid increases, more NPs are carried to the surface of the liquid and try to get closer to each other. As a consequence, the cohesion forces that occur between the molecules are stronger which results in an increase in the surface tension of the solution with nanoparticles. In addition, by increasing the concentration of nanoparticles it is possible to show that the space between them and the molecules is reduced.

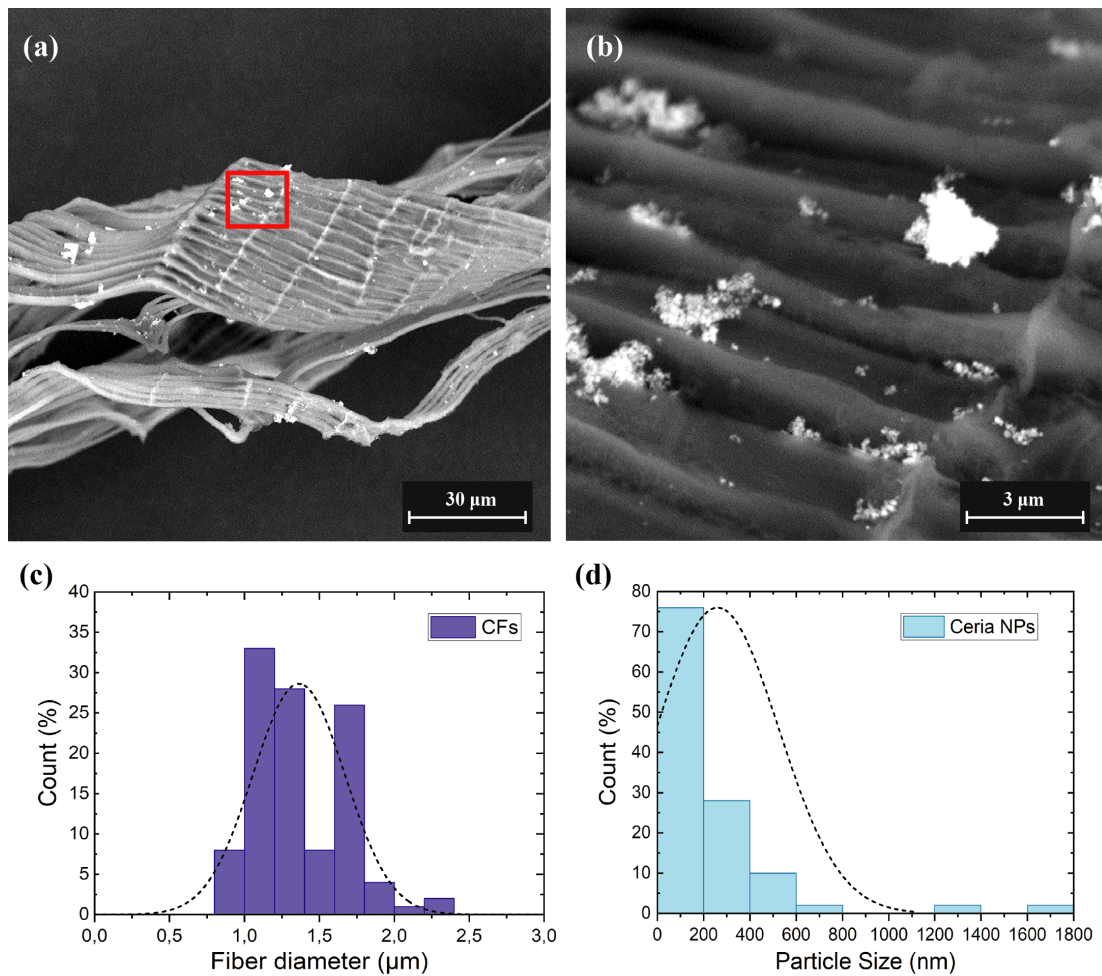


Figure 4.3: Characteristics surface morphology of banana CFs decorated with (CeO₂) NPs at [7.14] mM. (a) SEM images of CFs decorated with nanoceria. (b) Higher magnification view of the highlighted region in (a). (c) Histogram of the size distribution for (CeO₂)NPs/CFs extracted from (b). (d) Histogram for the distribution of cerium oxide particle size.

Thus, applying the attractive Van der Waals forces with respect to the electrostatic repulsion typical of molecules increases the surface tension of the nanofluid.

4.2 Raman Spectroscopy

As mentioned before, Raman spectroscopy aids the identification of crystalline phases present in most materials depending on the number of bands and wavenumbers detected. These characteristics are related to their bonds force constants and space group. According to the literature, pure cerium oxide exhibits a sharp intense peak at 464.8 cm^{-1} which is attributed to the F_{2g} cubic fluorite structure peak of (CeO_2) ¹³⁷.

In this study, Raman spectra of decorated CFs at both concentrations shows a slight peak at 450.30 cm^{-1} . The normalized Raman spectra of the pristine and decorated carbon fibers samples are displayed in Figure 4.4. Each spectrum is characterized by two main broad bands, the D band located at 1318.11 cm^{-1} and G band situated at 1588.63 cm^{-1} . In general, for the three different samples, the intensity of G band dominates which is originated from the interactions between C-C bonds assigned to the in-plane tangential stretching of all pairs of sp^2 atoms¹³⁸. In contrast, D band is related to the scattering from defects or disorders present in the carbon structure¹³⁹.

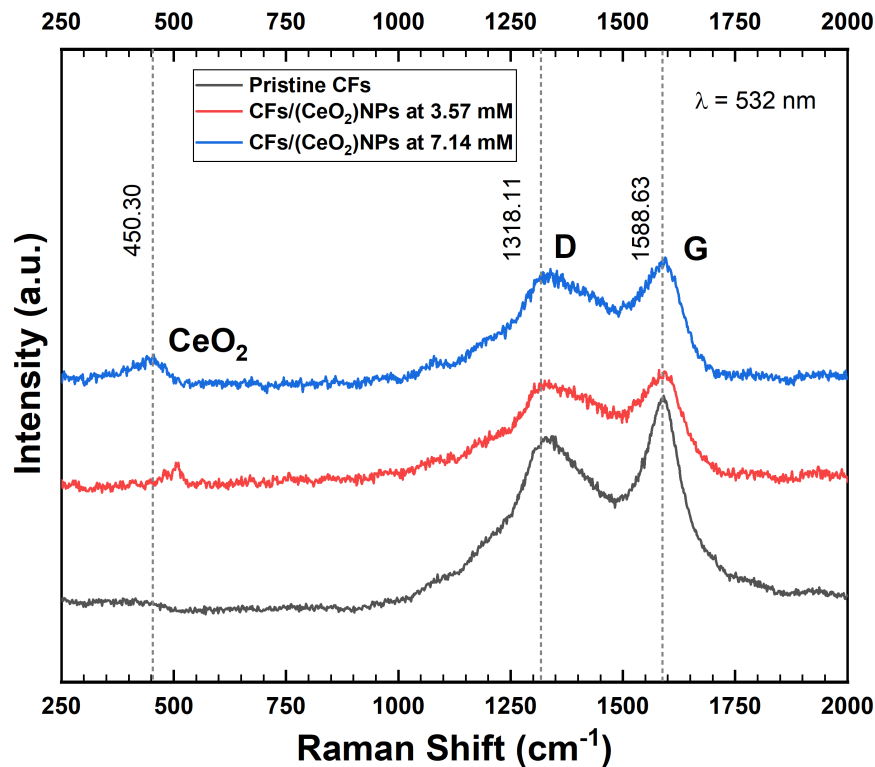


Figure 4.4: Raman spectra of banana CFs decorated with (CeO_2) NPs at 3.57 mM and 7.14 mM excited with 532 nm laser.

The G band nearly to 1588 cm^{-1} presents a sharp peak for pristine CFs, while it broadens along with the appearance of a shoulder at approximately 1560 cm^{-1} or a D' band due to the

presence of defects in the decorated carbon fiber structure. Concomitantly, an increase in the intensity of the D band at approximately 1318 cm^{-1} is observed for decorated samples. In this regard, the intensity of the D defect band can be attributed to the typical oxygen vacancies of cerium crystal structure¹⁴⁰.

Additionally, for those samples decorated with cerium oxide nanoparticles is shown a third peak that confirms the presence of nanoparticles along the carbon fiber surface. Raman spectra reported in Figure 4.4 contain shoulders on both sides of the F_{2g} band which explain minimal distortions at the typical fluorite structure¹⁴⁰. For CFs decorated at a concentration of 3.57 mM, the typical cerium oxide peak is narrower and redshifted at about 510 cm^{-1} which becomes a clear indicator of changes at crystalline composition¹⁴⁰. On the other hand, for CFs decorated with CeO_2 NPs at concentration of 7.14 mM the F_{2g} band was broader than the previous one.

4.2.1 Pristine CFs

In order to obtain an appropriate curve fitting and deconvolution of the spectral line profile, the Lorentzian functions are used to adjust the G and D bands successfully. According to Fung et al.¹⁴¹ and Hecht et al.¹⁴² it describes the shape of spectral lines which undergo homogeneous broadening, in which all atoms interact with the frequency range included in the line shape that allows us to obtain information on the contribution of both the sample and the spectrum.

Figure 4.5 compares the experimental spectra with the fitting curves as well as presents the proposed deconvolution of each band for Pristine carbon fibers measured at 532 nm laser excitation. After testing some deconvolution pathways with three and five contributions, the most accurate results ($R^2 = 0.9907$) were obtained using five peaks (G, D1, D2, D3 and D4) shown in Figure 4.5 (b) and summarized in Table 4.1. The main bands D and G are located at approximately 1318.11 cm^{-1} and 1588.63 cm^{-1} , respectively.

Table 4.1: Fitted parameters for D4, D3, D2, D1 and G bands.

Band	Amplitude	Center	FWHM
D4	32.6417197	418.002567	512.698815
D3	5.70534776	1087.12845	59.2825640
D1	271.631482	1338.91124	248.593092
D2	2.82159724	1393.31550	120.000000
G	286.975079	1584.35731	122.318343

D1 band, centered at 1338.91 cm^{-1} , is indexed to the vibration mode of microcrystalline graphite while D2, at approximately 1393.31 cm^{-1} , is assigned to the vibration mode typical of disordered graphitic lattice¹³⁹. Moreover, D3 band around 1087.13 cm^{-1} is attributed to an amorphous carbon contribution¹³⁹ and for D4 band centered at 418.00 cm^{-1} is qualified by a rich phase of sp^3 hybridized atoms that are related to C-H termination groups or, in general terms to adsorbed molecules or molecular fragments¹⁴³.

4.2.2 Carbon Fibers decorated with (CeO₂) NPs

The normalized Raman spectra, with a laser excitation of 532 nm for decorated carbon fibers samples with cerium oxide nanoparticles at a concentration of 3.57 and 7.14 mM are presented in Figure 4.6 and Figure 4.7, respectively. For both, in (a) is displayed the experimental Raman spectra with its respective Fitting curve and in (b) the proposed spectra deconvolution.

After testing some deconvolution pathways, the most accurate results in relation to their Pearson's coefficient for 3.57 mM ($R^2 = 0.9890$) and for 7.14 mM ($R^2 = 0.9830$) were obtained with five contributions for carbon constituents and three for cerium oxide. G, D1, D2, D3, and D4 bands as well as their related with presence of nanoparticles are shown in Figure 4.6 (b) for NPs at a concentration of 3.57 mM and in Figure 4.7 (b) for the variation at 7.14 mM. Additionally, to compare fitting parameters such as Amplitude, Center and the Full Width at Half Maximum (FWHM) measured for deconvolution are summarized in Table 4.2.

Table 4.2: Summarized Fitted parameters for D4, D3, D2, D1 and G bands of decorated carbon fibers at both concentrations 3.57 and 7.14 mM.

Band	At 7.14 mM			At 3.57 mM		
	Amplitude	Center	FWHM	Amplitude	Center	FWHM
D4	11.9535880	1146.37797	273.073055	14.2961793	1146.37818	316.160216
D3	27.8532738	1450.00052	104.040548	23.2533989	1450.00058	116.432048
D2	59.6220195	1556.49682	83.5437341	50.9025056	1556.49691	94.4876549
D1	93.1786211	1340.91093	187.308661	83.5494583	1340.91099	199.979013
G	72.3340551	1605.00028	56.2877081	62.7749768	1605.00034	67.3410062

At 3.57 mM and 7.14 mM, the main bands for D and G are located at 1340.91 cm^{-1} and 1605.00 cm^{-1} , respectively. As mentioned before, G band is assigned to planar sp^2 configured carbon atoms while D band is related to sp^2 carbon atoms with disorder and defects. According to Ammar and Rouzaud¹⁴⁴, in highly-oriented pyrolytic graphite (HOPG) is not exhibit the D band because of presents the highest degree of order at its three-dimensions.

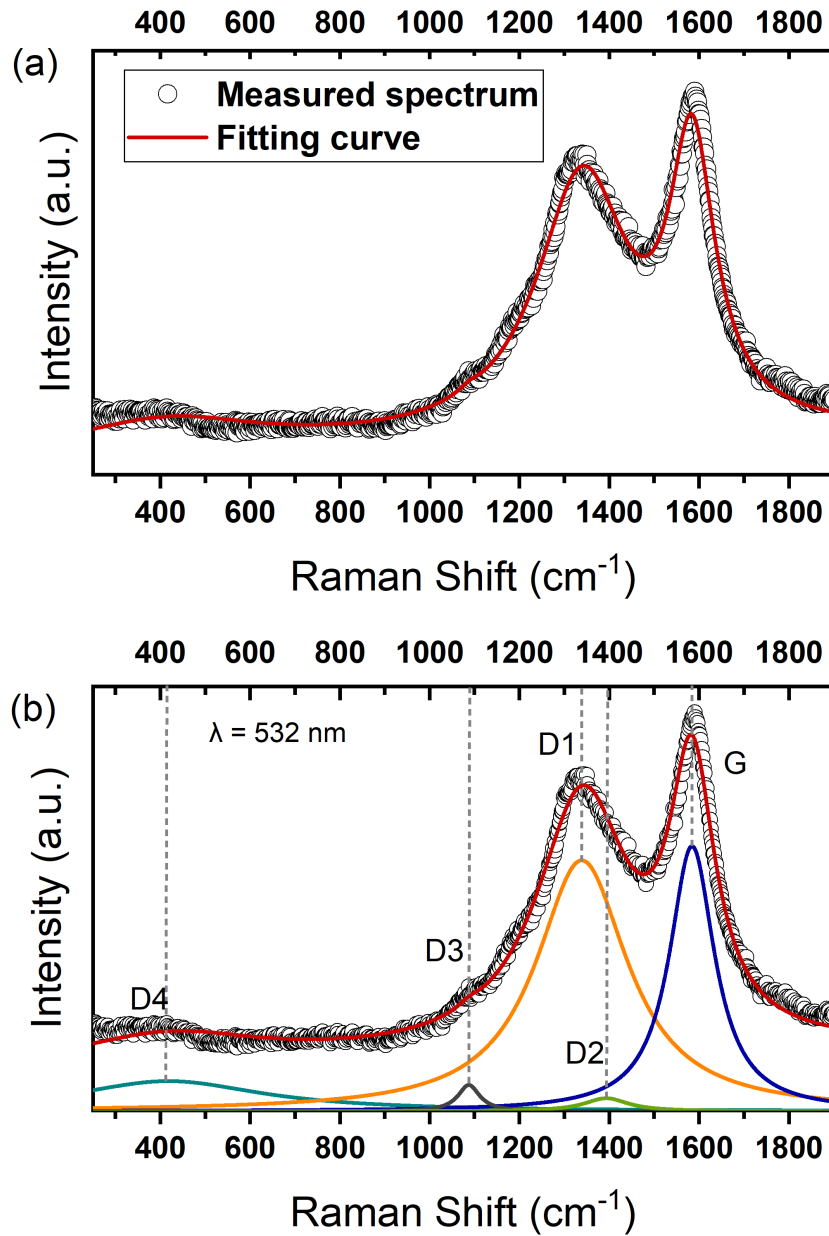


Figure 4.5: Raman spectroscopy of Pristine carbon fibers excited with 532 nm laser. In (a) Measured Raman spectra with respective Fitting curve and in (b) proposed spectra deconvolution.

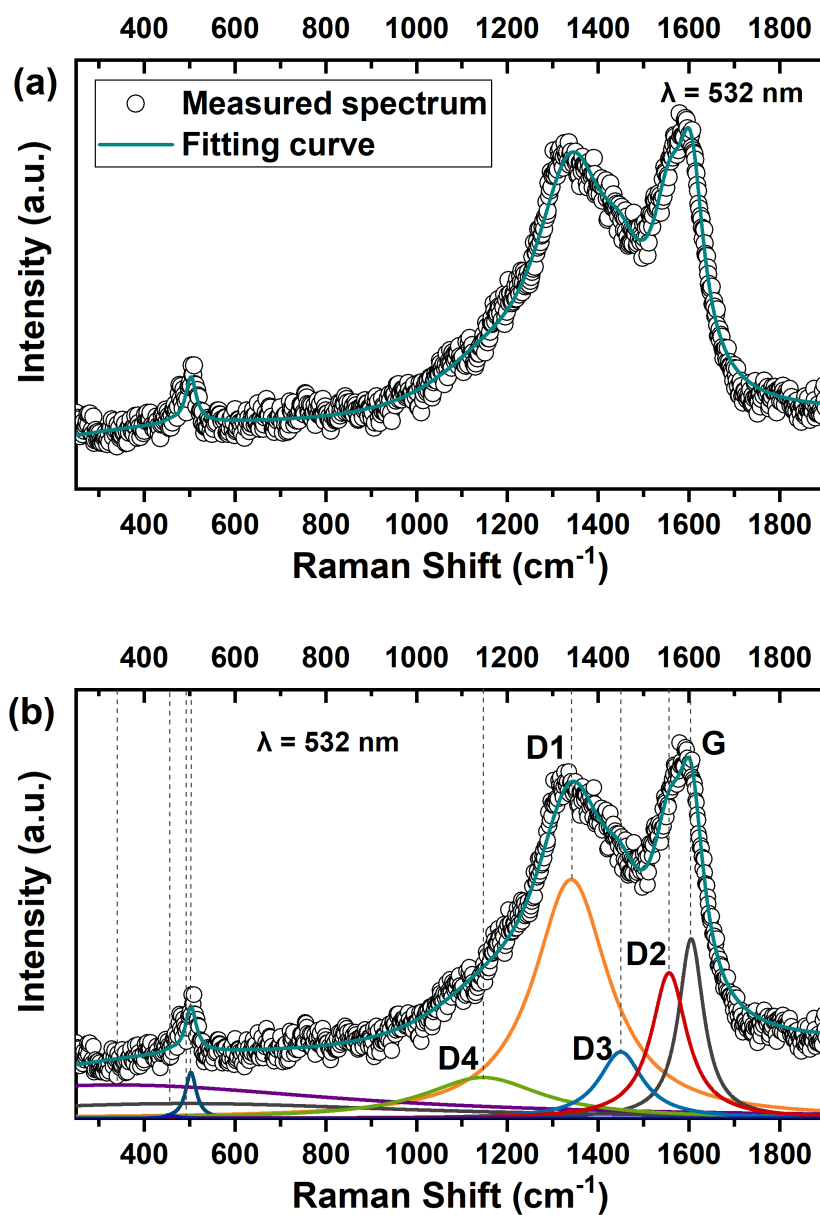


Figure 4.6: Raman spectroscopy of decorated carbon fibers at 3.57 mM excited with laser wavelength of 532 nm. In (a) Measured Raman spectra with respective Fitting curve and in (b) proposed spectra deconvolution.

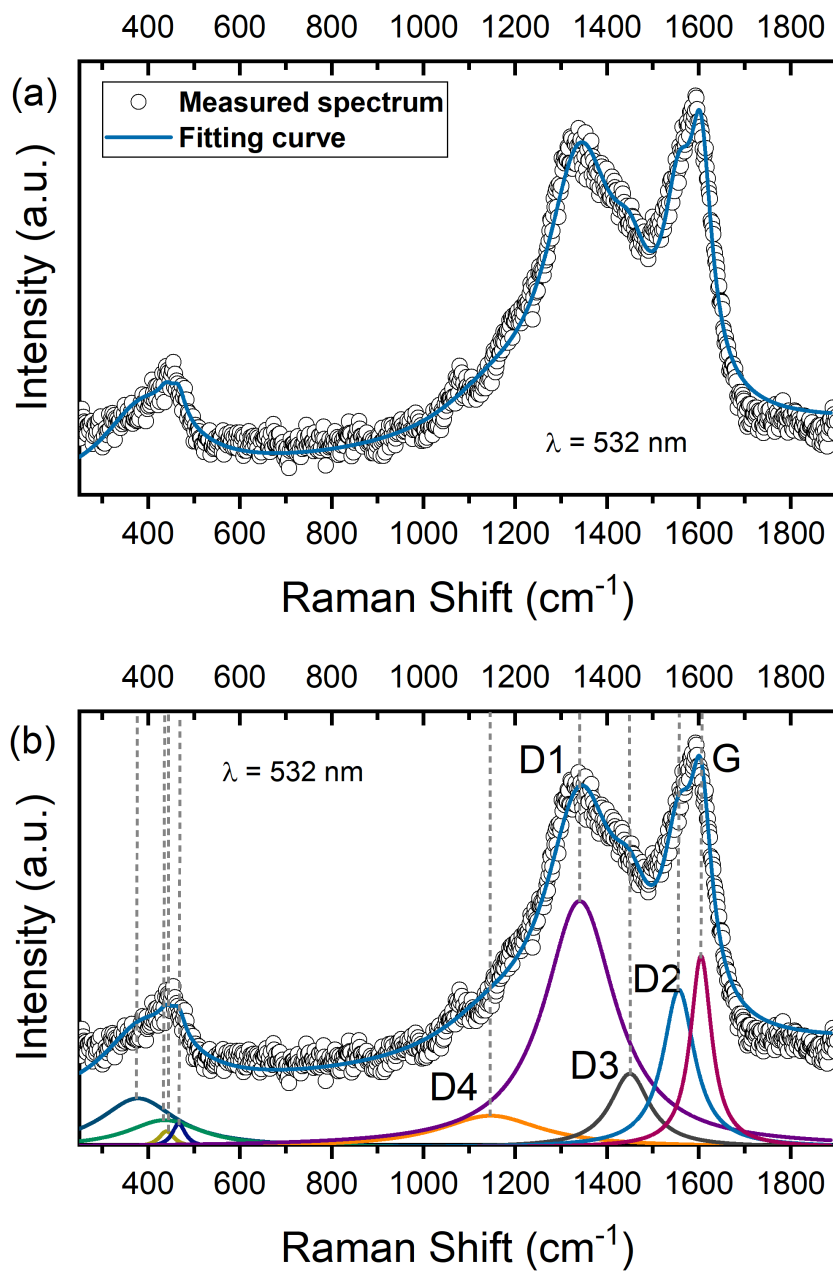


Figure 4.7: Raman spectroscopy of decorated carbon fibers at 7.14 mM excited with laser wavelength of 532 nm. In (a) measured Raman spectra with respective Fitting curve and in (b) proposed spectra deconvolution.

For that, in this study carbon contributions refers to a disordered or amorphous structure. In this regard, with respect to HOPG, the D bands for CFs samples are shown with a representative intensity that allows to determine that the carbon fibers maintain a disordered or amorphous structure. Interestingly, and attached to the real configuration for both concentrations each peak maintains the same position and very similar results for amplitude and FWHM.

D1 band is centered at 1340.91 cm^{-1} , D2 band is located at approximately 1556.49 cm^{-1} . Moreover, D3 and D4 bands, centered around 1450.00 cm^{-1} and 1146.37 cm^{-1} , respectively. As discussed earlier, D1 band is assigned to the vibration mode of microcrystalline graphite, while D2 band is attributed to the vibration mode typical of disordered graphitic lattice¹³⁹. Besides, D3 and D4 bands are indexed to the presence of amorphous carbon contributions¹³⁹ and as a rich phase of sp^3 hybridized atoms related with C-H terminations, respectively¹⁴³.

Besides, considering the crystal structure of ceria (cubic fluorite), Raman spectra provide crucial information for interpretation and analysis based on wave number, intensity and width of the F_{2g} band. To understand how the concentrations of cerium oxide nanoparticles affect the spectra and elucidates about structural configuration it is necessary to zoom in on the deconvoluted area between $250 - 800 \text{ cm}^{-1}$. In Table 4.3 are reported the amplitude or intensity, center and FWHM parameters for cerium oxide at both concentrations.

Also, Figure 4.8 compares the Raman spectra for both concentrations, in (a) a symmetrical peak with low intensity is shown at $\sim 494.096 \text{ cm}^{-1}$, which also presents a slight displacement to the right (red-shift) compared to the one with the highest concentration and the literature for pure cerium oxide 464.8 cm^{-1} . The last change can be attributed to the reduction of CeO_2 that leads to the formation of vacancies of oxygen and Ce^{+3} cations. In this regard, it leads to decreasing of bonds forces and increasing unit cell parameters which induces to red-shift of the F_{2g} band¹⁴⁵.

Table 4.3: Fitted parameters for cerium oxide contribution at 3.57 and 7.14 mM.

Peak	At 7.14 mM			At 3.57 mM		
	Amplitude	Center	FWHM	Amplitude	Center	FWHM
C1	18.5143654	377.926010	200.000000	11.6908810	339.696029	1205.83026
C2	10.2957852	436.001000	200.000000	0.86921447	459.920185	36.9546250
C3	6.07408390	439.999205	40.9464110	5.18604356	494.095906	1181.17895
C4	8.91511536	466.627087	35.4318751	16.0694551	503.000144	28.7450876

In Figure 4.8 (b) there is an asymmetrical peak, with an amplitude lower than the previous one and a much higher FWHM centered at 439.999 cm^{-1} . Also, it presents a slight displacement to the left (blue-shift) compared to the one with the lowest concentration and the literature for pure cerium oxide (464.8 cm^{-1}). This can be explained with an earlier study¹⁴⁶, which reports that peak of cerium oxide or fluorite structure band exhibits a low frequency as a consequence of the stabilizing effect of the oxygen structure in cerium oxide. According to the literature, the bands located at approximately 466 cm^{-1} are attributed to the F_{2g} band. This bands are related to symmetrical stretching vibrations of the $Ce - O_8$ units, that involves both O-O and Ce-O force

constants, where the contribution between oxygen species is larger than the stretching between cerium and oxygen¹⁴⁰.

The peak intensity ratios, which are assigned to compare the defect in carbon structures, are reported in Table 4.4. The I_D/I_G for pristine carbon fibers presents a value around 0.936, while for decorated carbon fibers are obtained a ratio of $I_D/I_G = 1.330$ and $I_D/I_G = 1.288$ for samples at 3.57 mM and 7.14 mM, respectively.

Table 4.4: Comparative intensity ratio for Pristine CFs and decorated CFs at 3.57 and 7.14 mM.

		Pristine CFs	At 3.57 mM	At 7.14 mM
D band	Center	1338.91124	1340.91099	1340.91093
	Intensity	271.631482	83.5494583	93.1786211
G band	Center	1584.35731	1605.00034	1605.00028
	Intensity	286.975079	62.7749768	72.3340551
I_D/I_G		0.936740781	1.33093571	1.28817085

Therefore, it can be assumed that cerium oxide nanoparticles are on the surface of banana stem carbon fibers. Having a greater intensity ratio at a concentration of 3.57 mM, can be assumed that this defect is due to a greater distribution of nanoparticles due to its smaller size and reduced amount of agglomerates on the carbon fibers. As evidenced in the study of morphology with SEM micrographs, at a higher concentration of nanoparticles during the immersion process it is possible to observe a lower distribution of NPs on the surface of the fiber.

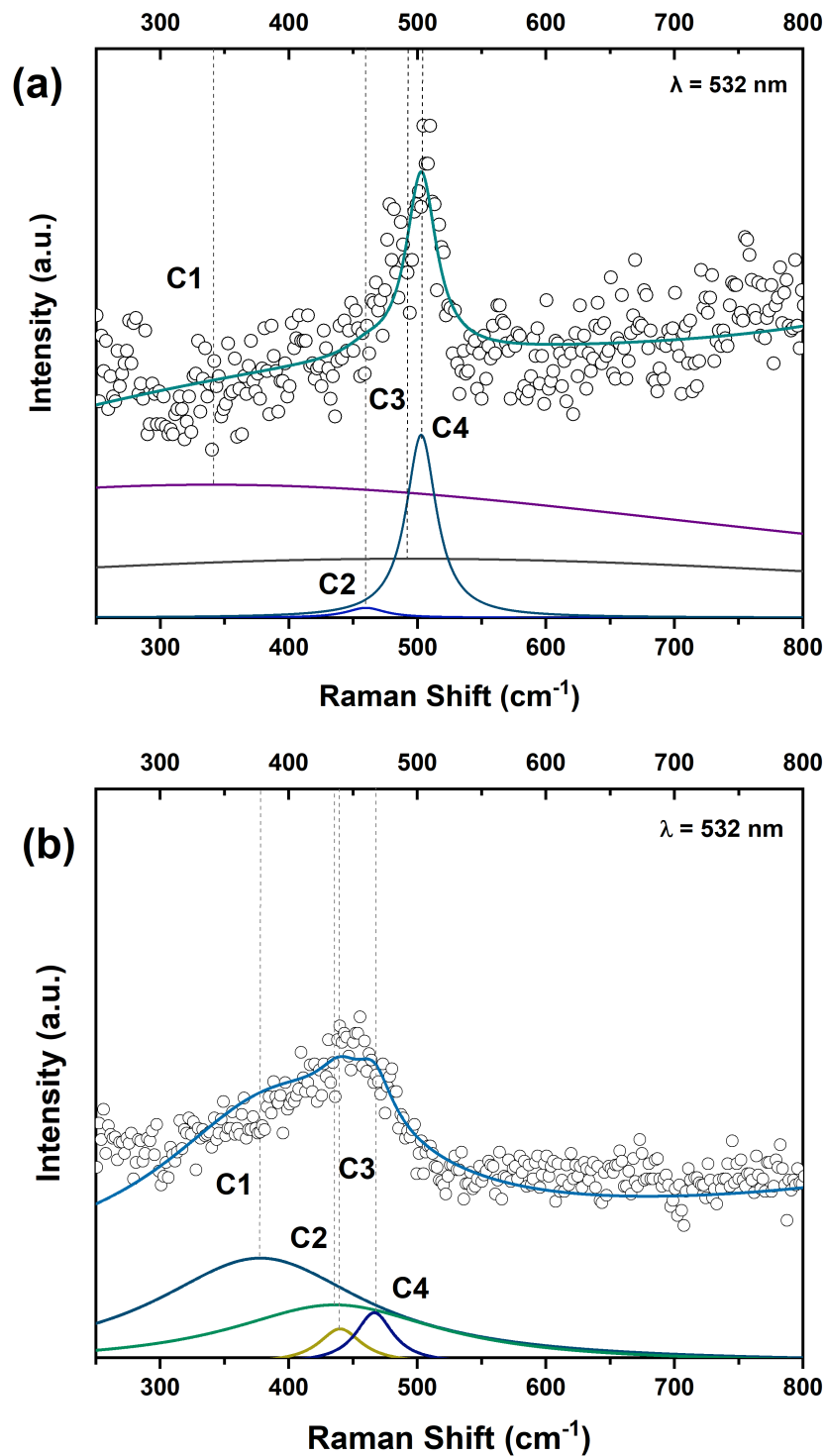


Figure 4.8: Raman spectroscopy of CeO_2 contribution at 3.57 and 7.14 mM excited with $\lambda = 532 \text{ nm}$. In (a) Measured Raman spectra with respective Fitting curve and deconvolution for 3.57 mM and in (b) measured spectra, fitting curve and proposed deconvolution for 7.14 mM.

Chapter 5

Conclusions and Outlook

In general, carbon fibers obtained from lignin or cellulose-based precursors need several studies for synthesis and thermal treatment conditions as well as many other parameters to enhance manufacturing of high-performance carbon fibers due to their low degree of orientation, amorphous structure and discontinuities. To summarize, this research project reports a comprehensive approach that involves Scanning electron microscopy as well as Raman spectroscopy supported by deconvolution of the different lattice vibrations to consider all the contributions of the different constituents. Indeed, morphological characteristics for CFs obtained from biomass precursors were determined.

Banana carbon fibers maintain a hair-like shape with several slender and elongated fibrils, that demonstrates hierarchical diameter scales which are generally arranged in networks of aligned and grouped in bundles. In relation of particles size, at lower concentration of cerium oxide nanoparticles there is a better distribution along the fibers, while at higher concentration is evident that particles are of relatively lower distribution because of presence of agglomerations. More in detail, if the concentration of nanoparticles is too high, there will be greater agglomeration. This tendency to come together and form agglomerations can be explained by the stronger cohesion forces that occur between the molecules when the spaces are reduced between them. All this is consistent with the results that tell us that having a higher concentration there are more agglomerations and therefore a low-grade of distribution along the fibers. On the contrary, at lower concentration the surfactant acts and allows the nanoparticles to be better distributed and therefore there are not so many agglomerations. With the above mentioned it is possible to report that concentration of nanoparticles maintain a direct influence on the formation of agglomerations and the final distribution at the surface of the fibers.

On the other hand, with vibrational analysis performed by Raman spectroscopy five contributions are presented (D1, D2, D3, D4 and G bands). The spectrum is characterized by two main broad bands (D1 and G), characteristic of carbon material constituents. The G band dominates and is related to the in-plane vibrational mode of graphene. As a result of carbon fiber structure there is a little bit disordered and the D1 band is related to the scattering from defects or disorders present in the carbon constituent. Which is not a bad feature since a high concentration of defects in the structure allows us to have an extremely high volume and density that is of great impor-

tance for biomedical applications. D2 bands are assigned to the vibration mode of disordered graphitic lattice. Besides, D3 and D4 bands are indexed to amorphous carbon contributions and sp^3 hybridized atoms in C-H terminations. With this, it can be determined that there is an interaction between the NPs and the hexagonal structure of the carbon atoms corresponding to the fibers. Furthermore, based on the crystal structure of cerium oxide (cubic fluorite), Raman spectra provide a characteristic peak which provides information on the wavenumber, intensity and width of the F_{2g} band. Also, due to the presence of shoulders in the intermediate structure between D1 and G bands it can be said that the nanoparticles are attached to the fibers.

Carbon fibers obtained from banana stem and functionalized with cerium oxide nanoparticles has been found to possess great potential for a broad range of biomedical applications, particularly as their similarity with hard carbon structure. However, there is a lot of work which has not achieved in this study to elucidate the intrinsic relation between the synthesis parameters and the final structure properties to propose a specific application. Therefore, it is necessary to conduct scientific research efforts to elucidate the precise relation between the synthesis parameters and the structural properties. In that way, the optimization of the hydrothermal carbonization process as well as that of graphitization at different temperatures and residence times become an important approach to define the final properties. Another significant approach to this research is related to the activation and post treatment process as well as the pre-functionalization of carbon fibers to obtain a better attachment of functional groups at the surface.

In this regard, multiple characterization techniques can be applied to obtain more detail about physical and chemical properties. In addition, the biosynthesis of ceria nanoparticles from natural precursors, in order to being an ecological alternative, will considerably improve acceptance in living organisms, guaranteeing the bio-availability of this nanocomposite in biomedical applications. Because of their phenomenal physicochemical properties, banana carbon fiber would be used as a reinforcement in both thermoplastic and thermoset matrices as an eco-friendly alternative for multiple purposes. In the future, these CFs can be combined with certain polymers, ceramics, metals and other composites for the reinforcement and/or to add functionalities in carbon fiber manufacturing applied for medical devices and orthopedic implants. Without a doubt, for a Latin American country and the society in general, through the management and waste treatment a new era of research, innovation and technological benefits is possible. In order to achieve this, it is indispensable to assure that carbon fibers present specific chemical and physical properties.

Bibliography

- [1] Wagner, W. R.; Sakiyama-Elbert, Shelly E. Zhang, G.; Yaszemski, M. J. *Biomaterials Science: An Introduction to Materials in Medicine*. Elsevier Inc., 4th ed.; Academic Press, 2020; p 1651.
- [2] Bose, S.; Bandyopadhyay, A. In *Characterization of Biomaterials*; Bandyopadhyay, A., Bose, S., Eds.; Academic Press: Oxford, 2013; pp 1–9.
- [3] Willyard, C. Timeline: Regrowing the body. *Nature* 2016 540:7632 **2016**, 540, S50–S51.
- [4] Crubezy, E.; Murail, P.; Girard, L.; Bernadou, J. P. False teeth of the Roman world [3]. *Nature* **1998**, 391, 29.
- [5] Boyle, M. O. Cultural Anatomies of the Heart in Aristotle, Augustine, Aquinas, Calvin, and Harvey. *Springer Nature* **2018**, 27.
- [6] Marin, E.; Boschetto, F.; Pezzotti, G. Biomaterials and biocompatibility: An historical overview. *Journal of Biomedical Materials Research - Part A* **2020**, 108, 1617–1633.
- [7] Bhat, S. V. *Biomaterials*; Springer Netherlands, 2002; p 273.
- [8] Williams, D. F. *Definitions in biomaterials: proceedings of a consensus conference of the European Society for Biomaterials, Chester, England, March 3-5, 1986 / edited by D.F. Williams*; Elsevier, 1987.
- [9] David, Williams. Xingdong, Z. *Definitions of Biomaterials for the Twenty-First Century*; Elsevier Inc. Academic Press, 2019; p 280.
- [10] NIBIB, *Biomaterial* | *National Institute of Biomedical Imaging and Bioengineering*; 2015.
- [11] Tranquilli L., P.; Merolli, A. In *Biomaterials in Hand Surgery*; Merolli, A., Joyce, T. J., Eds.; Springer Milan: Milano, 2009; pp 1–11.
- [12] Galletti, P. M.; Boretos, J. W. Report on the Consensus Development Conference on “Clinical Applications of Biomaterials,” 1–3 November 1983. *Journal of Biomedical Materials Research* **1983**, 17, 539–555.
- [13] Williams, D. F. On the mechanisms of biocompatibility. *Biomaterials* **2008**, 29, 2941–2953.

- [14] Ratner, B. D. The biocompatibility manifesto: Biocompatibility for the twenty-first century. *Journal of Cardiovascular Translational Research* **2011**, *4*, 523–527.
- [15] J.R. Davis, Handbook of Materials for Medical devices. *ASM International The Materials Information Society* **2003**, 318.
- [16] Huang, J.; Best, S. *Tissue Engineering Using Ceramics and Polymers: Second Edition*; 2014; pp 3–34.
- [17] Al-Maharma, A. Y.; Patil, S. P.; Markert, B. Effects of porosity on the mechanical properties of additively manufactured components: a critical review. *Materials Research Express* **2020**, *7*.
- [18] Physical and Chemical Properties of Matter - Chemistry LibreTexts.
- [19] Schnabelrauch, M. Chemical bulk properties of biomaterials. *Biomaterials in Clinical Practice: Advances in Clinical Research and Medical Devices* **2017**, 431–459.
- [20] Murphy, W.; Black, J.; Hastings, G. *Handbook of Biomaterial Properties, Second Edition*; 2016; pp 1–676.
- [21] Lasprilla, A. J.; Martinez, G. A.; Lunelli, B. H.; Jardini, A. L.; Filho, R. M. Poly-lactic acid synthesis for application in biomedical devices — A review. *Biotechnology Advances* **2012**, *30*, 321–328, Systems Biology for Biomedical Innovation.
- [22] SHABALOVSKAYA, S.; VAN HUMBEECK, J. In *Shape Memory Alloys for Biomedical Applications*; Yoneyama, T., Miyazaki, S., Eds.; Woodhead Publishing Series in Biomaterials; Woodhead Publishing, 2009; pp 194–233.
- [23] He, Y.; Wang, C.; Wang, C.; Xiao, Y.; Lin, W. An Overview on Collagen and Gelatin-Based Cryogels: Fabrication, Classification, Properties and Biomedical Applications. *Polymers* **2021**, *13*.
- [24] Fiume, E.; Magnaterra, G.; Rahdar, A.; Verné, E.; Baino, F. Hydroxyapatite for Biomedical Applications: A Short Overview. *Ceramics* **2021**, *4*, 542–563.
- [25] Biscarini, A.; Mazzolai, G.; Tuissi, A. Enhanced Nitinol Properties for Biomedical Applications. *Recent Patents on Biomedical Engineering* **2008**, *1*, 180–196.
- [26] Maitz, M. Applications of synthetic polymers in clinical medicine. *Biosurface and Biotechnology* **2015**, *1*, 161–176, SPECIAL ISSUE ON FUNCTIONAL SURFACES OF BIOMATERIALS.
- [27] Miranda, I.; Souza, A.; Sousa, P.; Ribeiro, J.; Castanheira, E.; Lima, R.; Minas, G. Properties and applications of PDMS for biomedical engineering: a review. *Journal of Functional Biomaterials* **2022**, *13*, 2.

- [28] Daniell, H.; Mangu, V.; Yakubov, B.; Park, J.; Habibi, P.; Shi, Y.; Gonnella, P. A.; Fisher, A.; Cook, T.; Zeng, L.; Kawut, S. M.; Lahm, T. Investigational new drug enabling angiotensin oral-delivery studies to attenuate pulmonary hypertension. *Biomaterials* **2020**, *233*, 119750.
- [29] Hu, L.; He, J.; gang Hou, L.; Wang, H.; Li, J.; Xie, C.; Duan, Z.; kui Sun, L.; Wang, X.; Zhu, C. Biological Evaluation of the Copper/Low-density Polyethylene Nanocomposite Intrauterine Device. *PLoS ONE* **2013**, *8*.
- [30] Nathaniel Huebsch, D. J. M. Inspiration and application in the evolution of biomaterials. *Nature* **2009**, *23*, 426–432.
- [31] Raghavendra, P.; Pullaiah, T. *Biomedical Imaging Role in Cellular and Molecular Diagnostics*; 2018; pp 85–111.
- [32] Lee, Y. C.; Moon, J. Y. *Introduction to Bionanotechnology*; 2020; pp 1–234.
- [33] Chisti, Y. *Bionanotechnology: Lessons from Nature*, D.S. Goodsell, Wiley-Liss, Hoboken. (2004), xii+337, ISBN: 0-471-41719-X. *Biotechnology Advances* **2006**, *24*.
- [34] Meyyappan, M.; Dastoor, M. Nanotechnology in Space Exploration - Report of the National Nanotechnology Initiative Workshop. *National Nanotechnology Coordination Office (NNCO)* **2006**, 84.
- [35] Gazit, E. *Plenty of Room for Biology at the Bottom: An Introduction to Bionanotechnology*; Imperial College Press, 2007.
- [36] Saleh, T. A. Nanomaterials: Classification, properties, and environmental toxicities. *Environmental Technology Innovation* **2020**, *20*, 101067.
- [37] Trotta, F.; Mele, A. *Nanosponges*; John Wiley Sons, Ltd, 2019; Chapter 1, pp 1–26.
- [38] qiang Li, Z.; Wang, L.; Li, Y.; Feng, Y.; Feng, W. Carbon-based functional nanomaterials: Preparation, properties and applications. *Composites Science and Technology* **2019**,
- [39] Marsh, H.; Rodríguez-Reinoso, F. *Activated Carbon*; Elsevier Science Ltd, 2006; pp 454–508.
- [40] Wang, F. In *Thermal Transport in Carbon-Based Nanomaterials*; Zhang, G., Ed.; Micro and Nano Technologies; Elsevier, 2017; pp 135–184.
- [41] Ahmadpour, A.; Do, D. The preparation of activated carbon from macadamia nutshell by chemical activation. *Carbon* **1997**, *35*, 1723–1732.
- [42] Saito, N.; Aoki, K.; Usui, Y.; Shimizu, M.; Hara, K.; Narita, N.; Ogihara, N.; Nakamura, K.; Ishigaki, N.; Kato, H.; Haniu, H.; Taruta, S.; Ahm Kim, Y.; Endo, M. Application of carbon fibers to biomaterials: A new era of nano-level control of carbon fibers after 30-years of development. *Chemical Society Reviews* **2011**, *40*, 3824–3834.

- [43] Edison, T. A. Electric lamp. 1880; US Patent 223898.
- [44] Bacon, R. Growth, Structure, and Properties of Graphite Whiskers. *Journal of Applied Physics* **1960**, *31*, 283–290.
- [45] Peebles, L.; Peebles, L. *Carbon Fibers: Formation, Structure, and Properties*; Raymond F. Boyer Library Collection; CRC-Press, 1995.
- [46] Ogale, A.; Zhang, M.; Jin, J. Recent advances in carbon fibers derived from biobased precursors. *Journal of Applied Polymer Science* **2016**, *133*.
- [47] Bengtsson, A.; Hecht, P.; Sommertune, J.; Ek, M.; Sedin, M.; Sjöholm, E. Carbon Fibers from Lignin-Cellulose Precursors: Effect of Carbonization Conditions. *ACS Sustainable Chemistry and Engineering* **2020**, *8*, 6826–6833.
- [48] Newcomb, B. A. Processing, structure, and properties of carbon fibers. *Composites Part A: Applied Science and Manufacturing* **2016**, *91*, 262–282.
- [49] Byrne, N.; De Silva, R.; Ma, Y.; Sixta, H.; Hummel, M. Enhanced stabilization of cellulose-lignin hybrid filaments for carbon fiber production. *Cellulose* **2018**, *25*, 723–733.
- [50] Zhou, X.; Wang, P.; Zhang, Y.; Zhang, X.; Jiang, Y. From Waste Cotton Linter: A Renewable Environment-Friendly Biomass Based Carbon Fibers Preparation. *ACS Sustainable Chemistry & Engineering* **2016**, *4*, 5585–5593.
- [51] Oroumei, A.; Fox, B.; Naebe, M. Thermal and Rheological Characteristics of Biobased Carbon Fiber Precursor Derived from Low Molecular Weight Organosolv Lignin. *ACS Sustainable Chemistry & Engineering* **2015**, *3*, 758–769.
- [52] Redelbach, M.; Klötzke, M.; E., F. Impact of lightweight design on energy consumption and cost effectiveness of alternative powertrain concepts. **2012**,
- [53] Hummel, M.; Michud, A.; Tantt, M.; Asaadi, S.; Ma, Y.; Hauru, L.; Parviainen, A.; King, A.; Kilpeläinen, I.; Sixta, H. In *Cellulose Chemistry and Properties*; Rojas, O., Ed.; Advances in Polymer Science; Springer-Verlag: Germany, 2016; Vol. 271; pp 133–168.
- [54] Takahashi, K.; Okita, K.; Nakagawa, M.; Yamanaka, S. Induction of pluripotent stem cells from fibroblast cultures. *Nature protocols* **2007**, *2*, 3081–3089.
- [55] Philbrick, S. "Generation of Germline-Competent Induced Pluripotent Stem Cells"(2007), by Keisuke Okita, Tomoko Ichisaka, and Shinya Yamanaka. *Embryo Project Encyclopedia* **2012**,
- [56] Liu, W.; Ma, J.; Yao, X.; Fang, R. *Materials for Biomedical Engineering*; Elsevier, 2019; pp 1–32.
- [57] Jan, C.; Grzegorz, K. The study of lifetime of polymer and composite bone joint screws under cyclical loads and in vitro conditions. *Journal of Materials Science: Materials in Medicine* **2005**, *16*, 1051–1060.

- [58] Rohner, B.; Wieling, R.; Magerl, F.; Schneider, E.; Steiner, A. Performance of a composite flow moulded carbon fibre reinforced osteosynthesis plate. *Veterinary and comparative orthopaedics and traumatology : V.C.O.T* **2005**, *18* 3, 175–82.
- [59] Park, S.-J.; Seo, M.-K. *Interface science and technology*; Elsevier, 2011; Vol. 18; pp 501–629.
- [60] Otawara, Y.; Ogasawara, K.; Kubo, Y.; Kashimura, H.; Ogawa, A.; Watanabe, K. Mechanical and surface properties of Yasargil Phynox aneurysm clips after long-term implantation in a patient with cerebral aneurysm. *Neurosurgical Review* **2008**, *32*, 193–197.
- [61] Takahama, T.; Onishi, K.; Kanai, F.; Hiraishi, M.; Yamazaki, Z.; Furuse, A.; Yoshitake, T. A new improved biodegradable tracheal prosthesis using hydroxy apatite and carbon fiber. *ASAIO transactions* **1989**, *35* 3, 291–3.
- [62] Egbo, M. K. A fundamental review on composite materials and some of their applications in biomedical engineering. *Journal of King Saud University - Engineering Sciences* **2021**, *33*, 557–568.
- [63] Steinberg, E. L.; Rath, E.; Shlaifer, A.; Chechik, O.; Maman, E.; Salai, M. Carbon fiber reinforced PEEK Optima—A composite material biomechanical properties and wear/debris characteristics of CF-PEEK composites for orthopedic trauma implants. *Journal of the Mechanical Behavior of Biomedical Materials* **2013**, *17*, 221–228.
- [64] Lu, S.-H.; Liang, G.-Z.; Zhou, Z.-W.; Li, F. Structure and properties of UHMWPE fiber/carbon fiber hybrid composites. *Journal of Applied Polymer Science* **2006**, *101*, 1880–1884.
- [65] Campbell, M.; Bureau, M.; Yahia, L. Performance of CF/PA12 composite femoral stems. *Journal of materials science. Materials in medicine* **2008**, *19*, 683–93.
- [66] Claes, L. Kohlenstoffaserverstärktes Polysulfon - ein neuer Implantatwerkstoff - Carbonfibre Reinforced Polysulfone - A New Biomaterial. 1989, *34*, 315–319.
- [67] Geary, C.; Birkinshaw, C.; Jones, E. L. Characterisation of Bionate polycarbonate polyurethanes for orthopaedic applications. *Journal of Materials Science: Materials in Medicine* **2008**, *19*, 3355–3363.
- [68] Pilliar, R. M.; Blackwell, R.; Macnab, I.; Cameron, H. U. Carbon fiber-reinforced bone cement in orthopedic surgery. *Journal of Biomedical Materials Research* **1976**, *10*, 893–906.
- [69] Parsons, J. R.; del Rosario, A.; Weiss, A. B.; Alexander, H. Achilles Tendon Repair with an Absorbable Polymer-Carbon Fiber Composite. *Foot & Ankle International* **1984**, *5*, 49 – 53.
- [70] Ogale, A. A.; Zhang, M.; Jin, J. Recent advances in carbon fibers derived from biobased precursors. *Journal of Applied Polymer Science* **2016**, *133*.

- [71] Ko, T.-H. The effect of pyrolysis on the mechanical properties and microstructure of carbon fiber-reinforced and stabilized fiber-reinforced phenolic resins for carbon/carbon composites. *Polymer Composites* **1993**, *14*, 247–256.
- [72] Basu, P. In *Biomass Gasification, Pyrolysis and Torrefaction (Third Edition)*, third edition ed.; Basu, P., Ed.; Academic Press, 2018; pp 155–187.
- [73] Rajendran, K.; Lin, R.; Wall, D. M.; Murphy, J. D. In *Sustainable Resource Recovery and Zero Waste Approaches*; Taherzadeh, M. J., Bolton, K., Wong, J., Pandey, A., Eds.; Elsevier, 2019; pp 65–78.
- [74] Naqvi, S.; Prabhakara, H. M.; Bramer, E.; Dierkes, W.; Akkerman, R.; Brem, G. A critical review on recycling of end-of-life carbon fibre/glass fibre reinforced composites waste using pyrolysis towards a circular economy. *Resources, conservation and recycling* **2018**, *136*, 118–129.
- [75] Demirbas, A.; Arin, G. An Overview of Biomass Pyrolysis. *Energy Sources* **2002**, *24*, 471–482.
- [76] Chum, H. L. Polymers from biobased materials. **1991**,
- [77] Chen, Z.; Leng, E.; Zhang, Y.; Zheng, A.; Peng, Y.; Gong, X.; Huang, Y.; Qiao, Y. Pyrolysis characteristics of tobacco stem after different solvent leaching treatments. *Journal of Analytical and Applied Pyrolysis* **2018**, *130*, 350–357.
- [78] Van de Velden, M.; Baeyens, J.; Brems, A.; Janssens, B.; Dewil, R. Fundamentals, kinetics and endothermicity of the biomass pyrolysis reaction. *Renewable Energy* **2010**, *35*, 232–242.
- [79] Mullen, C. A.; Boateng, A. A. Characterization of water insoluble solids isolated from various biomass fast pyrolysis oils. *Journal of Analytical and Applied Pyrolysis* **2011**, *90*, 197–203.
- [80] Zhang, L.; Hu, X.; Hu, K.; Hu, C.; Zhang, Z.; Liu, Q.; Hu, S.; Xiang, J.; Wang, Y.; Zhang, S. Progress in the reforming of bio-oil derived carboxylic acids for hydrogen generation. *Journal of Power Sources* **2018**, *403*, 137–156.
- [81] Hu, X.; Gholizadeh, M. Biomass pyrolysis: A review of the process development and challenges from initial researches up to the commercialisation stage. *Journal of Energy Chemistry* **2019**, *39*, 109–143.
- [82] Jahirul, M. I.; Rasul, M. G.; Chowdhury, A. A.; Ashwath, N. Biofuels Production through Biomass Pyrolysis —A Technological Review. *Energies* **2012**, *5*, 4952–5001.
- [83] Amutio, M.; Lopez, G.; Aguado, R.; Bilbao, J.; Olazar, M. Biomass oxidative flash pyrolysis: autothermal operation, yields and product properties. *Energy & fuels* **2012**, *26*, 1353–1362.

- [84] Suhani, N.; Mohamed, R. M. S. R.; Latiff, A. A. A.; Nasir, N.; Ahmad, B.; Oyekanmi, A. A.; Awang, H.; Daud, Z. Removal of COD and ammoniacal nitrogen by banana trunk fiber with chitosan adsorbent. *Malaysian Journal of Fundamental and Applied Sciences* **2020**, *16*, 243–247.
- [85] Wang, G.; Dai, Y.; Yang, H.; Xiong, Q.; Wang, K.; Zhou, J.; Li, Y.; Wang, S. A Review of Recent Advances in Biomass Pyrolysis. *Energy & Fuels* **2020**, *34*, 15557–15578.
- [86] Frank, E.; Steudle, L. M.; Ingildeev, D.; Spörl, J. M.; Buchmeiser, M. R. Carbon Fibers: Precursor Systems, Processing, Structure, and Properties. *Angewandte Chemie International Edition* **2014**, *53*, 5262–5298.
- [87] Tang, M.; Bacon, R. Carbonization of cellulose fibers—I. Low temperature pyrolysis. *Carbon* **1964**, *2*, 211–220.
- [88] Brunner, P. H.; Roberts, P. V. The significance of heating rate on char yield and char properties in the pyrolysis of cellulose. *Carbon* **1980**, *18*, 217–224.
- [89] Dumanli, A. G.; Windle, A. H. Carbon fibres from cellulosic precursors: a review. *Journal of Materials Science* **2012**, *47*, 4236–4250.
- [90] Singh, K. R.; Nayak, V.; Sarkar, T.; Singh, R. P. Cerium oxide nanoparticles: properties, biosynthesis and biomedical application. *RSC Adv.* **2020**, *10*, 27194–27214.
- [91] Singh, K. R.; Nayak, V.; Sarkar, T.; Singh, R. P. Cerium oxide nanoparticles: properties, biosynthesis and biomedical application. *RSC Advances* **2020**,
- [92] Wang, B.; Zhu, B.; Yun, S.; Zhang, W.; Xia, C.; Afzal, M.; Cai, Y.; Liu, Y.; Wang, Y.; Wang, H. Fast ionic conduction in semiconductor CeO_{2-δ} electrolyte fuel cells. *NPG Asia Materials* **2019**, *11*, 1–12.
- [93] Reed, K.; Cormack, A.; Kulkarni, A.; Mayton, M.; Sayle, D.; Klaessig, F.; Stadler, B. Exploring the properties and applications of nanoceria: is there still plenty of room at the bottom? *Environ. Sci.: Nano* **2014**, *1*, 390–405.
- [94] Cafun, J.; Kvashnina, K.; Casals, E.; Puentes, V.; Glatzel, P. Absence of Ce³⁺ sites in chemically active colloidal ceria nanoparticles. *ACS Nano* **2013**, *7*, 10726–10732.
- [95] Gao, Y.; Guo, X.; Qiu, Z.; Zhang, G.; Zhu, R.; Zhang, Y.; Pang, H. Printable electrode materials for supercapacitors. *ChemPhysMater* **2022**, *1*, 17–38.
- [96] Korsvik, C.; Patil, S.; Seal, S.; Self, W. T. Superoxide dismutase mimetic properties exhibited by vacancy engineered ceria nanoparticles. *Chem. Commun.* **2007**, 1056–1058.
- [97] Singh, S.; Dosani, T.; Karakoti, A. S.; Kumar, A.; Seal, S.; Self, W. T. A phosphate-dependent shift in redox state of cerium oxide nanoparticles and its effects on catalytic properties. *Biomaterials* **2011**, *32*, 6745–6753.

- [98] Ijaz, I.; Gilani, E.; Nazir, A.; Bukhari, A. Detail review on chemical, physical and green synthesis, classification, characterizations and applications of nanoparticles. *Green Chemistry Letters and Reviews* **2020**, *13*, 223–245.
- [99] Kumar, P. S.; Pavithra, K. G.; Naushad, M. In *Nanomaterials for Solar Cell Applications*; Thomas, S., Sakho, E. H. M., Kalarikkal, N., Oluwafemi, S. O., Wu, J., Eds.; Elsevier, 2019; pp 97–124.
- [100] Waris, G.; Ahsan, H. Reactive oxygen species: role in the development of cancer and various chronic conditions. *Journal of carcinogenesis* **2006**, *5*, 14.
- [101] Ansari, A. A.; Kaushik, A.; Solanki, P.; Malhotra, B. Sol–gel derived nanoporous cerium oxide film for application to cholesterol biosensor. *Electrochemistry Communications* **2008**, *10*, 1246–1249.
- [102] Burello, E.; Worth, A. P. A theoretical framework for predicting the oxidative stress potential of oxide nanoparticles. *Nanotoxicology* **2011**, *5*, 228–235.
- [103] Ranjbar, A.; Soleimani Asl, S.; Firozian, F.; Heidary Dartoti, H.; Seyedabadi, S.; Taheri Azandariani, M.; Ganji, M. Role of Cerium Oxide Nanoparticles in a Paraquat-Induced Model of Oxidative Stress: Emergence of Neuroprotective Results in the Brain. *Journal of Molecular Neuroscience* **2018**, *66*, 420–427.
- [104] Karakoti, A. S.; Tsigkou, O.; Yue, S.; Lee, P. D.; Stevens, M. M.; Jones, J. R.; Seal, S. Rare earth oxides as nanoadditives in 3-D nanocomposite scaffolds for bone regeneration. *J. Mater. Chem.* **2010**, *20*, 8912–8919.
- [105] Adeniyi, A. G.; Ighalo, J. O.; Onifade, D. V. Banana and plantain fiber-reinforced polymer composites. *Journal of Polymer Engineering* **2019**, *39*, 597–611.
- [106] Alavudeen, A.; Thiruchitrabalam, M.; Venkateshwaran, N.; Athijayamani, A. Review of natural fiber reinforced woven composite. *Rev. Adv. Mater. Sci* **2011**, *27*, 146–150.
- [107] Syahirah, N.; Deraman, M.; Suleman, M.; M.R.M.Jasni, M. R.; J.G.Manjunantha,; Othman, M. A. R. Supercapacitors using Binderless Activated Carbon Monoliths Electrodes consisting of a Graphite Additive and Pre-carbonized Biomass Fibers. *International journal of electrochemical science* **2017**, *12*, 2520–2539.
- [108] van der Heide, P. *X-ray Photoelectron Spectroscopy: An Introduction to Principles and Practices*, first edit ed.; John Wiley Sons, Inc: Hoboken, New Jersey, 2012; p 283.
- [109] Mathur, V. Composite materials from local resources. *Construction and Building Materials - CONSTR BUILD MATER* **2006**, *20*, 470–477.
- [110] Taj, S.; Munawar, M.; Khan, S. Natural fiber-reinforced polymer composites. *Proc. Pakistan Acad. Sci.* **2007**, *44*, 129–144.
- [111] Baker, D. A.; Rials, T. G. Recent advances in low-cost carbon fiber manufacture from lignin. *Journal of Applied Polymer Science* **2013**, *130*, 713–728.

- [112] Smole, M. S.; Hribernik, S.; Kleinschek, K. S.; Kreže, T. In *Advances in Agrophysical Research*; Grundas, S., Stepniewski, A., Eds.; IntechOpen: Rijeka, 2013; Chapter 15.
- [113] Mallick, P. *Fiber-Reinforced Composites: Materials, Manufacturing, and Design, Third Edition*; Mechanical Engineering; CRC Press, 2007.
- [114] Sivaranjana, P.; Arumugaprabu, V. A brief review on mechanical and thermal properties of banana fiber based hybrid composites. *SN Applied Sciences* **2021**, *3*, 1–8.
- [115] Al Rashid, A.; Khalid, M. Y.; Imran, R.; Ali, U.; Koc, M. Utilization of banana fiber-reinforced hybrid composites in the sports industry. *Materials* **2020**, *13*.
- [116] Farideh Namvar, Mohammad Jawaid, Paridah Md Tahir, Rosfarizan Mohamad, Susan Azizi, Alireza Khodavandi, H. S. R.; Nayeri, M. D.; Namvar, F.; Jawaid, M.; Tahir, P. M.; Mohamad, R.; Susan Azizi, d. A. K.; Rahman, H. S.; Nayeri, M. D. Potential Use of Plant Fibres and their Composites for Biomedical Applications. *Bioresources* **2016**, *9*, 5688–5706.
- [117] Holmes, M. H. Global carbon fibre market remains on upward trend. *Reinforced Plastics* **2014**, *58*, 38–45.
- [118] Chang, H.; Luo, J.; Liu, H. C.; Zhang, S.; Park, J. G.; Liang, R.; Kumar, S. Carbon fibers from polyacrylonitrile/cellulose nanocrystal nanocomposite fibers. *Carbon* **2019**, *145*, 764–771.
- [119] FAO, Food and Agriculture Organization of the United Nations - Banana market review – Preliminary results 2020. **2021**, 18.
- [120] Das, R. S.; Agrawal, Y. Raman spectroscopy: Recent advancements, techniques and applications. *Vibrational Spectroscopy* **2011**, *57*, 163–176.
- [121] Xu, Z.; Zhongdu, H.; Song, Y.; Fu, X.; Rommel, M.; Luo, X.; Hartmaier, A.; Zhang, J.; Fang, F. Topic Review: Application of Raman Spectroscopy Characterization in Micro/Nano-Machining. *Micromachines* **2018**, *9*, 361.
- [122] Inkson, B. In *Materials Characterization Using Nondestructive Evaluation (NDE) Methods*; Hübschen, G., Altpeter, I., Tschuncky, R., Herrmann, H.-G., Eds.; Woodhead Publishing, 2016; pp 17–43.
- [123] Akhtar, K.; Khan, S. A.; Khan, S. B.; Asiri, A. M. In *Handbook of Materials Characterization*; Sharma, S. K., Ed.; Springer International Publishing: Cham, 2018; pp 113–145.
- [124] Gaona Torres, S. J.; González Vásquez, G.; Briceño, S.; Corredor, L. Structural characterization and electrochemical properties of natural carbon fibers decorated with nanoparticles. Yachay Tech University. School of Physical Sciences and Nanotechnology. **2021**,
- [125] Maldonado, P.; González Vásquez, G.; Bastardo, E. Natural and Doped Diatoms for Photodegradation under Visible Light. Yachay Tech University. School of Chemical Sciences and Engineering. **2020**, 96.

- [126] Brabazon, D.; Raffer, A. In *Emerging Nanotechnologies for Manufacturing*; Ahmed, W., Jackson, M. J., Eds.; Micro and Nano Technologies; William Andrew Publishing: Boston, 2010; pp 59–91.
- [127] Goldstein, J. I.; Newbury, D. E.; Michael, J. R.; Ritchie, N. W.; Scott, J. H. J.; Joy, D. C. *Scanning electron microscopy and X-ray microanalysis*; Springer, 2017.
- [128] Harris, D. C. *Symmetry and spectroscopy : an introduction to vibrational and electronic spectroscopy*; Oxford University Press: New York, 1977.
- [129] Dietzek, B.; Cialla, D.; Schmitt, M.; Popp, J. In *Confocal Raman Microscopy*; Toporski, J., Dieing, T., Hollricher, O., Eds.; Springer International Publishing: Cham, 2018; pp 47–68.
- [130] Xu, Z.; He, Z.; Song, Y.; Fu, X.; Rommel, M.; Luo, X.; Hartmaier, A.; Zhang, J.; Fang, F. Topic Review: Application of Raman Spectroscopy Characterization in Micro/Nano-Machining. *Micromachines* **2018**, *9*.
- [131] Harris, D.; Bertolucci, M. *Symmetry and Spectroscopy: An Introduction to Vibrational and Electronic Spectroscopy*; Dover Books on Chemistry Series; Dover Publications, 1989.
- [132] Mercier, B.; Castelain, T.; Jondeau, E.; Bailly, C. Density Fluctuations Measurement by Rayleigh Scattering Using a Single Photomultiplier. *AIAA Journal* **2018**, *56*, 1310–1316.
- [133] Baker, M. J.; Hughes, C. S.; Hollywood, K. A. *Biophotonics: Vibrational Spectroscopic Diagnostics*; 2053-2571; Morgan Claypool Publishers, 2016.
- [134] Baker, M.; Hughes, C.; Hollywood, K. *Biophotonics: Vibrational spectroscopic diagnostics*; 2016; pp 1–94.
- [135] Tschöpe, A.; Sommer, E. M.; Birringer, R. Grain size-dependent electrical conductivity of polycrystalline cerium oxide: I. Experiments. *Solid State Ionics* **2001**, *139*, 255–265.
- [136] Tanvir, S.; Qiao, L. Surface tension of nanofluid-type fuels containing suspended nanomaterials. *Western States Section of the Combustion Institute Spring Technical Meeting 2012* **2012**, 551–573.
- [137] Singhanía, A.; Bhaskarwar, A. N. Synthesis, Characterization and Catalytic Activity of CeO₂ and Ir-doped CeO₂ Nanoparticles for Hydrogen Iodide Decomposition. *Chemistry Letters* **2018**, *47*, 1224–1227.
- [138] Ferrari, A. C. Raman spectroscopy of graphene and graphite: Disorder, electron–phonon coupling, doping and nonadiabatic effects. *Solid State Communications* **2007**, *143*, 47–57, Exploring graphene.
- [139] Marino, C.; Cabanero, J.; Povia, M.; Villevieille, C. Biowaste Lignin-Based Carbonaceous Materials as Anodes for Na-Ion Batteries. *Journal of The Electrochemical Society* **2018**, *165*, A1400–A1408.

- [140] Loridant, S. Raman spectroscopy as a powerful tool to characterize ceria-based catalysts. *Catalysis Today* **2020**,
- [141] Fung, A.; Rao, A.; Kuriyama, K.; Dresselhaus, M.; Dresselhaus, G.; Endo, M.; Shindo, N. Raman scattering and electrical conductivity in highly disordered activated carbon fibers. *Journal of Materials Research* **1993**, *8*, 489–500.
- [142] Hecht, E.; Zajac, A. *Optics*; Addison-Wesley world student series edition; Addison-Wesley, 1987.
- [143] Herdman, J. D.; Connelly, B. C.; Smooke, M. D.; Long, M. B.; Miller, J. H. A comparison of Raman signatures and laser-induced incandescence with direct numerical simulation of soot growth in non-premixed ethylene/air flames. *Carbon* **2011**, *49*, 5298–5311.
- [144] Ammar, M. R.; Rouzaud, J.-N. How to obtain a reliable structural characterization of polished graphitized carbons by Raman microspectroscopy. *Journal of Raman Spectroscopy* **2012**, *43*, 207–211.
- [145] Loridant, S. Raman spectroscopy as a powerful tool to characterize ceria-based catalysts. *Catalysis Today* **2021**, *373*, 98–111.
- [146] Kim, N.-W.; Lee, D.-K.; Yu, H. Selective shape control of cerium oxide nanocrystals for photocatalytic and chemical sensing effect. *RSC Adv.* **2019**, *9*, 13829–13837.

Abbreviations

AFM Atomic force microscopy 24

CFs carbon fibers 13, 14, 16, 28, 34

CNTs carbon nanotubes 14

DNA deoxyribonucleic acid 11

EFB empty fruit bunches 27

ESB European Society of Biomaterials 4

FAO Food and Agriculture Organization of the United Nations 28

FDA Food and Drug Administration 3

FOV Field of View 38

FT-IR Fourier transform infrared spectroscopy 24

FWHM full width at half maximum 40, 57

HA Hydroxyapatite 16

HM High-modulus 13

HT Standard elastic modulus type 13

IM Intermediate-modulus 13

LM Low elastic modulus type 13

NFC natural fiber composite 27

NIBIB National Institute of Biomedical Imaging and Bioengineering 3

NIH National Institutes of Health 4

NPs nanoparticles 12, 13, 23, 25, 33

PAN poly(acrylonitrile) 14, 15, 17, 21, 28

PEEK polyether ether ketone 16

PSU polysulfone 16

RNS reactive nitrogen species 24

ROS reactive oxygen species 24

SEM Scanning Electron Microscopy 29, 38, 45

SOD Superoxide Dismutase 23

TEM Transmission electron microscopy 24

UHM Ultrahigh-modulus 13

XRD X-ray diffraction 24